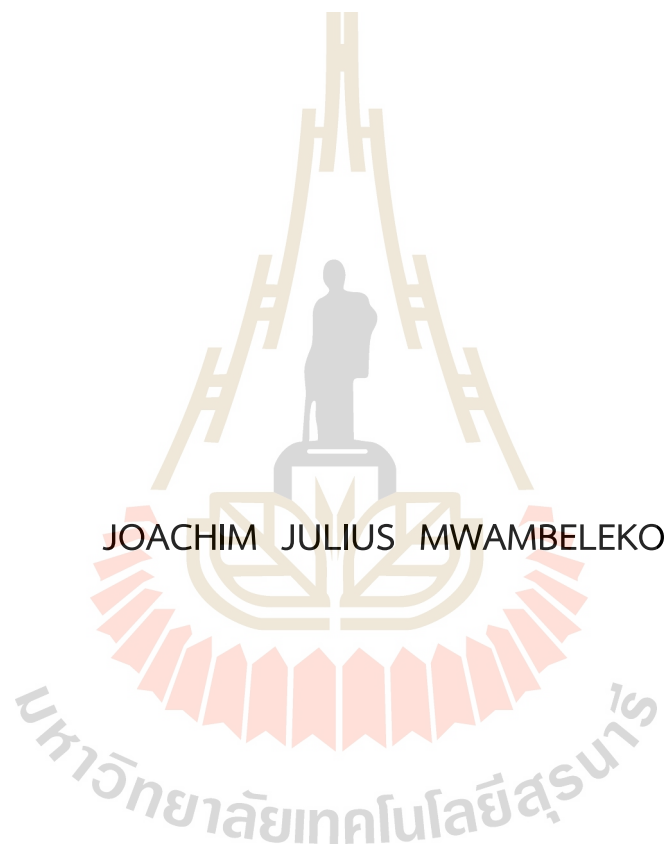


ENHANCING ON-BOARD ENERGY STORAGE SYSTEM USING  
ACCELERATING CONTACT LINES



JOACHIM JULIUS MWAMBELEKO

A Thesis Submitted in Partial Fulfillment of the Requirements for the  
Degree of Doctor of Philosophy in Electrical Engineering  
Suranaree University of Technology  
Academic Year 2020

การทำระบบกักเก็บพลังงานบนขบวนรถไฟดีเซลด้วยสายลัมผัสช่วยเร่ง



นายโจอะคิม จูเลียส มวมเบเลโก

วิทยานิพนธ์นี้เป็นส่วนหนึ่งของการศึกษาตามหลักสูตรปริญญาวิศวกรรมศาสตรดุษฎีบัณฑิต

สาขาวิชาวิศวกรรมไฟฟ้า

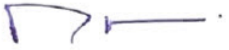
มหาวิทยาลัยเทคโนโลยีสุรนารี


ปีการศึกษา 2563


ENHANCING ON-BOARD ENERGY STORAGE SYSTEM USING  
ACCELERATING CONTACT LINES


Suranaree University of Technology has approved this thesis submitted in partial fulfillment of the requirements for the Degree of Doctor of Philosophy.


Thesis Examining Committee


  
\_\_\_\_\_  
(Assoc. Prof. Dr. Kaan Kerdchuen)  
Chairperson


  
\_\_\_\_\_  
(Assoc. Prof. Dr. Thanatchai Kulworawanichpong)  
Member (Thesis Advisor)

  
\_\_\_\_\_  
(Asst. Prof. Dr. Uthen Leeton)  
Member

  
\_\_\_\_\_  
(Assoc. Prof. Dr. Keerati Chayakulkeeree)  
Member

  
\_\_\_\_\_  
(Asst. Prof. Dr. Tosaphol Ratniyomchai)  
Member

  
\_\_\_\_\_  
(Assoc. Prof. Dr. Chatchai Jothityangkoon)  
Vice Rector for Academic Affairs  
and Quality Assurance

  
\_\_\_\_\_  
(Assoc. Prof. Dr. Pornsiri Jongkol)  
Dean of Institute of Engineering

โจอะคิม จูเลียส มวมเบเลโก : การทำระบบกักเก็บพลังงานบนขบวนรถให้ดีขึ้น  
ด้วยสายสัมผัสช่วยเร่ง (ENHANCING ON-BOARD ENERGY STORAGE SYSTEM USING  
ACCELERATING CONTACT LINES) อาจารย์ที่ปรึกษา : รองศาสตราจารย์ ดร.ธนิตชัย  
กุลรวรานิชพงษ์, 147 หน้า.

คำสำคัญ: อุปกรณ์กักเก็บพลังงานบนขบวนรถ/รถราง/ตัวเก็บประจุยิ่งยวด/สายสัมผัสช่วยเร่ง

วิทยานิพนธ์นี้ทำระบบกักเก็บพลังงานบนขบวนรถให้ดีขึ้นโดยใช้สายสัมผัสช่วยเร่ง  
(Accelerating Contact Line: ACL) ซึ่งเป็นสายสัมผัสระยะสั้นที่ยื่นออกมาจากรางสัมผัสสำหรับ  
ประจุไฟฟ้าทั่วไปที่ติดตั้งอยู่ที่สถานีรถราง เพื่อให้รถรางดึงกำลังไฟฟ้าไปใช้ในช่วงเร่งออกจากสถานี  
เนื่องจากรถรางใช้กำลังไฟฟ้าสูงในการเร่ง การใช้สายสัมผัสช่วยเร่งจึงสามารถช่วยลดขนาดของ  
อุปกรณ์ระบบกักเก็บพลังงานบนขบวนรถได้ ซึ่งนำไปสู่การลดต้นทุนของระบบกักเก็บพลังงานบน  
ขบวนรถ น้ำหนักของรถราง และการใช้พลังงานของรถราง นอกจากนี้ สายสัมผัสช่วยเร่งยังมีความ  
สะดวกและเหมาะสมเมื่อนำไปใช้กับเส้นทางที่ไม่ได้รับการจ่ายไฟฟ้าทั้งหมดตลอดเส้นทางด้วยเหตุผล  
ประการต่าง ๆ เช่น (1) การรักษาทัศนียภาพที่สวยงามบริเวณใจกลางเมืองและโบราณสถาน (2) การ  
ลดความซับซ้อนของระบบจ่ายไฟฟ้าอันเนื่องมาจากทางข้ามรถไฟ สะพาน และการขาดสิทธิในการใช้  
ที่ดินหรือเส้นทาง และ (3) ต้นทุนการสร้างระบบจ่ายไฟฟ้าที่สูงสำหรับเส้นทางที่มีผู้ใช้งานน้อยหรือ  
ให้บริการไม่ถี่มากนัก

การศึกษานี้ใช้โปรแกรม MATLAB ในการสร้างแบบจำลองและจำลองผลระบบรถรางที่ใช้ตัว  
เก็บประจุยิ่งยวดเพียงอย่างเดียวในการขับเคลื่อน (cap-Tram) และระบบรถรางที่ใช้ตัวเก็บประจุ  
ยิ่งยวดควบคู่กับสายสัมผัสช่วยเร่งที่นำเสนอ (cap-ACL-Tram) จากผลการจำลอง พบว่า เมื่อ  
เปรียบเทียบกับระบบ cap-Tram ระบบ cap-ACL-Tram ลดขนาดของอุปกรณ์กักเก็บพลังงานบน  
ขบวนรถได้ถึงร้อยละ 44 ลดน้ำหนักของรถรางได้ร้อยละ 4.8 และลดการใช้พลังงานของรถรางร้อยละ  
1.5 เมื่อพิจารณาราคาของตัวเก็บประจุยิ่งยวดในปัจจุบัน ขนาดที่ลดได้ของอุปกรณ์กักเก็บพลังงาน  
ดังกล่าวมีนัยสำคัญต่อการลดต้นทุน ยิ่งไปกว่านั้น ขนาดที่ลดได้จากการจำลองผลพิจารณาจากการใช้  
งานรถรางเพียงขบวนเดียวในเส้นทาง ถ้าจำนวนขบวนที่ใช้งานเพิ่มขึ้นสองเท่า อุปกรณ์ กักเก็บ  
พลังงานบนขบวนรถทั้งหมดก็จะลดลงสองเท่าเช่นเดียวกัน แต่ต้นทุนของสายสัมผัสช่วยเร่งยังคงเท่าเดิม



JOACHIM JULIUS MWAMBELEKO : ENHANCING ON-BOARD ENERGY STORAGE SYSTEM USING ACCELERATING CONTACT LINES. THESIS ADVISOR : ASSOC. PROF. THANATCHAI KULWORAWANICHPONG, Ph.D., 147 PP.

Keyword: On-Board Energy Storage/Tram/Supercapacitor/Accelerating Contact Lines

This thesis enhances on-board energy storage systems using accelerating contact lines. An Accelerating Contact Line (ACL) is a short extension of a conventional charging bar at a tram station. The ACL is intended to supply tram's acceleration power demand. Since trams consume high energy during acceleration, ACLs reduce the required size of On-Board Energy Storage Device (OBESD). Consequently, cost of the OBESD and effective tram weight are reduced. The latter reduces tram energy consumption. Accelerating contact lines come in handy when a railway route cannot be fully electrified, for reasons such as i) aesthetic in city centers and historical sites, ii) electrification complexity due to level crossings, bridges, and not enough right of way, and iii) electrification cost on idle routes. In the study, conventional supercapacitor tram system, that is, a tram powered solely by supercapacitors (cap-Tram) and the proposed supercapacitor and accelerating contact line tram system (cap-ACL-Tram) are modelled and simulated using MATLAB. The cap-ACL-tram system reduces the required size of OBESD by 44%, tram effective weight by 4.8%, and energy consumption by 1.5%.

School of Electrical Engineering  
Academic Year 2020

Student's Signature Joachimjm  
Advisor's Signature [Signature]

## ACKNOWLEDGEMENTS

This thesis work was possible through the generosity of several people in various ways. I take the opportunity to mention just a few.

I would like to express my deepest gratitude to my advisor, Assoc. Prof. Dr. Thanatchai Kulworawanichpong for his overly support, enlightening guidance, patience, inspiration, and encouragement throughout the course of my study. Even though his guidance was highly insightful, I always had free room to work on my thoughts in my own ways.

My sincere appreciation is extended to thesis committee members, for their insightful and invaluable comments and suggestions.

It is my great pleasure to express my sincere gratitude to colleagues, and staffs from electrical engineering school for their kindness, and support.

I am very grateful to Suranaree University of Technology (SUT), school of electrical engineering, for the scholarship that covered my tuition fee during the period of the study.

I am greatly indebted to the constant love and support from family members. In a very special way, I thank my lovely mother and aunt.

Finally, I would like to express my gratitude to all whom I have failed to mention, but they have generously supported me.

Joachim Julius Mwambeleko

# TABLE OF CONTENTS

	Page
ABSTRACT (THAI).....	I
ABSTRACT (ENGLISH).....	II
ACKNOWLEDGEMENTS.....	III
TABLE OF CONTENTS.....	IV
LIST OF TABLES.....	VIII
LIST OF FIGURES.....	IX
SYMBOLS AND ABBREVIATIONS.....	XI
<b>CHAPTER</b>	
<b>I INTRODUCTION.....</b>	<b>1</b>
1.1 Background.....	1
1.1.1 The beauty of electric traction.....	1
1.1.2 The need for on-board energy storage.....	2
1.1.3 The supercapacitor-powered tram.....	4
1.1.4 Tram tractive energy demand.....	5
1.1.5 The proposed idea.....	6
1.2 Problem definition.....	8
1.3 Research motivation.....	9
1.4 Research objective.....	10
1.5 Methodology.....	11
1.6 Research assumptions.....	11
1.7 Scope and limitations of the study.....	11
1.8 Expected benefits.....	12
1.9 Organization of the thesis.....	12
<b>II BRIEF REVIEW.....</b>	<b>13</b>
2.1 Introduction.....	13
2.2 Energy storage technologies in LRVs.....	13

## TABLE OF CONTENTS (Continued)

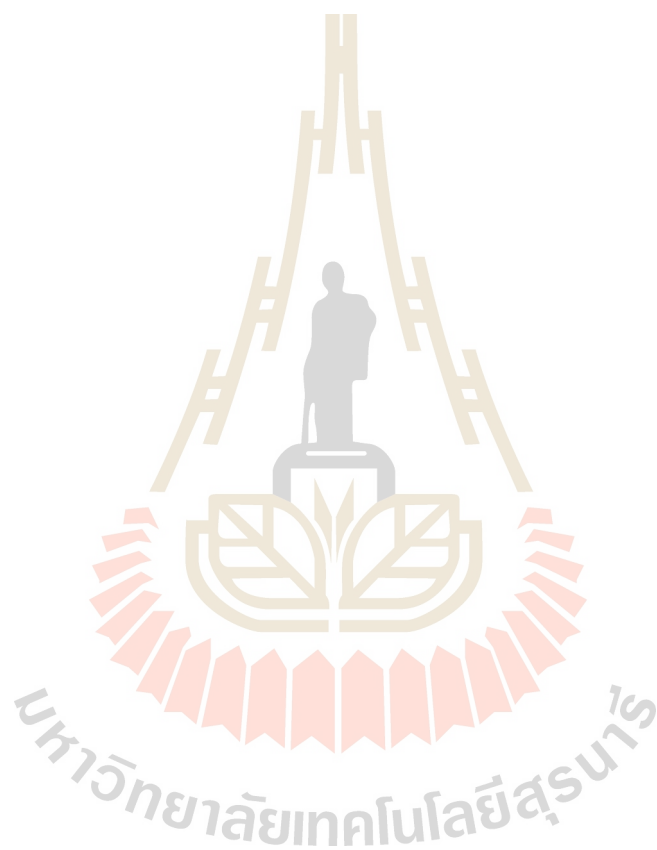
	Page
2.3 Accelerating contact lines, previous works.....	14
2.4 Supercapacitors .....	15
2.4.1 Capacitor energy and voltage .....	16
2.4.2 Capacitor energy and power densities.....	18
2.5 Supercapacitors versus batteries .....	21
2.6 Tram motion .....	23
2.6.1 Tram longitudinal forces.....	25
2.6.2 Acceleration force during motoring.....	29
2.6.3 Tractive effort force during cruising.....	29
2.6.4 Tram forces during coasting .....	31
2.6.5 Tram forces during braking.....	33
2.6.6 Tram power demand.....	33
<b>III TRAM SYSTEM MODEL .....</b>	<b>35</b>
3.1 Introduction.....	35
3.2 Capacitor bank model .....	36
3.2.1 Capacitor module constructor .....	36
3.2.2 Charge-discharge method.....	37
3.2.3 Capacitor bank constructor.....	38
3.2.4 Capacitor bank other methods .....	38
3.3 Sizing capacitor bank.....	39
3.3.1 Capacitor bank energy target.....	39
3.3.2 Energy target to capacitor bank size .....	40
3.3.3 Capacitor bank mass question/effect .....	42
3.4 Contact line model .....	43
3.4.1 Contact line constructor.....	44
3.4.2 Update state method.....	44

## TABLE OF CONTENTS (Continued)

	Page
3.5 Contact line length.....	45
3.6 Tram movement model.....	46
3.6.1 Tram speed modes.....	47
3.6.2 Speed profile generation.....	49
3.6.3 Tram power and energy demand.....	53
3.7 Power dispatcher.....	57
3.7.1 Power mode dwell.....	59
3.7.2 Power mode ACL.....	60
3.7.3 Power mode autonomous.....	62
<b>IV SIMULATION RESULTS AND DISCUSSION.....</b>	<b>64</b>
4.1 Introduction.....	64
4.2 Route and speed profile.....	64
4.3 Results for a cap-Tram.....	66
4.4 Results for a cap-ACL-Tram.....	73
4.5 Discussion.....	78
4.5.1 Capacitor bank reduction.....	78
4.5.2 Effect of gradient.....	79
4.5.3 Significance of ACLs.....	81
4.5.4 Supercapacitors and ACLs.....	81
<b>V CONCLUSION AND FUTURE WORKS.....</b>	<b>82</b>
5.1 Conclusion.....	82
5.2 Future works.....	83
REFERENCES.....	84
APPENDICES	
APPENDIX A SIMULATION SETUP MATLAB CODE.....	88
APPENDIX B CAPACITOR MODULE AND CAPACITOR BANK MATLAB CODE.....	93

## TABLE OF CONTENTS (Continued)

	Page
APPENDIX C CONTACT LINE MATLAB CODE.....	108
APPENDIX D PUBLICATIONS.....	117
BIOGRAPHY.....	147





## LIST OF TABLES

Table	Page
2.1 Supercapacitor modules from various manufacturers.....	20
2.2 Altairnano Lithium Titanate cell.....	22
2.3 Maxwell DuraBlue supercapacitor cell.....	23
3.1 Capacitor bank sizing algorithm.....	41
3.2 Tram movement algorithm.....	47
3.3 A peek view of tram speed profile.....	53
3.4 Power dispatcher modes summary.....	59
4.1 Route sections' elevation trajectory of interest for the study.....	65
4.2 Simulation results summary for cap-Tram.....	72
4.3 Simulation results summmary for cap-ACL-Tram.....	78
4.4 Trams performance comparison summary.....	78

## LIST OF FIGURES

Figure		Page
1.1	Reasons and advantages of on-board energy storage .....	4
1.2	Supercapacitor tram unveiled in China.....	5
1.3	Tram speed profile and energy consumption .....	6
1.4	Tram systems a) conventional (cap-Tram) b) proposed (cap-ACL-Tram).....	7
1.5	Accelerating contact line as an extension of a charging bar .....	7
1.6	Block diagram of a supercapacitor and contact line tram system .....	8
1.7	Layered view of a problem definition.....	9
2.1	Supercapacitor cells .....	18
2.2	Supercapacitor modules .....	19
2.3	Supercapacitor bank from supercapacitor modules .....	19
2.4	General tram speed profile.....	24
2.5	Typical tractive effort, braking effort and resistance force curves .....	25
2.6	Forces affecting tram longitudinal dynamics .....	26
2.7	Acceleration and speed limit during cruising .....	30
2.8	Acceleration and speed limit during coasting.....	32
3.1	Tram system model .....	35
3.2	Capacitor bank circuit model .....	36
3.3	Flowchart of an iterative process to find capacitor bank energy target .....	43
3.4	Contact line model .....	44
3.5	Accelerating contact line length, a) description b) computing function .....	46
3.6	Tram speed modes .....	48
3.7	Tram tractive effort, braking effort, and running resistance curves.....	49
3.8	Tram general power flow diagram .....	54
3.9	Tram power demand diagram.....	55

## LIST OF FIGURES (Continued)

Figure	Page
3.10 Power dispatcher inputs and outputs .....	57
3.11 Power dispatcher modes a) cap-ACL-Tram system b) cap-Tram system .....	58
3.12 Power flows in PM-Dwell .....	59
3.13 Power flows in PM-ACL (applicable only for a cap-ACL-Tram).....	61
3.14 Powers flows in PM-Autonomous .....	62
4.1 Tram route used in the study a) route profile, b) gradient.....	65
4.2 Trams' speed profile used in the study.....	66
4.3 Capacitor bank echoed input for a cap-Tram.....	67
4.4 Tram echoed input for a cap-Tram.....	68
4.5 Tractive effort and speed profile results for a cap-Tram .....	69
4.6 Tram power demand, power from contact line (charging bar), and power from capacitor bank results for a cap-Tram.....	70
4.7 Capacitor bank SOE, voltage, and current results for a cap-Tram.....	71
4.8 Distance travelled, net energy consumption, and capacitor bank state of charge results for a cap-Tram .....	72
4.9 Capacitor bank echoed input for a cap-ACL-Tram .....	73
4.10 Tram echoed input for a cap-ACL-Tram .....	74
4.11 Tractive effort and speed profile results for a cap-ACL-Tram.....	75
4.12 Power demand, power from contact line (ACL), and power from capacitor bank results for a cap-ACL-Tram .....	76
4.13 Capacitor bank SOE, voltage, and current results for a cap-ACL-Tram .....	77
4.14 Distance travelled, net energy consumption, and capacitor bank SOE results for a cap-ACL-Tram.....	77
4.15 Effect of gradient on power and current demand (cap-ACL-Tram).....	80

## SYMBOLS AND ABBREVIATIONS

- $\beta_{cb}$  = Capacitor bank state of energy.
- $\beta_{cb}^{arv}$  = Arrival capacitor bank state of energy ( $\beta_{cb}$  when a tram arrives at a station).
- $\beta_{cb}^{dep}$  = Departure capacitor bank state of energy ( $\beta_{cb}$  when a tram leaves a station).
- $\Delta E_{cb}$  = Change in energy stored in a capacitor bank [kWh]
- $\Delta t$  = Simulation step time interval (Change in time from  $i$  to  $i + 1$ ) [s]
- ACL = Accelerating contact line
- APU = Auxiliary power unit
- $C_{cb}$  = Capacitance of a capacitor bank [F]
- $C_{cm}$  = Capacitance of a capacitor module [F]
- ESC = Energy storage capacity
- ESD = Energy storage device
- ESR = Equivalent series resistance
- $E_{cb}^{dw}$  = Energy from capacitor bank during dwell [kWh]
- $E_{cl}^{dw}$  = Energy from contact line during dwell [kWh]
- $E_{cb}^{tr}$  = Net energy from capacitor bank during interstation travel [kWh]
- $E_{cl}^{tr}$  = Energy from contact line during interstation travel [kWh]
- $F_{acc}$  = Acceleration force [kN]
- $F_{curv}$  = Curvature resistance force [kN]

## SYMBOLS AND ABBREVIATIONS (Continued)

$F_{frdr}$	=	Frictional drag force [kN]
$F_{grad}$	=	Gradient force [kN]
$F_{trt}$	=	Tractive effort force [kN]
$\tau_{hs}$	=	A constant used to convert hours to seconds ( $\tau_{hs} = 3600$ )
$\tau_{sh}$	=	A reciprocal of $\tau_{hs}$ used to convert seconds to hours
$i$	=	Simulation step index number. $i = 1, 2, 3, \dots, n_i$
$k$	=	Interstation section index number
$n_{cm}$	=	Total number of capacitor modules
$n_{cms}$	=	Number of capacitor modules in series
$n_i$	=	Total number of simulation steps
$n_{st}$	=	Total number of stopping stations
$P_{ax}$	=	Average tram auxiliary power demand (power injected into APU) [kW]
$P_{cb}$	=	Power from capacitor bank, at capacitor bank terminals [kW]
$P_{cbls}$	=	Power loss in a capacitor bank due to $r_{cb}$ [kW]
$P_{cl}$	=	Power from contact line at a point of contact with tram current collector [kW]
$P_{tr}$	=	Tram tractive power demand [kW]
$P_{dm}$	=	Tram total power demand [kW]
$r_{cb}$	=	Capacitor bank equivalent series resistance [ $\Omega$ ]
$r_{mcl}$	=	Contact line resistance per meter [ $\Omega.m^{-1}$ ]
$r_{sb}$	=	Substation resistance [ $\Omega$ ]

## SYMBOLS AND ABBREVIATIONS (Continued)

$s$	= Tram distance from a starting station [m]
SOE	= State of energy
$s_{sb}$	= Tram distance from a feeding substation [m]
$T_{bs}$	= Travel time between two successive stations ( $t_p - t_s$ )
$T_{bsd}$	= $T_{bs}$ plus dwell time
$T_{cmd}$	= Cumulative $T_{bsd}$
$T_{jn}$	= Journey time
$t_p$	= Time at which a tram stops at the next station
$t_s$	= Time at which a tram leaves a station
$v$	= Tram speed [ $m \cdot s^{-1}$ ]
$V_{cb}$	= Capacitor bank terminal voltage [V]
$V_{cbo}$	= Capacitor bank no-load voltage [V]
$V_{cm}^{rated}$	= Capacitor module rated voltage [V]
$V_{cb}^{rated}$	= Capacitor bank rated voltage [V]
$V_{cb-cv}^{min}$	= Converter minimum input voltage limit on capacitor bank side [V]
$V_{cb-cv}^{max}$	= Converter maximum input voltage limit on capacitor bank side [V]
$V_{cl}$	= Contact line voltage at point of contact with tram current collector [V]
$V_{clo}$	= Contact line no-load voltage [V]. $V_{clo} = V_{sbo}$ for a given route section
$V_{sb}$	= Substation voltage [V]
$V_{sbo}$	= Substation no-load voltage [V]



# CHAPTER I

## INTRODUCTION

### 1.1 Background

With the growing population and economy, mobility demand in urban areas is on the rise, and so is the resulting traffic congestion and air pollution. Safe, reliable, comfortable, traffic efficient, economical, and environmentally friendly means of transportation have always been a constant goal of city authorities (Mwambeleko and Kulworawanichpong, 2017) and (Mwambeleko, 2015).

Trams and light rail vehicles (LVRs) have proven to be one of the best solutions to urban mobility challenges. Thanks to their high passenger capacity and low energy consumption per passenger-kilometer. Rail transport is characterized by the guided movement of steel wheels on steel rails. The metal-to-metal contact that has considerably low rolling resistance (Mwambeleko, 2015).

Today's railroad vehicles can be driven by diesel-powered Internal Combustion Engines (ICEs), electric traction motors, or the combination of the two. Electric traction is not only more efficient and environmentally friendly than diesel traction, but also more comfortable (due to little noise and vibration) and more economical (due to low maintenance cost) (Mwambeleko, 2015).

#### 1.1.1 The beauty of electric traction

The driving engine of an electric traction system is an Electric Traction Motor (ETM), whereas the driving engine of a non-electric traction (mainly diesel traction, for heavy vehicles) system is an Internal Combustion Engine (ICE). Compared to an ICE, an electric traction motor has several significant advantages: -

- i. efficiency of an ETM is more than twice the efficiency of an ICE. With frequent stops, which is a characteristic of urban transport system, the ICE highly inefficient,

- ii. electric traction motor has considerably lower maintenance cost and lower downtime per maintenance, mainly due to less frequent maintenance requirement and easy to maintain,
- iii. electric traction motor has higher power to weight ratio than that of an ICE,
- iv. electric traction motor has higher acceleration capability than an ICE,
- v. electric traction motor can recover braking energy (can take a generator role during braking), which means an increase in energy efficiency and decrease in maintenance cost of braking shoes, and
- vi. electric motor operates with less vibration which means less track damage, and increased ride comfort.

It is interesting to note that, except for regenerative braking and less vibration, the advantages of an ETM over an ICE are very similar to the advantages that an ICE had over a steam engine (Mwambeleko, 2015) and (Mwambeleko and Kulworawanichpong, 2017).

In addition to the advantages of an ETM over an ICE, in many countries, electricity is more economical than diesel. Moreover, electricity can be produced from environmentally friendly and sustainable sources such as hydro, wind, and solar, and even if electricity is produced from sources such as coal and natural gas, emission level per kilowatt-hour output from such sources at a power plant is much lower than that of an ICEs installed in a vehicle (Mwambeleko, 2015).

### **1.1.2 The need for on-board energy storage**

Despite of all the benefits of electric traction, some railway routes are either partially electrified or not electrified at all, for reasons such as: -

- i. electrification cost,
- ii. electrification complexity (difficulty and safety issues), and
- iii. visual impact (aesthetic reasons).

Electrification cost is particularly true for lightly used routes. That is, routes with not enough density of traffic movement to justify capital and maintenance

costs (Mwambekeko, Hayasaka, and Kulworawanichpong, 2020) and (Mwambekeko, 2015).

Electrification complexity is true for routes that are difficult to electrify such as crossing routes (where two or more railways cross), routes passing under bridges (or in tunnels) with not enough clearance and, routes with not enough right of way. Electrification difficulty and cost often come bundled when trying to electrify old routes which were constructed without electrification consideration (Mwambekeko, Hayasaka, and Kulworawanichpong, 2020).

Visual impact is particularly true for routes passing through historical sites and city centers. For aesthetic reasons, in some areas, catenaries (overhead contact lines) are out of the question (Mwambekeko, Hayasaka, and Kulworawanichpong, 2020) and (Mwambekeko, 2015).

Under such circumstances (when a route cannot be fully electrified), On-Board Energy Storage Devices (OBESDs) such as batteries and supercapacitors are often used, as depicted in Figure 1.1. Aside from supplying tram power demand on non-electrified section(s), the OBESDs come with an added benefit, which is the ability to store regenerative braking energy (Shiraki, Tokito, Yokozutsumi, 2015), (Mwambekeko, 2015), (Mwambekeko, Hayasaka, and Kulworawanichpong, 2020), and (Wang, et al., 2020).

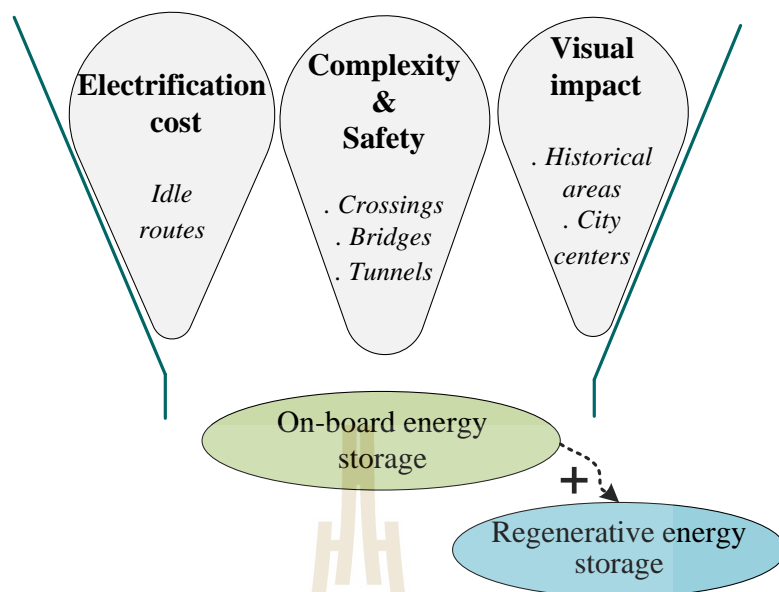


Figure 1.1 Reasons and advantages of on-board energy storage

### 1.1.3 The supercapacitor powered tram

Recently a tram powered solely by supercapacitors shown in Figure 1.2 rolled out in China. The four cars tram is 36.5 meters long, has a maximum speed of 70 km/h, and a capacity of 380 passengers. The supercapacitor bank is fully recharged at each stopping station within 30 seconds as passengers board and deboard, giving the tram an autonomy to the next stop (Saracco, 2016) and (Barrow, 2014).



**Figure 1.2** Supercapacitor tram unveiled in China (railjournal.com, Barrow, 2014)

Having low energy density, several supercapacitor modules are needed to store enough energy to move a tram from one station (charging point) to the next. This imposes cost challenges given that supercapacitors are costly. A Maxwell 125 V, 63 F supercapacitor modules costs around 5,000 USD (Mouser Electronics, Inc., 2018) and (Arrow Electronics, Inc, 2018). Moreover, increasing the number of supercapacitor modules increases tram weight and consequently increasing energy consumption.

#### 1.1.4 Tram tractive energy demand

Rail vehicles are characterized by high inertia and low rolling friction. The former accounts for high energy consumption during acceleration, the latter accounts for low energy consumption during cruising, and the two combined accounts for the ability to coast a long distance and high regenerative braking recuperation. Trams and LRVs operating in urban areas are characterized by frequent stops (short distances between stations) and low speed (about 40 kph to 50 kph). A tram consumes high energy during acceleration (due to inertia resistance). Energy demand drops significantly during cruising as the inertia resistance is out of the equation. During coasting, and braking, tractive energy demand is zero, the only energy needed is to supply auxiliary loads. General tram speed profile and its mapping to energy demand

are presented in Figure 1.3 (Mwambeleko, Kulworawanichpong, and Greyson, 2015), (Mwambeleko and Kulworawanichpong, 2017), and (Mwambeleko, Hayasaka, and Kulworawanichpong, 2020).

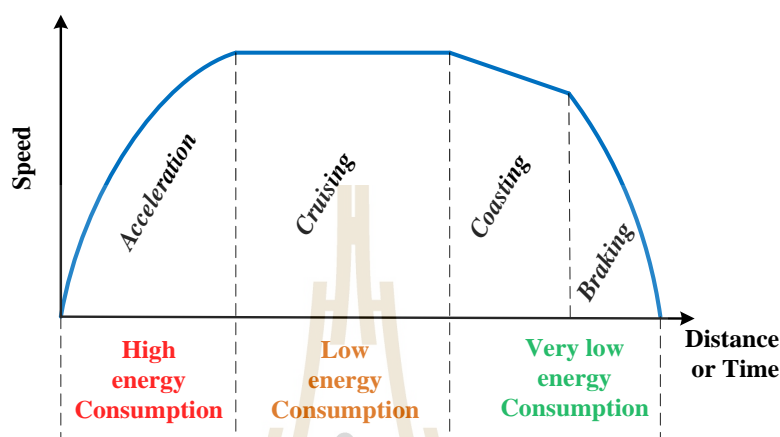


Figure 1.3 Tram speed profile and energy consumption

#### 1.1.5 The proposed idea

Accelerating Contact Lines (ACLs) which are short extension of existing charging feeders are proposed in the study. With ACLs and OBESD hybrid tram system, high energy demand during acceleration is supplied by an ACL, the rest of the energy demand (after acceleration to the next station) is supplied by a small size OBESD as depicted in Figure 1.4 through Figure 1.6 (Mwambeleko, Hayasaka, and Kulworawanichpong, 2020).



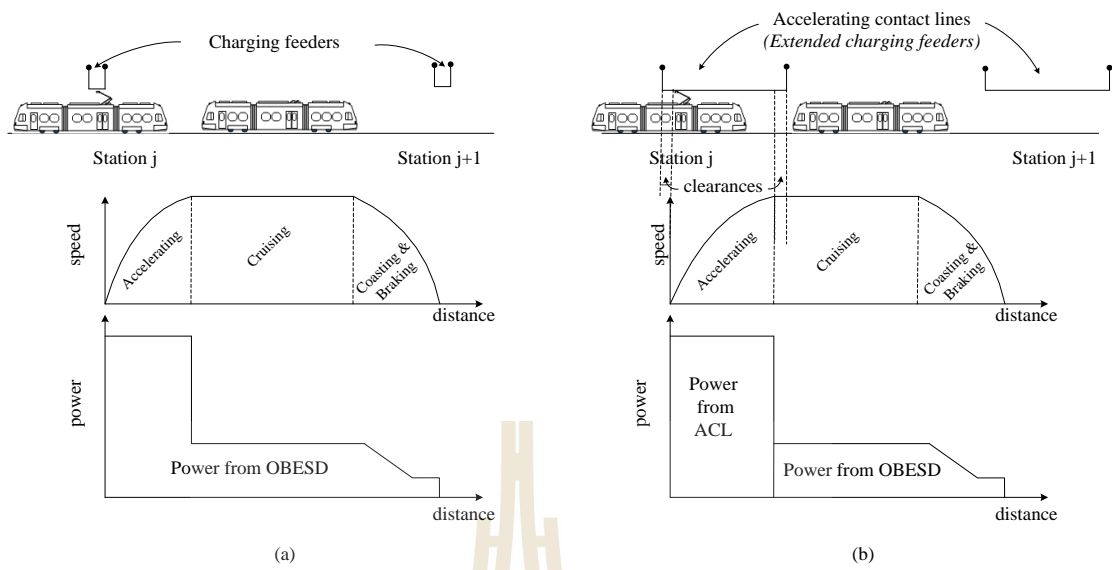


Figure 1.4 Tram systems a) conventional (cap-Tram) b) proposed (cap-ACL-Tram)

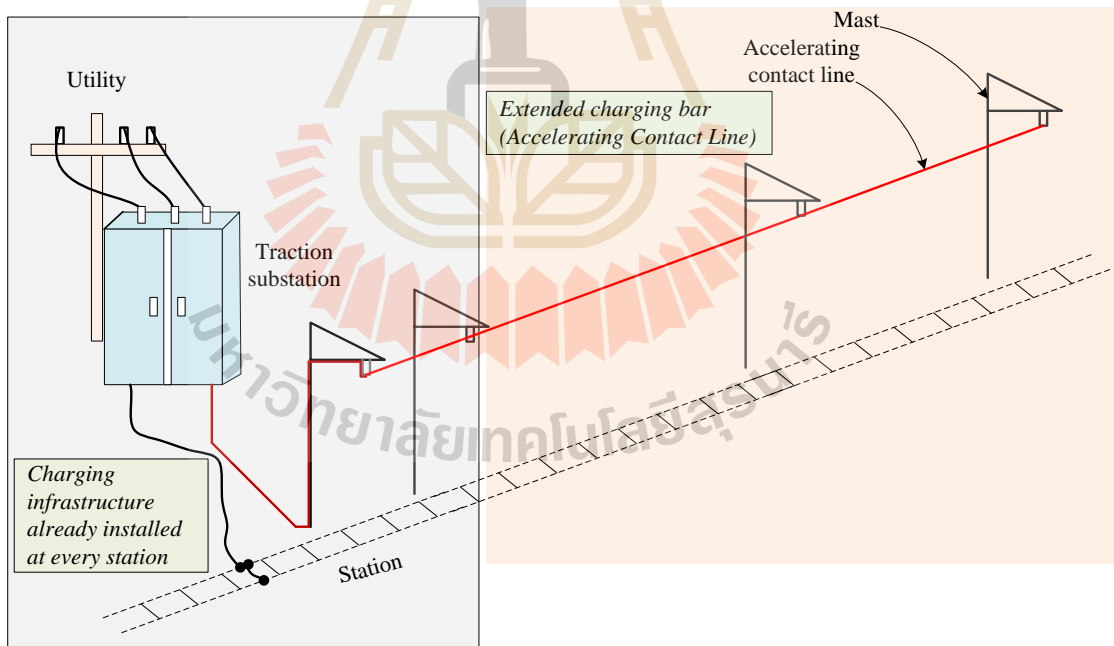


Figure 1.5 Accelerating contact line as an extension of a charging bar

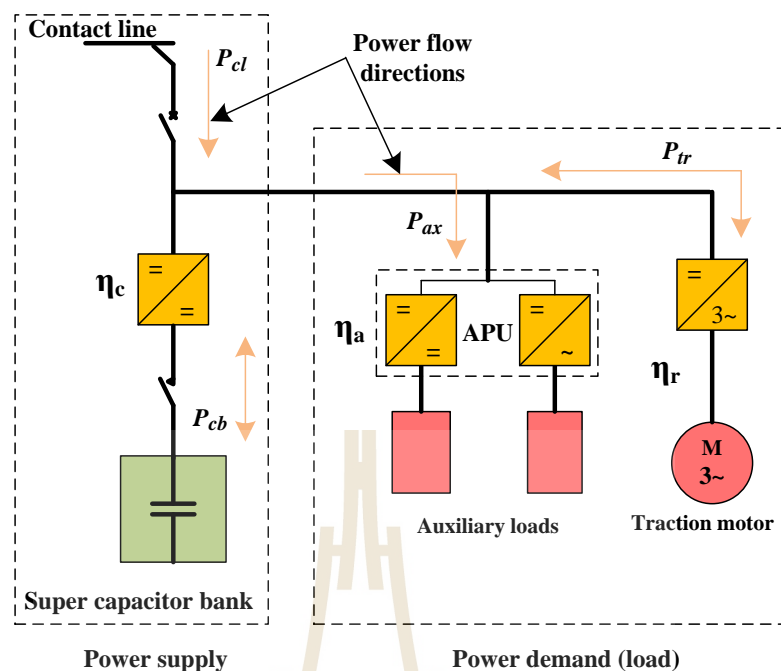


Figure 1.6 Block diagram of a supercapacitor and contact line tram system

## 1.2 Problem definition

Electrified tram systems are highly recommended for urban mass transport due to their efficiency, cost effectiveness, and environmental friendliness. However, attributed to electrification cost (or difficulty) and aesthetic concerns, some railway routes are either partly electrified, or not electrified at all. This is true for i) routes with low traffic movement that cannot justify electrification cost, ii) routes that are difficult to electrify for reasons such as not enough right of way, not enough clearance in a tunnel or under a bridge, and presence of level crossover(s), and iii) routes passing through historical areas and city squares (Mwambeleko, 2015).

Under such circumstances, trams and LRVs are often equipped with OBESDs. The OBESDs are not only costly, but they also increase vehicle weight. Therefore, the idea of accelerating contact lines is introduced to reduce the required size of the OBESD. A layered view of a problem definition is depicted in Figure 1.7.

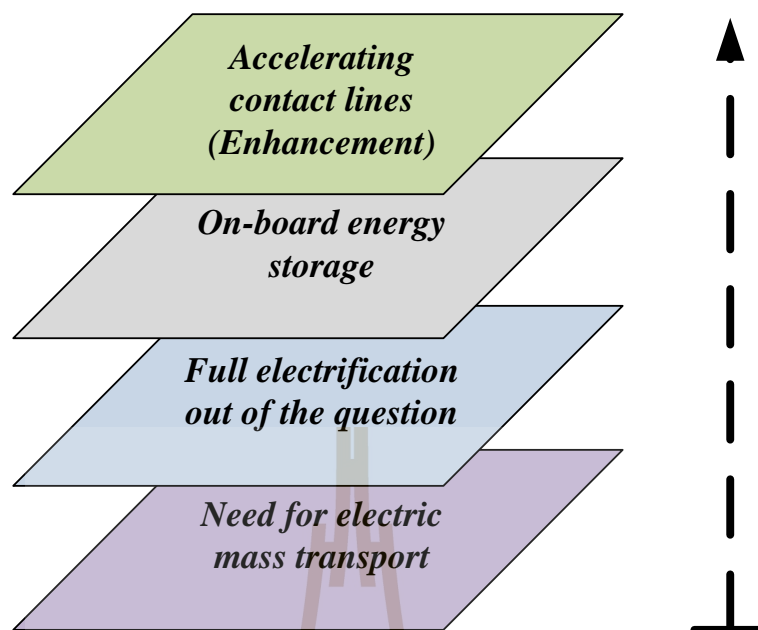


Figure 1.7 Layered view of a problem definition

### 1.3 Research motivation

Trams and LRVs play a significant role addressing urban mobility challenges, fuel efficiency and subsequently environmental concerns. Electric trains are much more efficient, cost effective and environmentally friendly than the conventional diesel trains. For reasons such as electrification cost and visual impacts some railway routes (or route sections) are not electrified. Trams operation on those routes are often equipped with OBESDs. Thanks to technological advancements, the cost of OBESDs is decreasing while the performance is increasing. Subsequently, electric vehicles are increasingly being manufactured. In most of electric buses, the capacity of OBESD is of the order of hundreds of kWh. Interestingly, a tram having low coefficient of rolling friction, consumes less energy per passenger kilometer than a bus (Mwambeleko, 2015) and (Mwambeleko and Kulworawanichpong, 2017). Recently, a concept of supercapacitor tram came to live, supercapacitor powered tram rolled out in China. Supercapacitors have high power density but, they have low energy density and are costly. They need to be recharged at every stopping station. Low energy density means many supercapacitor modules are needed to move a tram from one station to the

next, and since they are costly, this imposes cost challenges (Saracco, 2016) and (Barrow, 2014). Owing to their high inertial, trams and LRVs consume high energy during acceleration. During cruising the energy demand is low, thanks to the low rolling friction. During coasting and braking, energy demand is very low. Introducing accelerating contact lines by just extending the existing charging bar means, the high energy during acceleration is supplied from the contact line and thus, the size and cost of the OBESD (supercapacitor bank in this study) is reduced. Moreover, reducing the size of the OBESD, reduces vehicle weight and consequently energy consumption (Mwambeleko, Kulworawanichpong, and Greyson, 2015) and (Mwambeleko, Hayasaka, and Kulworawanichpong, 2020).

#### 1.4 Research objective

The main objective of the research is to reduce size and subsequently cost and weight of OBESD required for trams (supercapacitor powered trams) operating on non-electrified urban railway routes, taking into account visual impact concerns. Accelerating contact lines (ACLs) and on-board energy storage (OBES) hybrid system is introduced and, supercapacitor powered tram system is used as a case study.

To achieve the main objective the research work is divided into the following subobjectives: -

- i. To establish speed profile for a given route.
- ii. To model a tram powered solely by on-board supercapacitors (cap\_Train) and a hybrid tram powered on-board supercapacitors and ACLs (cap\_ACL\_Train), and then simulate them.
- iii. To analyze by how much the proposed tram (cap\_ACL\_Train) system reduces size and cost of the required OBESD and, tram energy consumption.

## 1.5 Methodology

Aiming at enhancing supercapacitor powered tram system (reducing the required size of the onboard supercapacitor bank) using ACLs; tram data, supercapacitor data, and route data are acquired and prepared for simulation. With the available literature, supercapacitor powered tram modeling is done using MATLAB. Tram movement is simulated and, the results are analyzed as to what extent the ACLs reduces required size of on-board supercapacitor bank.

## 1.6 Research assumptions

The following assumptions have been made in this study: -

- i. Charging infrastructure is already installed at each stopping station as required for a supercapacitor powered tram.
- ii. Contact line system is capable of supplying tram system maximum power demand.
- iii. Tram tractive effort is continuous.

## 1.7 Scope and limitations of the study

Power loss and voltage drop across ACL is not of interest in this study, the ACL is very short (just 150 m) and only one tram will be drawing power from an ACL at a time. With low line resistance (such as  $170 \text{ m}\Omega/\text{km}$ ), there will be just a little power loss and voltage drop across the ACL, which can be neglected without noticeable effect.

Tram speed profile generation (optimization) is out of scope of this study for two reasons: -

- i. to avoid idea “clouding”. The focus of this work is to present the new ACL idea in tram and light rail urban systems and,
- ii. as long as a tram accelerates fast when it is in ACL (or in power mode ACL, to be explained in Chapter II), any (feasible) speed profile after that will work fine. The proposed system does not necessarily need speed profile to be optimized, what is important is high acceleration when a tram is leaving a station.

## 1.8 Expected benefits

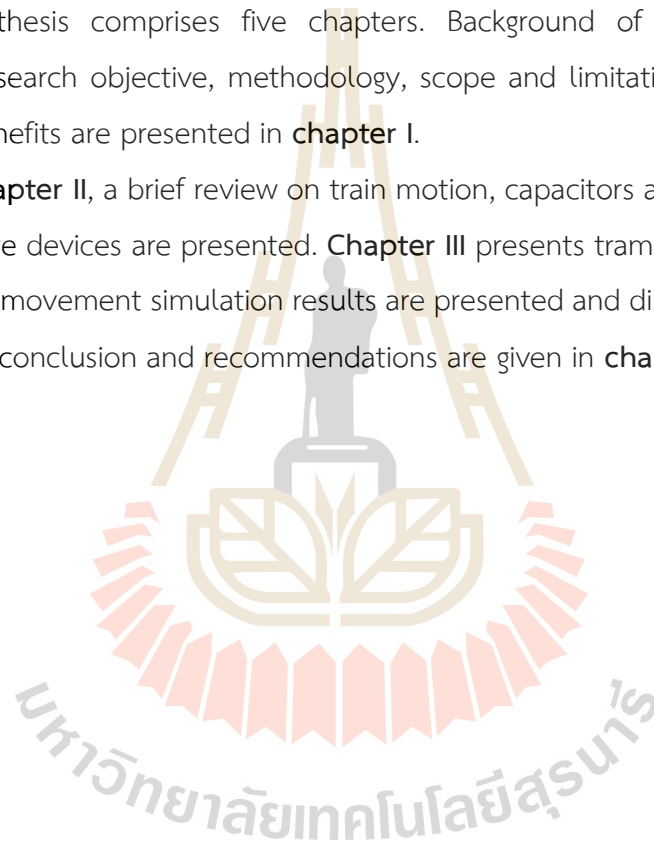
Results from this research work are expected to be a great help and reference to policy makers, city authorities, railway operators, tram and LRV manufacturers and, other stakeholders interested in having electric trams and LRVs in urban areas with low operating cost and visual impact.

## 1.9 Organization of the thesis

The thesis comprises five chapters. Background of the study, problem definition, research objective, methodology, scope and limitation, assumptions and, expected benefits are presented in **chapter I**.

In **chapter II**, a brief review on train motion, capacitors and supercapacitors as energy storage devices are presented. **Chapter III** presents tram system modelling.

Tram movement simulation results are presented and discussed in **chapter IV**, and finally a conclusion and recommendations are given in **chapter V**.





## CHAPTER II

### BRIEF REVIEW

#### 2.1 Introduction

Electrified public transport systems such as trams and Light Rail Vehicles (LRVs) play a significant role in providing green commuter transport services in cities. Traffic congestion and urban air pollution is a concern to city authorities. Railway operators would like to reduce travel cost and time. Realizing the benefit of electric traction, trams and LRVs operating on routes that are not fully electrified are often equipped with OBESDs such as supercapacitors (Mwambeleko, 2015).

Given their high inertial, low rolling friction, and the nature of their operation (frequent stops and low speed), trams present an interesting power/energy demand profile. During acceleration, power demand is considerably high. However, thereafter when no power is drained to change tram inertial, the power demand drops significantly. Different power sources hybrids have been proposed for tram drive. One of them is Accelerating Contact Lines (ACLs) and OBESD hybrid system (Mwambeleko, Hayasaka, and Kulworawanichpong, 2020).

In this chapter, a brief literature review on OBESD, ACL, supercapacitors, and tram movement is presented.

#### 2.2 Energy storage technologies in LRVs

Owing to the significant technological advancements in Energy Storage Devices (ESDs) over the past two decades, Light Rail Vehicles (LRVs) with OBESDs have attracted the attention of several researchers, companies, and authorities. Common energy storage technologies currently used in LRVs include batteries (Lithium-ion batteries in particular), supercapacitors, flywheels, and fuel cells. Among these, batteries and supercapacitors are the most common. Compared to batteries, supercapacitors have high power densities but low energy densities, they can deliver and absorb high power but cannot store high energy per unit mass (or volume) as batteries (Arboleya P,

Bidaguren P, and Armendariz U, 2016), (Iwase, et al., 2015) (Shiraki, Tokito, and Yokozutsumi, 2015) and (Wang, et al., 2020).

On account of their high-power density, supercapacitors located either on ground (trackside) or inside a vehicle (on-board) are employed to reduce peak power, and to increase voltage stability and energy efficiency. That is done by storing braking energy when a vehicle brakes and supplying it back when a vehicle starts accelerates (Barrero, Mierlo, and Tackoen, 2008) and (Sumpavakup, Ratniyomchai, and Kulworawanichpong, 2017).

Supercapacitors are sometimes hybridized with batteries particularly for an autonomous On-Board Energy Storage System (OBESS) since the two have complimenting characteristics on energy and power densities (Wang, et al., 2020)

Utilizing Li-ion batteries, some railway operators such as JR East, JR West, and JR Kyushu Japanese railway operators have been replacing Diesel Multiple Units (DMUs) with battery and catenary hybrid trams. Battery-powered rail vehicles (replacement of DMU with battery-powered vehicles) dates back to 1950s (Mwambeleko, Hayasaka, and Kulworawanichpong, 2020).

Until very recently (within the decade), light railway vehicles powered entirely by on-board supercapacitors have not been popular. The main reason is the fact that currently, supercapacitor technology suffers from low energy density (Wang Y, Yang Z, and Li F, 2018) and (Saracco, 2016)

### **2.3 Accelerating contact lines, previous works**

An ACL is a short contact line extending from a tram stopping station. Its main use is to supply power to a tram during acceleration (as the tram departs from a station, accelerating to the desired speed). Therefore, relieving the OBESD from supplying the high acceleration power. To reduce the required size of OBESD in trams, the ACL concept was introduced by Mwambeleko and Kulworawanichpong. Lithium titanate battery pack was used as an OBESD (Mwambeleko and Kulworawanichpong, 2017).

Compared to a tram powered solely by battery, a battery-ACL (BACL) tram system (with a total electrified distance of 1.8 km out of a 25 km route) reduced the

battery pack size by 62.5%. Compared to a conventional battery-contact line tram system having 12.2 km electrified, the BACL showed equivalently performance (Mwambeleko, Hayasaka and Kulworawanichpong, 2020).

If there already is a charging infrastructure at a tram station, then the ACL can be realized by just extending the charging bar (or feeder). Such a modification will increase the utilization of the charging infrastructure and reduce the required size and cost of the OBESD (Mwambeleko and Kulworawanichpong, 2017) and (Mwambeleko, Hayasaka and Kulworawanichpong, 2020).

If an ACL system is installed at a station where there was no charging infrastructure, it will act as a charging point to rail vehicles that don't have the capability to draw power while moving (Mwambeleko and Kulworawanichpong, 2017) and (Mwambeleko, Hayasaka and Kulworawanichpong, 2020).

## 2.4 Supercapacitors

A capacitor comprises two conducting plates separated by a dielectric. Applying a DC voltage across a capacitor, charges the capacitor by accumulating opposite charges to the two conduction plates. A dielectric between the plates, keeps the opposite charges separated, creating an electric field by which capacitors store energy. The ratio of accumulated charge to the applied voltage is called capacitance. It is proportional to the surface area of the conducting plates and inversely proportional to the distance between the plates (Raghavendra, et al., 2020) and (Moghbeli, Hajisadeghian, and Asadi, 2016).

As the name suggests, a supercapacitor is a general term referring to a capacitor with much higher capacitance than a conventional capacitor. Consequently, the former has much higher energy density than the latter. Thanks to its high surface area, and small distance between conducting plates. Thus, a supercapacitor can technically be considered (modeled) just like a conventional capacitor, the only difference being capacitance value. In this work therefore, the terms capacitor and supercapacitor are used interchangeably (Moghbeli, Hajisadeghian, and Asadi, 2016).

Supercapacitors are used in many applications to store electrical energy and supply it on demand. The applications range from voltage stabilization (buffer), backup

system, to autonomous on-board energy source (Barrero, Mierlo, and Tackoen, 2008) and (Wang, Yang, and Li, 2018).

#### 2.4.1 Capacitor energy and voltage

Energy stored in a capacitor is proportional to its capacitance and square of the voltage difference between capacitor conducting plates (terminals), as expressed in Equation (2.1) (Wang, Guo, Xu, Wu, and Lin, 2019).

$$E = \frac{1}{2} C \times V^2 \times \tau_{sh} \Rightarrow V = \sqrt{\frac{2E}{\tau_{sh} C}} \quad (2.1)$$

Where,  $E$  is energy stored in a capacitor (Wh),  $C$  is capacitor capacitance (F),  $V$  is voltage difference between capacitor terminals (V), and  $\tau_{sh}$  is a constant used to convert seconds to hours so as to convert energy from watt-second to watt-hour.

From Equation (2.1) it can be seen that, unlike batteries, capacitor voltage varies *widely* with the amount of energy stored in it (it's state of energy). If energy stored in a capacitor decreases to 25% of the full charge energy, capacitor voltage decreases to 50% of the full charge voltage. This is a substantial voltage variation. Thus, capacitor banks are usually used with (connected to) DC-DC converters (Wang, et al., 2019).

Since voltage converters have a limited acceptable input voltage range, capacitor minimum voltage is normally constrained such that the voltage range is acceptable. Moreover, for a given power demand, low voltage necessitates high current. A tram system (switching converters, circuit breakers, and cables) capable to handle high current may prove to be uneconomical (Golchoubian and Azad, 2017).

If a capacitor is considered fully charged at rated voltage  $V_{rated}$  (which is normally the case, and it is so done in this study), then given capacitor minimum voltage limit  $V_{min}$ , energy harvestable  $E_{harv}$  from a fully charged capacitor is as expressed in Equation (2.2) (Wang, et al., 2019) and (Moghbeli, Hajisadeghian, and Asadi, 2016).

$$\boxed{E_{harv} = \frac{1}{2}C(V_{rated}^2 - V_{min}^2)\tau_{sh}} \quad (2.2)$$

Where,  $E_{harv}$  is harvestable energy (Wh),  $C$  is capacitor capacitance (F),  $V_{min}$  is minimum voltage limit (V), and  $\tau_{sh}$  is a constant used to convert seconds to hours.

It follows that, if capacitor minimum voltage is set to half of the rated (full charge) voltage (that is,  $V_{min} = \frac{1}{2}V_{rated}$ ), then energy harvestable  $E_{harv}$  from the capacitor is 75% of the full charge energy  $E_{fc}$ , as expressed in Equation (2.3).

$$\begin{aligned} E_{harv} &= \frac{1}{2}C\left(V_{rated}^2 - \left(\frac{V_{rated}}{2}\right)^2\right)\tau_{sh} \\ &= \frac{1}{2}C\left(V_{rated}^2 - \frac{V_{rated}^2}{4}\right)\tau_{sh} \\ &= \frac{1}{2}C\left(\frac{3}{4}V_{rated}^2\right)\tau_{sh} \\ &= \frac{3}{4}\left(\frac{1}{2}C(V_{rated}^2)\tau_{sh}\right) \end{aligned} \quad (2.3)$$

Substituting  $E_{fc}$  for  $\frac{1}{2}CV_{rated}^2\tau_{sh}$

$$E_{harv} = \frac{3}{4}E_{fc}, \quad V_{min} = \frac{1}{2}V_{rated}$$

Where,  $E_{harv}$  is harvestable energy (Wh),  $E_{fc}$  is energy stored in a capacitor at full charge (Wh),  $C$  is capacitor capacitance (F),  $V_{rated}$  is capacitor rated voltage, which is considered as a full charge voltage (V),  $V_{min}$  is minimum voltage limit (V), and  $\tau_{sh}$  is a constant used to convert seconds to hours.

Generally, harvestable energy  $E_{harv}$  can be derived from capacitor State Of Energy (SOE) which is defined as the ratio of energy stored in a capacitor to capacitor's energy storage capacity (energy stored in a capacitor at full charge) as expressed in Equation (2.4) (Wang, et al., 2019).

$$\beta = \left( \frac{V}{V_{rated}} \right)^2 \Rightarrow \beta_{min} = \left( \frac{V_{min}}{V_{rated}} \right)^2$$

At full charge, capacitor SOE is 1 (100%)

$$E_{harv} = (1 - \beta_{min}) E_{fc}$$

$$E_{harv} = \left( 1 - \left( \frac{V_{min}}{V_{rated}} \right)^2 \right) E_{fc}$$
(2.4)

Where,  $\beta$  is capacitor SOE,  $\beta_{min}$  capacitor minimum SOE limit,  $V_{rated}$  is capacitor rated voltage, which is considered as a full charge voltage (V),  $V_{min}$  is minimum voltage limit (V) and  $E_{fc}$  is energy stored in a capacitor at full charge (capacitor energy storage capacity).

#### 2.4.2 Capacitor bank from capacitor modules

To increase energy storage and power capabilities, several identical capacitors (capacitor cells) as shown in Figure 2.1 are often connected to make a capacitor module as shown in Figure 2.2, and several capacitor modules may then be connected to make a capacitor bank as shown in Figure 2.3.



Figure 2.1 Supercapacitor cells (Maxwell Technologies, Inc, 2021).



Figure 2.2 Supercapacitor modules (Maxwell Technologies, Inc, 2021).

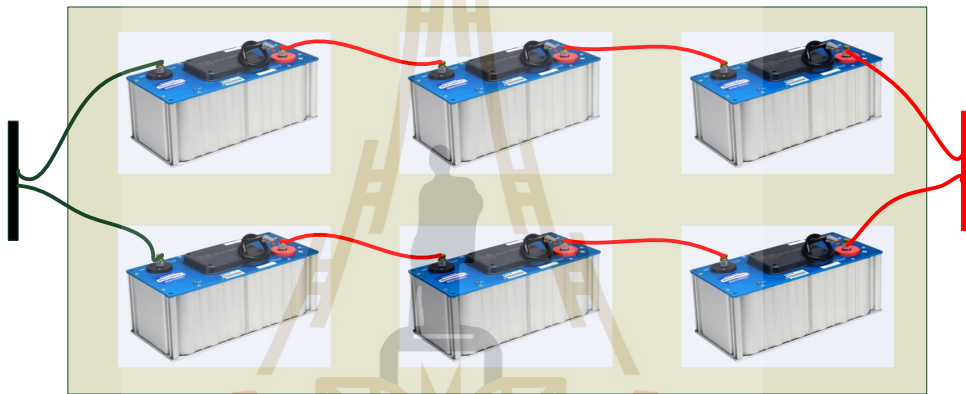






Figure 2.3 Supercapacitor bank from supercapacitor modules.

Examples of supercapacitor modules from various manufacturers are shown in Table 2.1



**Table 2.1** Supercapacitor modules from various manufacturers

	<ul style="list-style-type: none"> <li><input type="checkbox"/> XLR-48 Supercapacitor</li> <li><input type="checkbox"/> 48 V, 166 F</li> </ul> <p>Dimensions (mm): L x W x H: 421 x 177 x 196</p> <p>Mass (kg): 14.7</p> <p>Source: <a href="https://www.eaton.com/us/en-us/catalog/electronic-components/xlr-supercapacitor-module.html">https://www.eaton.com/us/en-us/catalog/electronic-components/xlr-supercapacitor-module.html</a></p>
	<ul style="list-style-type: none"> <li><input type="checkbox"/> SkelMod 51V Supercapacitor</li> <li><input type="checkbox"/> 51V, 177F</li> </ul> <p>Dimensions (mm): L x W x H: 422 x 194 x 198</p> <p>Mass (kg): 16</p> <p>Source: <a href="https://www.skeletontech.com/skelmod-51v-ultracapacitor-module">https://www.skeletontech.com/skelmod-51v-ultracapacitor-module</a></p>
	<ul style="list-style-type: none"> <li><input type="checkbox"/> BMOD0165 P048 C01</li> <li><input type="checkbox"/> 48V, 165F</li> </ul> <p>Dimensions (mm): L x W x H: 418 x 194 x 179</p> <p>Mass (kg): 14.2</p> <p>Source: <a href="https://www.maxwell.com/images/documents/48V_ds_DuraBlue_3000685_4.pdf">https://www.maxwell.com/images/documents/48V_ds_DuraBlue_3000685_4.pdf</a></p>
	<ul style="list-style-type: none"> <li><input type="checkbox"/> BMOD0063 P125 B08</li> <li><input type="checkbox"/> 125V, 63F</li> </ul> <p>Dimensions (mm): L x W x H: 789 x 425 x 313</p> <p>Mass (kg): 63.4</p> <p>Source: <a href="https://www.maxwell.com/images/documents/125V_Module_datasheet.pdf">https://www.maxwell.com/images/documents/125V_Module_datasheet.pdf</a></p>

Capacitance and internal equivalent resistance of a capacitor bank comprising identical capacitor modules connected in series, parallel, and series-parallel are expressed in Equation (2.5) (Maxwell Technologies, 2019) and (Kermani, et al., 2020).



$$\left\{ \begin{array}{l} C_{cb} = \frac{C_{cm}}{n_{cms}} \\ r_{cb} = n_{cms} r_{cm} \end{array} \right., \text{ Series configuration } (n_{ps} = 1)$$

$$\left\{ \begin{array}{l} C_{cb} = n_{ps} C_{cm} \\ r_{cb} = \frac{r_{cm}}{n_{ps}} \end{array} \right., \text{ Parallel configuration } (n_{cms} = 1) \quad (2.5)$$

$$\left\{ \begin{array}{l} C_{cb} = \frac{n_{ps}}{n_{cms}} C_{cm} \\ r_{cb} = \frac{n_{cms}}{n_{ps}} r_{cm} \end{array} \right., \text{ Series-parallel configuration}$$

Where,  $C_{cb}$  and  $C_{cm}$  are capacitor bank and capacitor module capacitances (F) respectively,  $r_{cb}$  and  $r_{cm}$  are internal equivalent resistances (Ohms) of a capacitor bank and capacitor module respectively,  $n_{cms}$  is number of capacitor modules in series, and  $n_{ps}$  is number of parallel strings.

Regardless of how capacitor modules (identical modules) are connected (series, parallel, or series-parallel), the total energy storage capacity of a capacitor bank equals the sum of energy storage capacity of individual capacitor modules.

## 2.5 Supercapacitors versus batteries

Currently, the most common OBESDs are supercapacitors and lithium-ion batteries (Wang, et al., 2020). Among the lithium-ion battery chemistries, lithium titanate is the leading candidate in terms of power density (Liu, et al., 2015). However, compared to supercapacitors, the lithium titanate battery comes far behind, particularly in power density and cycle life.

It is possible to full charge a supercapacitor within 30 seconds, whereas a battery would need around 30 minutes (Sengupta, et al., 2018). Life cycle of a

supercapacitor is in the order of millions, whereas that of a battery is in the order of thousands (Farhadi and Mohammed, 2016).

Except for low energy densities, a supercapacitor exhibits key performance characteristics for an OBESD. Its low energy ratios drawback can be addressed by fast charging at stopping stations. This well suits urban transport systems characterized by short distances between stations (Saracco, 2016) and (Barrow, 2014)..

Performance and life characteristics of a lithium titanate cell from Altairnano, and DuraBlue supercapacitor cell from Maxwell are presented in Table 2.2 and Table 2.3 respectively.

**Table 2.2** Altairnano Lithium Titanate cell (Altairnano, 2021)

Attribute	Value	Unit
<i>Performance characteristics</i>		
Nominal voltage	2.22	V
Capacity typical <sup>1</sup>	66.8	Ah
Typical discharge energy <sup>2</sup>	148	Wh
Internal charge impedance <sup>3</sup>	0.32	mΩ
Internal discharge impedance <sup>3</sup>	0.38	mΩ
Maximum continuous charge/discharge current	500	A
<i>Life characteristics</i>		
Cycle life at 2C charge/discharge, 100% DOD, 25°C <sup>4</sup>	> 25,000	
Cycle life at 2C charge/discharge, 100% DOD, 55°C <sup>4</sup>	> 6,000	
Calendar life at 25°C <sup>5</sup>	25	years
<i>Physical characteristics</i>		
Width x Height x Thickness	256 x 263 x 12.6	mm
Weight	1.81	kg

<sup>1</sup>At 70 Amps, 25°C, CCCV charge

<sup>2</sup>At 70 Amps, 25°C, CCCV discharge

<sup>3</sup>At 10 sec DC pulse, 50% SOC, 25°C

<sup>4</sup>To 80% initial capacity

<sup>5</sup>25°C is the optimal temperature.

**Table 2.3** Maxwell DuraBlue supercapacitor cell (Maxwell, 2019)

Attribute	Value	Unit
<i>Performance characteristics</i>		
Nominal voltage	2.70	V
Capacitance typical	3000	F
Stored energy	3.04	Wh
Equivalent series resistance (ESR)	0.29	m $\Omega$
Maximum continuous charge/discharge current	1900	A
<i>Life characteristics</i>		
Cycle life at 25 <sup>0</sup> C*	1,000,000	
DC life at 25 <sup>0</sup> C, rated voltage*	10	years
Calendar life at 25 <sup>0</sup> C, uncharged*	4	years
<i>Physical characteristics</i>		
Height x Diameter	138 x 60.7	mm
Weight	0.51	kg

\*Capacitance 80% of initial value, ESR 200% of rated value

For the reasons explained above (in this section), this work uses on-board supercapacitor storage instead of battery storage which was used in the previous works. Moreover, cost analysis is done in this study, it is not done in the two previous works (Mwambeleko and Kulworawanichpong, 2017) and (Mwambeleko, Hayasaka and Kulworawanichpong, 2020).

## 2.6 Tram motion

Tram motion can be expressed using Newton's second law of motion and kinematic equations. Generally, when a tram moves from one station to the next, its speed profile consists of four parts namely i) accelerating or motoring, ii) constant speed or cruising, iii) coasting or freewheeling, and iv) braking as shown in Figure 2.4 (Mwambeleko, 2015) and (Mwambeleko and Kulworawanichpong, 2017).

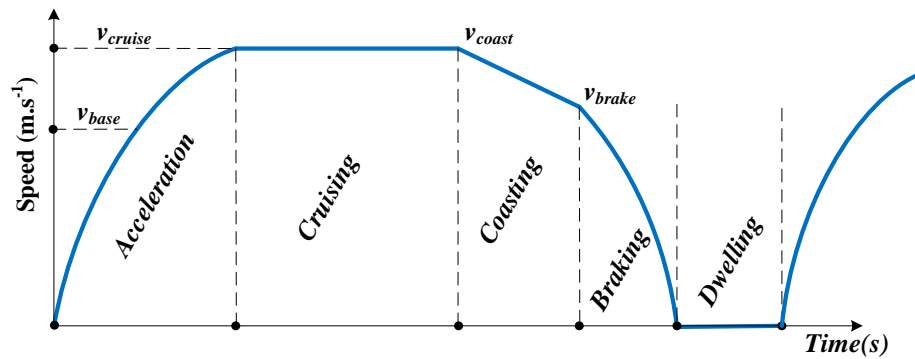


Figure 2.4 General tram speed profile

Normally, when a train starts moving, it accelerates with approximately constant acceleration, using constant (normally maximum) tractive effort to a speed called base speed  $v_{base}$ . From the base speed to cruising (desired) speed  $v_{cruise}$  tractive power is kept constant and tractive effort reduces (as it has to) inversely to speed until it balances resistance forces. To avoid slipping, the tractive effort is always limited to a certain maximum value, depending on the number of driving axels and the adhesion between the driving wheels and the track. Maximum tractive effort is also a function of train speed (Mwambeleko, 2015).

When the tractive effort balances the forces opposing the motion, the train moves with a constant speed (zero acceleration) drawing constant tractive power, this is called cruising mode (Mwambeleko, 2015).

As a technique to minimize tractive energy consumption, before brakes are applied, tractive power is cut off, and the train is left to move with its own kinetic energy, this is called coasting or freewheeling. The train speed starts decreasing on account of resistance to motion. Coasting has long been recognized as one of the techniques to save energy, though it increases interstation run time (Mwambeleko, 2015).

Finally, brakes are applied, and the train is brought to a stop. As with the tractive effort, braking effort is also limited to a maximum allowable value, which is also a function of train speed. Typical tractive effort, braking effort, and resistance force curves are as shown in Figure 2.5, data for these curves have been retrieved from

Rotem tram (using curve fitting), the same data will be used in this study (Mwambeleko, 2015), (ITCgroup, 2014) and (Hyundai Rotem; Hyundai Motor Group, 2014).

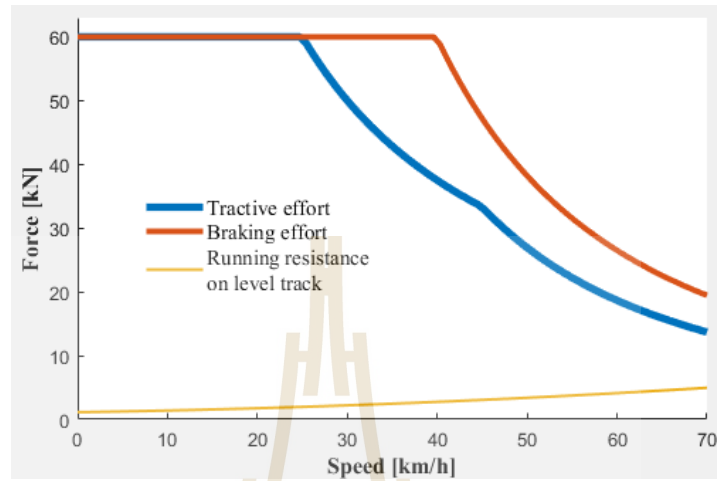


**Figure 2.5** Typical tractive effort, braking effort and resistance force curves

Modern trains use regenerative braking to recapture train's kinetic energy. Some trains just use rheostatic braking, where the braking energy is dissipated in a bank of resistors as heat. As opposed to friction braking dynamic braking (regenerative or rheostatic braking) has proven to minimize maintenance cost of the braking system (Mwambeleko, 2015)

### 2.6.1 Tram longitudinal forces

Tram longitudinal dynamics are due to five main forces, namely i) tractive effort force  $F_{tr}$ , ii) gradient force  $F_{grad}$  iii) frictional drag force  $F_{fdr}$ , iv) curvature resistance force  $F_{curv}$  and, v) acceleration resistance (or inertial) force  $F_{acc}$  as shown in Figure 2.6 (Chymera and Goodman, 2014) and (Nicholson, 2014).

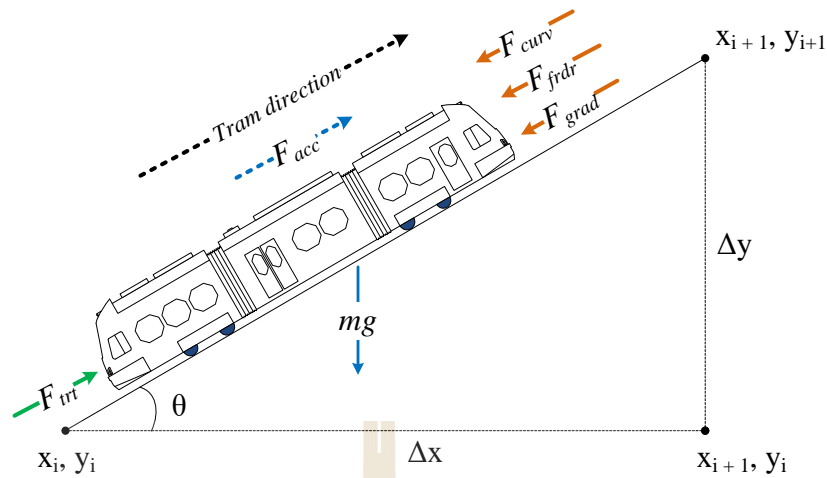


**Figure 2.6** Forces affecting tram longitudinal dynamics

- i) Tractive effort force.

Tractive effort force  $F_{trt}$  is the force applied to move (or brake) a tram. It is positive if it is applied to move the tram, and negative if it is applied to stop (oppose) the tram (Mwambeleko, Kulworawanichpong, and Greyson, 2015).

- ii) Curvature resistance force.

Curvature resistance force  $F_{curv}$  is the force opposing tram motion as the tram goes through a curve (corner). The curvature resistance force is usually very small and thus, ignored (Yihui Wang, 2011), (Ahmadi, Dastfan, and Assili, 2017). (Chymera and Goodman, 2014) and (Nicholson, 2014).

- iii) Frictional-drag Force.

Frictional-drag force  $F_{fldr}$  is the force opposing tram motion due to friction (axle bearing friction and wheel-track friction) and air drag. Wind (wind drag) may be in the same direction or in opposite direction to tram direction. In this work, however, wind effect is neglected. Normally, frictional-drag force (for a particular train) is given using Davis equation as expressed in Equation (2.6) (Nicholson, 2014).

$$F_{fldr} = \begin{cases} A + Bv_{kph} + Cv_{kph}^2 & v \text{ in km/h} \\ A + 3.6Bv + 12.96Cv^2 & v \text{ in m/s} \end{cases} \quad (2.6)$$

Where,  $F_{frdr}$  is frictional drag force (kN),  $A$  and  $B$  are coefficients for static friction (losses at the wheel-rail interface) and dynamic friction (axle bearing losses) respectively and,  $C$  is aerodynamic drag coefficient (Nicholson, 2014).

iv) Gradient Force.

Gradient force  $F_{grad}$  is the force due to route gradient, therefore it can either be positive (opposing tram motion on uphill section) or negative (supporting tram motion on downhill section). With reference to Figure 2.6, gradient force is computed as expressed in Equation (2.7) (Chymera and Goodman, 2014) and (Nicholson, 2014).

$$\begin{aligned} F_{grad} &= mg \sin \theta \\ &= mg \frac{\Delta y}{\sqrt{\Delta y^2 + \Delta x^2}} \end{aligned} \quad (2.7)$$

Where,  $F_{grad}$  is gradient force (N),  $m$  is vehicle (tram) mass (kg),  $g$  is gravitational acceleration ( $m/s^2$ ),  $\theta$  is gradient angle (radian),  $\Delta y$  is change in vertical distance (altitude) (m), and  $\Delta x$  is change in horizontal distance (m).

For small route gradients, Equation (2.7) can be approximated to an easier to compute equation as expressed in Equation (2.8) (Mwambeleko and Kulworawanichpong, 2017).

$$\begin{aligned} F_{grad} &= mg \sin \theta \approx mg \tan \theta \\ &\approx mg \frac{\Delta y}{\Delta x} \end{aligned} \quad (2.8)$$

Where,  $F_{grad}$  is gradient force (N),  $m$  is vehicle (tram) mass (kg),  $g$  is gravitational acceleration ( $m/s^2$ ),  $\theta$  is gradient angle (radian),  $\Delta y$  is change in vertical distance (altitude) (m), and  $\Delta x$  is change in horizontal distance (m).

v) Acceleration Force.

Acceleration force  $F_{acc}$  is a *result* of forces imbalance between tractive effort force and the summation of other (motion-opposing) longitudinal forces.

It is, therefore, the force responsible for tram change of speed. It is expressed in Equation (2.9) (Chymera and Goodman, 2014) and (Nicholson, 2014).

$$F_{acc} = F_{trt} - R$$

$$\boxed{F_{acc} = F_{trt} - (F_{curv} + F_{frdr} + F_{grad})}$$
(2.9)

Where,  $F_{grad}$  is gradient force (N),  $F_{trt}$  is tractive effort force (N),  $R$  is the sum of resistance forces (N),  $F_{curv}$  is curvature resistance force (N),  $F_{frdr}$  is frictional-drag force (N), and  $F_{grad}$  is gradient force (N).

Acceleration force  $F_{acc}$  as a function of tram's speed-change (acceleration) is expressed in Equation (2.10) (Chymera and Goodman, 2014).

$$\left\{ \begin{aligned} F_{acc} &= m_{eff} \frac{v(i+1) - v(i)}{t(i+1) - t(i)} \\ &= m_{eff} \frac{\Delta v}{\Delta t} \\ &= m_{eff} \alpha \end{aligned} \right.$$
(2.10)

Where,  $\Delta v$  is change in tram speed (m/s),  $\Delta t$  is change in time (s),  $m_{eff}$  is effective tram mass (kg) to be explained later,  $\alpha$  is tram acceleration (m/s<sup>2</sup>) and  $F_{acc}$  is acceleration force (N).

When a tram accelerates, the total mass  $m$  ( $m = m_{tare} + m_{load}$ ) is accelerated linearly but the rotating parts such as motor rotors, gear sets, and wheel sets are also accelerated rotationally. It is usual to express this rotational inertia effect as an increase in tram mass expressed as a fraction of the tare weight of the train. Thus, tram effective mass  $m_{eff}$  is given as  $m_{eff} = \lambda m_{tare} + m_{load}$  Where,  $\lambda$  is a rotary allowance, its value varies from 0.05 to 0.15 depending on the number of motored axles, the gear ratio, and the type of car construction. It is magnified by the gear-ratio squared (assuming motors are geared to rotate faster than the wheels, which is



normally the case). If the exact value is unknown, 0.01 is a reasonable assumption (Chymera and Goodman, 2014) and (Nicholson, 2014).

### 2.6.2 Acceleration force during motoring

As previously mentioned, during motoring, tractive effort force is applied to accelerate a tram to the desired cruising speed. There are three scenarios based on which tram acceleration force can be computed: -

- i) speed profile (speed or acceleration at each iteration) is known,
- ii) speed profile is not known; therefore, it has to be generated by providing *proposed(requested)* acceleration value and,
- iii) tractive effort is known, for example if the aim is to accelerate with maximum tractive effort.

For these (the above) three scenarios, acceleration force is computed as expressed in Equation (2.11).

$$F_{acc}(i) = \begin{cases} m_{eff} a(i), & \text{given requested acceleration } a \\ m_{eff} \frac{v(i+1) - v(i)}{Dt}, & \text{given speed profile} \\ F_{irt}(i) - (F_{curv}(i) + F_{frdr}(i) + F_{grad}(i)), & \text{given tractive effort force} \end{cases} \quad (2.11)$$

Where,  $F_{acc}$  is acceleration force (N),  $m_{eff}$  is tram effective mass (kg),  $a$  is requested acceleration ( $m/s^2$ ),  $v$  is speed (m/s),  $Dt$  is change in time (s) from simulation step index  $i$  to  $i+1$ ,  $F_{irt}$  is tractive effort force (N),  $F_{curv}$  is curvature resistance force (N),  $F_{frdr}$  is frictional drag force (N),  $F_{grad}$  is gradient force (N), and  $i$  is simulation step index number.

### 2.6.3 Tractive effort force during cruising

Generally, during cruising the objective is to maintain speed, therefore acceleration force would be zero ( $F_{acc} = 0$ ). That is, tractive effort force  $F_{irt}$  is expressed as in Equation (2.12) (Mwambeleko, 2015) and (Mwambeleko and Kulworawanichpong, 2017).

$$\begin{cases} F_{acc} = F_{trt} - (F_{curv} + F_{frdr} + F_{grad}) \\ \text{Letting } F_{acc} = 0 \\ F_{trt} = F_{curv} + F_{frdr} + F_{grad} \end{cases} \quad (2.12)$$

Where,  $F_{acc}$  is acceleration force (kN),  $F_{trt}$  is tractive effort force (kN),  $F_{curv}$  is curvature resistance force (kN),  $F_{frdr}$  is frictional drag force, and  $F_{grad}$  is gradient force (kN).

However, due to route profile (uphill), maximum tractive effort constraint, and maximum cruising power constraint, constant speed may not be achieved. That is, Equation (2.12) may not hold.

The Equation (2.12) may also not hold on a downslope such that  $F_{curv} + F_{frdr} + F_{grad} < 0$  and a tram is allowed to accelerate, or when tram speed is greater than cruising speed ( $v > v_{cruise}$ ) due to a prior downslope. Consequently, acceleration force  $F_{acc}$  may come into the scene and alter tram speed from the intended cruising speed, as depicted in Figure 2.7.

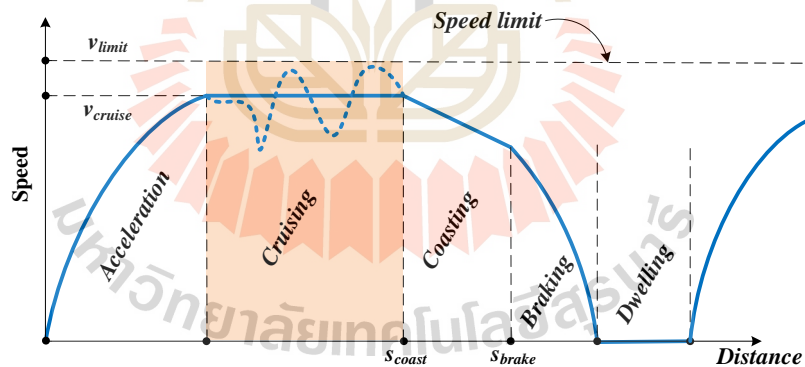


Figure 2.7 Acceleration and speed limit during cruising.

It may also be necessary to apply brakes during cruising on a downhill section with speed limit, or any other section with speed limit less than the cruising speed. In programming implementation, this can be handled by changing operation mode (not speed mode) from cruising mode to braking mode whenever brakes are applied. That is, whenever tractive effort force  $F_{trt}$  is less than zero ( $F_{trt} < 0$ ).

### 2.6.4 Tram forces during coasting

During coasting tram tractive power is cut off. That is, tractive effort force is set to zero  $F_{trt} = 0$ . Thus, the tram moves using its own momentum (kinetic energy) (Mwambeleko, Kulworawanichpong, and Greyson, 2015). Normally, coasting takes place on a flat or a downhill route section. However, in a simulation, if the “tram mover” algorithm (simulator) has no knowledge of the route profile ahead, coasting may also take place on an uphill section.

Acceleration force during coasting is expressed in Equation (2.13). It is clear from the Equation (2.13) that even if there is no tractive effort, if gradient force is negative (down slope), a tram may accelerate (positive acceleration force).

$$\left\{ \begin{array}{l} F_{acc} = F_{trt} - (F_{curv} + F_{frdr} + F_{grad}) \\ \text{Offsetting } F_{trt} \quad (F_{trt} = 0) \\ F_{acc} = -(F_{curv} + F_{frdr} + F_{grad}) \end{array} \right. \quad (2.13)$$

Where,  $F_{acc}$  is acceleration force (kN),  $F_{trt}$  is tractive effort force (kN),  $F_{curv}$  is curvature resistance force (kN),  $F_{frdr}$  is frictional drag force, and  $F_{grad}$  is gradient force (kN).

Though rare, two abnormal scenarios may happen (need to be taken care of) during coasting, namely, i) acceleration and ii) stalling.

- i) Acceleration and speed limitation during coasting: -

Acceleration, and eventually overspeeding may occur due to high and/or prolonged negative gradient (long section with steep downslope). Tram maximum speed in this study is set to 70 kph, which is the vehicle maximum speed. Therefore, during coasting on downhill sections, brakes may be applied to reinforce speed limit as illustrated in Figure 2.8.

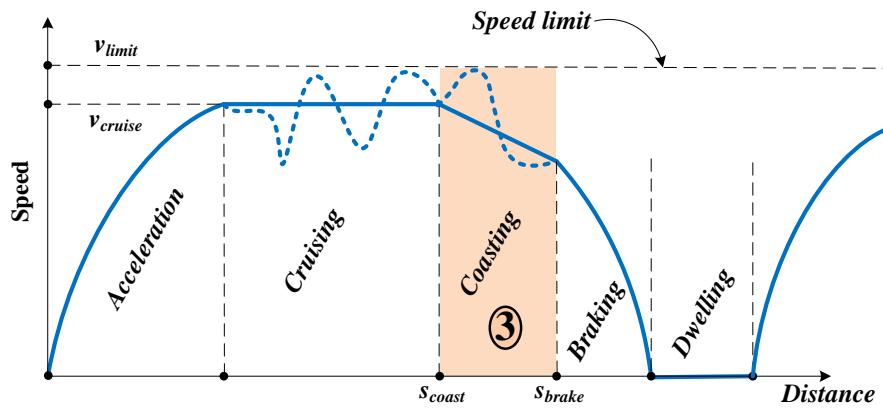


Figure 2.8 Acceleration and speed limit during coasting.

It might be worth mentioning that, when brakes are applied, the braking force appears as negative tractive effort  $-F_{trt}$ .

Force balance and tractive effort (braking) force equation during coasting with brakes applied to limit tram speed is expressed in Equation (2.14).

$$\begin{cases} F_{acc} = F_{trt} - (F_{curv} + F_{frdr} + F_{grad}) \\ \text{Applying brakes to offset } F_{acc} \quad (F_{acc} = 0) \\ F_{trt} = F_{curv} + F_{frdr} + F_{grad} \end{cases} \quad (2.14)$$

Where,  $F_{acc}$  is acceleration force (kN),  $F_{trt}$  is tractive effort force (kN),  $F_{curv}$  is curvature resistance force (kN),  $F_{frdr}$  is frictional drag force, and  $F_{grad}$  is gradient force (kN).

ii) Stalling during coasting: -

Stalling may happen due to prolonged coasting on flat or uphill sections, that is, sections where gradient is greater than or equal to zero ( $F_{grad} \geq 0$ ). In this work, whenever tram speed is less than or equal to zero ( $v \leq 0$ ), away from stopping station, then the tram is considered to have entered stalling mode, and the simulation (trip) is aborted (considered invalid). It is essential therefore, during speed profile generation, to make sure stalling during coasting is avoided. This is done by choosing acceptable coasting points for every interstation section ( $coastingPoint(k)$ ).

### 2.6.5 Tram forces during braking

During braking speed mode, brakes are applied such that a tram will stop smoothly at a stopping station. That is tram speed decreases gradually. Force equation during tram braking is similar to the force equation during acceleration with braking force appearing as negative tractive effort. If speed profile is not known, one technique to calculate braking acceleration is to use critical braking distance as expressed in Equation (2.15) (Chymera and Goodman, 2014).

$$\left\{ \begin{array}{l} \alpha = \frac{-v^2}{2s_{brcr}} \\ F_{acc} = m_{eff}\alpha \\ F_{trt} = F_{acc} + F_{curv} + F_{frdr} + F_{grad} \end{array} \right. \quad (2.15)$$

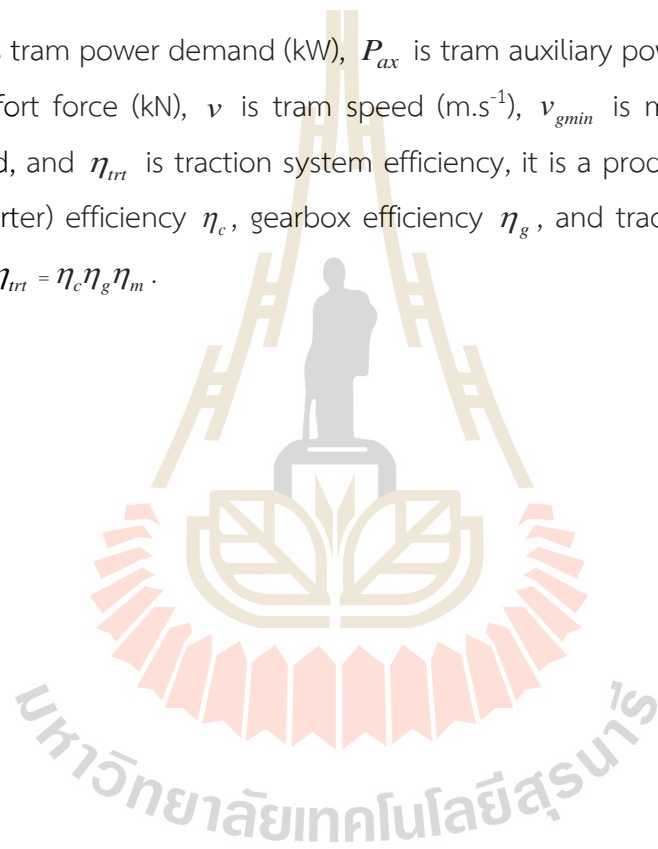
Where,  $\alpha$  is acceleration ( $m/s^2$ ),  $v$  is speed ( $m/s$ ) and,  $s_{brcr}$  is critical braking distance (m). That is, from speed  $v$ , tram speed has to decrease to zero after covering the distance  $s_{brcr}$ .

### 2.6.6 Tram power demand

Given tractive effort force and speed, tram power demand is calculated as a sum of auxiliary power demand  $P_{ax}$  and tractive power demand  $P_{trt}$  which is the product of tractive effort force and speed as expressed in Equation (2.16) (Chymera and Goodman, 2014) and (Mwambeleko, Hayasaka and Kulworawanichpong, 2020).

$$P_{dm} = P_{ax} + \begin{cases} \frac{F_{trt}v}{\eta_{trt}}, & F_{trt} > 0 \\ \eta_{trt}F_{trt}v, & F_{trt} < 0 \text{ and } v \geq v_{gmin} \\ 0 & \text{otherwise} \end{cases} \quad (2.16)$$

Where,  $P_{dm}$  is tram power demand (kW),  $P_{ax}$  is tram auxiliary power demand (kW),  $F_{trt}$  is tractive effort force (kN),  $v$  is tram speed ( $\text{m}\cdot\text{s}^{-1}$ ),  $v_{gmin}$  is minimum regenerative braking speed, and  $\eta_{trt}$  is traction system efficiency, it is a product of traction motor driver (converter) efficiency  $\eta_c$ , gearbox efficiency  $\eta_g$ , and traction motor efficiency  $\eta_m$ . That is,  $\eta_{trt} = \eta_c\eta_g\eta_m$ .



## CHAPTER III

### TRAM SYSTEM MODEL

#### 3.1 Introduction

This chapter presents tram systems models used in the study. The models comprise four main components, namely i) supercapacitor bank model, ii) contact line model, iii) tram movement model and, iv) power dispatch strategy, as presented in

Figure 3.1. It is worth noting that, for a conventional on-board supercapacitor powered tram system, the contact line is just a charging bar (where a tram stops for charging), whereas, for the proposed tram system, it is an accelerating contact line (ACL).

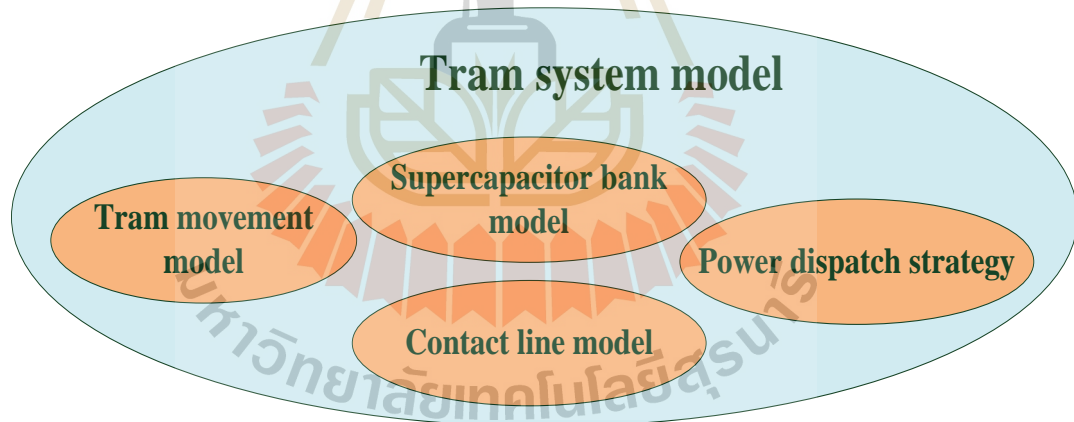


Figure 3.1 Tram system model

### 3.2 Capacitor bank model

A capacitor bank is a series-parallel combination of capacitor modules as explained in chapter II. Therefore, in this study a capacitor bank (CapBank) class is a subclass of a capacitor module (CapModule) class. A capacitor bank is modeled as a voltage source in series with a constant internal resistance as shown in Figure 3.2 (Cheng, Wang, Wei, Lin, and Jia, 2018). Its open-circuit voltage is a function of its state of energy as explained in chapter II

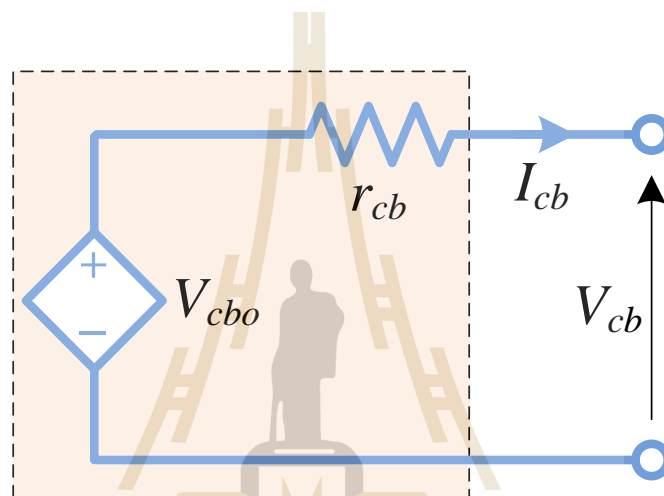


Figure 3.2 Capacitor bank circuit model

#### 3.2.1 Capacitor module constructor

The CapModule constructor can take one to three inputs, which are i) capacitor module data, ii) capacitor module SOE (optional), and iii) a boolean value “setForSim” (optional), i.e., set the object for simulation. Capacitor module data are obtained from manufacturer’s datasheet. A Maxwell 125V, 63F supercapacitor module was used in the study (Maxwell Technologies, 2021).

If capacitor module SOE is given, initial capacitor module voltage  $V_{cb}^{initial}$  is computed using Equation (3.1) (Wang, Guo, Xu, Wu, and Lin, 2019).



$$\begin{cases} \beta_{cb} = \left( \frac{V_{cbo}}{V_{cb}^{fc}} \right)^2 & \Rightarrow V_{cbo} = V_{cb}^{fc} \sqrt{\beta_{cb}} \\ V_{cb}^{initial} = V_{cbo} \end{cases} \quad (3.1)$$

Where,  $\beta_{cb}$ ,  $V_{cbo}$ ,  $V_{cb}^{fc}$ , and  $V_{cb}^{initial}$  are capacitor bank's SOE, no-load (open-circuit) voltage (V), full-charge voltage (V), and initial voltage (V), respectively

If “setForSim” is given as true, storage for power (“powerArray”), current (“currentArray”), SOE (“soeArray”) and voltage (“voltageArray”) will be initiated.

### 3.2.2 Charge-discharge method

A capacitor module (CapModule) class has a chargeDischarge method, which needs one input, power at capacitor bank terminals. Briefly, the method does the following: -

- a) checks if the given power is not beyond maximum power capability,
- b) computes current using instance voltage value,
- c) checks if the computed current is not beyond maximum current capability,
- d) computes change in stored energy using power, current, and internal resistance,
- e) computes the next SoE, and checks if it ranges from 0 to 1, inclusively,
- f) updates array variables, i.e., powerArray, currentArray, soeArray, and voltageArray, and
- g) updates state variables, i.e., soe and voltage

Key expressions/equations encapsulated in the chargeDischarge method of the CapModule class are expressed in Equation (3.2) (Wang, Yang, and Li, 2018), (Cheng, Wang, Wei, Lin, and Jia, 2018) and (Wang, Guo, Xu, Wu, and Lin, 2019)

$$\left\{ \begin{array}{l} I(i) = P(i) / V(i-1) \\ \Delta e = \left( P(i) + (I(i))^2 r_{cb} \right) \Delta t \tau_{sh} \\ \beta_{cb}(i) = \beta_{cb}(i-1) - \frac{\Delta e}{Y_{cb}} \\ V_{cbo}(i) = V_{cb}^{fc} \sqrt{\beta_{cb}(i)} \\ V_{cb}(i) = V_{cbo}(i) - I(i) r_{cb} \end{array} \right. \quad (3.2)$$

Where,  $I$  is current (A),  $P$  is power (W),  $V$  is voltage (V),  $\Delta e$  is change in energy (Watt-hour),  $r_{cb}$  is internal resistance (Ohms),  $\Delta t$  is simulation time step (sec),  $\tau_{sh}$  is a factor used to convert seconds into hours,  $Y_{cb}$  is energy storage capacity (Watt-hour),  $V_{cbo}$  is open-circuit voltage, and  $V_{cb}$  is terminal voltage (V).

The value for simulation time step  $\Delta t$  was set to 0.5. Through trials, it was found to suffice. The smaller the value, the more accurate is the model, and the more computational expensive it is.

### 3.2.3 Capacitor bank constructor

A capacitor bank object is instantiated with four inputs, i) capacitor module data, ii) number of (capacitor) modules in series  $n_{ms}$ , iii) number of parallel strings  $n_{ps}$ , and iv) simulation data  $simData$ , which is a structure. The  $simData$  contains three fields, i) SOE (i.e., initial SOE), ii) capacitor bank converter minimum voltage limit, and iii) capacitor bank converter maximum voltage limit.

In the CapBank constructor, the first statement is a call to CapModule constructor, passing to it capacitor module data, initial SOE, and true (setForSim). Then values for properties inherited from CapModule class such as capacitance, full charge voltage, initial voltage, internal resistance, energy storage capacity, and mass are modified/computed accordingly.

### 3.2.4 Capacitor bank other methods

Other CapBank class methods include: -

- a) `updateState`, which checks for voltage limits and then calls `chargeDischarge` method of the CapModule class. The input to the method is power at capacitor bank terminals,

- b) `getPowerToFullCharge`, which computes power to fully charge the capacitor bank. The input to the method is time. That is, time to fully charge the capacitor bank, and
- c) `guiCapBankSimData`, which displays capacitor bank and capacitor module simulation data in a GUI.

For more information on the capacitor bank model see the appendices section.

### 3.3 Sizing capacitor bank

A capacitor bank has to meet (be able to deliver) the required energy for a tram to move from one station (charging point) to the next without violating its minimum voltage limit constraint  $V_{cb}^{\min}$ . As previously mentioned, capacitor bank minimum voltage limit constraint dictates capacitor bank minimum SOE constrain  $\beta_{cb}^{\min}$ .

Given a capacitor bank with enough (needed) energy storage capacity  $Y_{cb}$ , capacitor bank current (power) capability is normally not a threat to supercapacitors since they have high power density. However, should power demanded from a capacitor bank exceed what a capacitor bank can deliver, then tram tractive effort is reduced.

#### 3.3.1 Capacitor bank energy target

A capacitor bank is sized targeting capacitor bank energy target  $E_{cbtg}$  as expressed in Equation (3.3).

$$\begin{cases} E_{cb}(i) = E_{cb}(i-1) + \tau_{sh} P_{cb}(i) \Delta t \\ E_{cbtg} = 1.25 \max(E_{cb}(i|_k)), \quad \forall i, k \end{cases} \quad (3.3)$$

Where,  $E_{cbdm}$  is energy demanded from a capacitor bank,  $i$  is simulation step counter (index),  $k$  is interstation section counter (index),  $\tau_{sh}$  is a constant used to convert seconds to hours,  $\Delta t$  is simulation time step (s),  $P_{cb}$  is power from capacitor bank (kW), which is obtained from power dispatcher, explained later in the chapter. A factor of 1.25 is added to the equation to account for losses in capacitor bank due to internal resistance.

In Equation (3.3), it is important to notice that capacitor bank energy target  $E_{cbtg}$  is a function of energy from a capacitor bank at each iteration for all interstation sections and not net energy from a capacitor bank for each interstation section. This avoids (what could have been wrong) the reduction in capacitor bank energy target due to regenerative braking.

The capacitor bank energy target  $E_{cbtg}$  is determined by simulating a tram movement down to just a level of power dispatcher. That is, down to only a level of power from contact line  $P_{cl}$  and power from capacitor bank  $P_{cb}$  without calculating currents, voltages, and capacitor bank SOE. Power dispatcher and tram movement simulator are explained later in this chapter.

### 3.3.2 Energy target to capacitor bank size

Knowing capacitor bank energy target  $E_{cbtg}$ , procedure to size capacitor bank is as follows: -

- i) Start with one array of capacitors connected in series ( $n_{ps} = 1$ ) such that capacitor bank voltage is just above the minimum voltage limit,
- ii) Keep increasing number of parallel strings ( $n_{ps} = 2, 3, \dots$ ) until capacitor bank size meets energy target,
- iii) Record number of capacitor modules in series  $n_{cms}$ , number of parallel strings  $n_{ps}$ , and total number of capacitor modules
 
$$n_{cm} = n_{cms}n_{ps}$$
- iv) Reset number of parallel strings to 1 ( $n_{ps} = 1$ ),
- v) Add one capacitor module in series,
- vi) While capacitor bank voltage is less than maximum voltage limit, go to step ii) else go to step vii),
- vii) Take the option with minimum number of capacitor modules.

Capacitor bank sizing algorithm is presented in Table 3.1. It is an exhaustive search algorithm.

Table 3.1 Capacitor bank sizing algorithm

---

*Load capacitor module data*

*Load capacitor bank energy target*  $E_{cbtg}$

*Load system (converter capacitor bank input) maximum voltage*  $V_{max\_conv}^{in\_cb}$

*Load system (converter capacitor bank input) minimum voltage*  $V_{min\_conv}^{in\_cb}$

*Calculate capacitor bank maximum voltage*  $V_{cb}^{max} = \min(V_{cb}^{max\_series}, V_{max\_conv}^{in\_cb})$

*Let capacitor bank minimum voltage*  $V_{cb}^{min} = V_{min\_conv}^{in\_cb}$

*Calculate minimum number of capacitor modules in series*  $n_{cms}^{min}$

$$n_{cms}^{min} = \text{ceiling} \left( \frac{V_{cb}^{min}}{V_{cm}^{fc}} \right)$$

*Initiate*  $n_{cms}$  *as minimum*  $n_{cms}$  ( $n_{cms} = n_{cms}^{min}$ )

*Calculate capacitor bank full charge voltage*  $V_{cb}^{fc} = V_{cm}^{fc} n_{cms}$

*Calculate energy available in capacitor bank*  $E_{cbav}$

$$E_{cbav} = E_{cb}(V_{cb}^{fc}) - E_{cb}(V_{cb}^{min})$$

*Set iteration counter*  $j$  *to zero* ( $j = 0$ ). *Comment* : MATLAB indexing starts from 1

---

*while1*  $V_{cb}^{fc} + V_{cm}^{fc} \leq V_{cb}^{max}$  *and*  $E_{cbav} < E_{cbtg}$

*Increment*  $j$

*Set(reset) number of parallel strings to 1* ( $n_{ps} = 1$ )

*Increment number of capacitor modules in series* ( $n_{cms} = n_{cms} + 1$ )

*Calculate*  $V_{cb}^{fc}, E_{cbav}$

*while2*  $E_{cbav} < E_{cbtg}$

*Increment*  $n_{ps}$

*Calculate*  $E_{cbav}$

*end while2*

*Calculate number of capacitor modules*  $n_{cm}(j) = n_{cms}(j) n_{ps}(j)$

*Store*  $n_{cms}(j), n_{ps}(j), n_{cm}(j)$

*end while1*

---

*Get optimal number of capacitor modules*  $n_{cm}^{optimal} = \min(n_{cm}(j)), \forall j$

*Get*  $n_{cms}$  *and*  $n_{ps}$  *associated with*  $n_{cm}^{optimal}$

---

In this study, nominal system voltage is taken as 750 V DC, and system (capacitor bank DC-DC converter) voltage window is taken as 100% to 70% of the full charge voltage. Therefore, minimum capacitor bank SOE is 50%. Thus, the converter for a cap\_Train may be different from that of a cap\_ACL\_Train.

### 3.3.3 Capacitor bank mass question/effect

As aforementioned, capacitor bank energy target is obtained by simulating tram movement down to just power dispatcher. The challenge/question is, *what will be total tram weight (not knowing capacitor bank weight)?* Estimating capacitor bank weight may not be a good idea. If it is overestimated, it may increase tram tractive energy consumption which in turn may require addition of several capacitors.

When a capacitor bank is not just one string (which is normally the case), but several parallel strings, addition to capacitor bank size (due to increased weight) is not just adding a single capacitor module, but several of them. That is, adding a capacitor module to every string, or adding a new string of capacitor modules.

To address this challenge (the challenge explained above), the initial capacitor bank weight is set to zero. That is, initially, tram weight does not include capacitor bank weight. The process to find capacitor bank energy target  $E_{cbtg}$  becomes an iterative process as shown in Figure 3.3 That is, if the capacitor bank energy target  $E_{cbtg}$  results to a capacitor bank size that does not satisfy minimum capacitor bank voltage (or state of energy), mass of the obtained(sized) capacitor bank is added to tram mass, and the process is repeated.

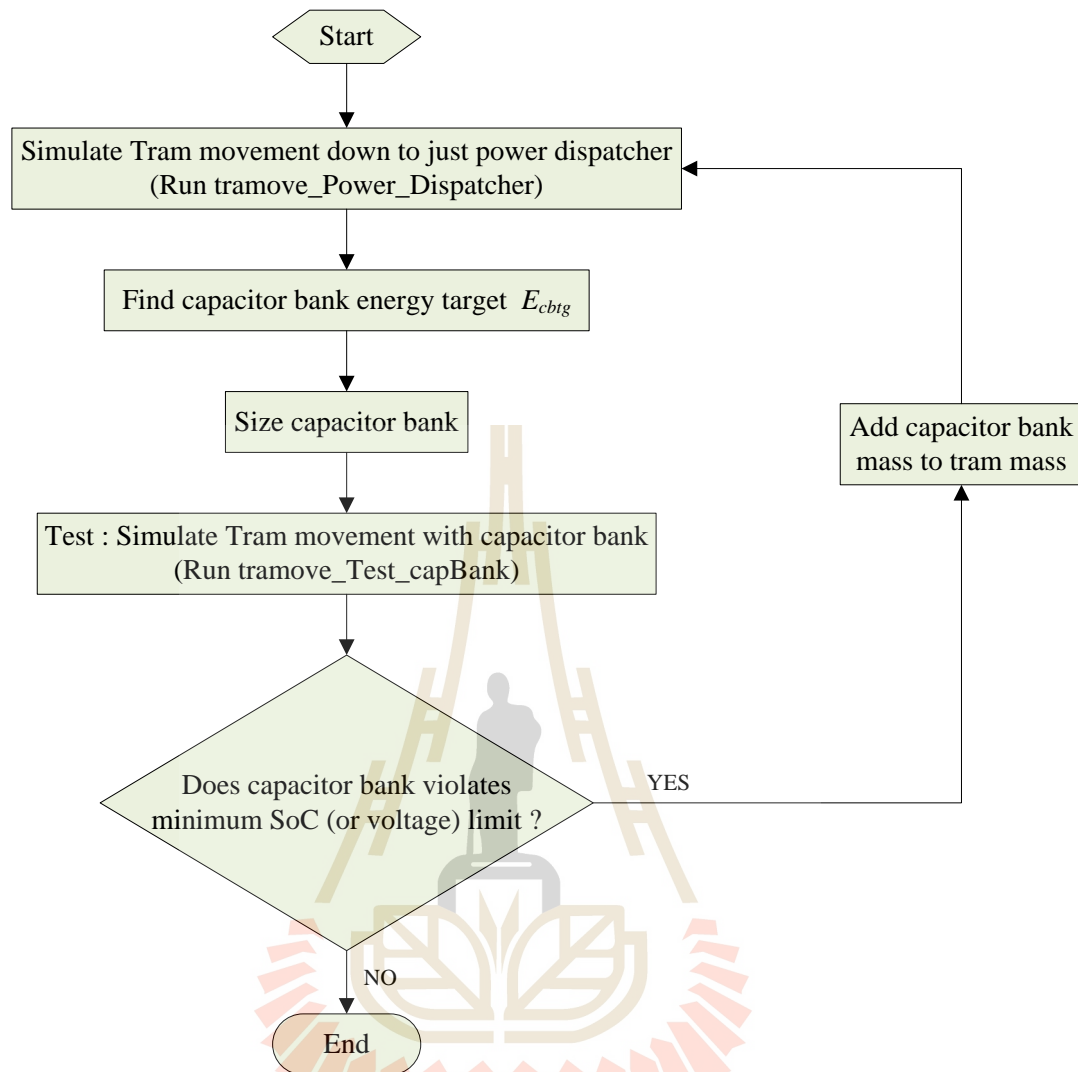


Figure 3.3 Flowchart of an iterative process to find capacitor bank energy target.

### 3.4 Contact line model

Contact line supply system comprises a substation (stepdown transformer, diode rectifier, and unidirectional converter), feeder line, and return rails (running rails are used as return rails). It is modelled as a constant voltage source in series with a constant resistance (substation resistance) and varying resistances (contact line resistance and running rails resistance) as shown in Figure 3.4 (Xiao, Sun, Wang, Zhu, and Feng, 2018).

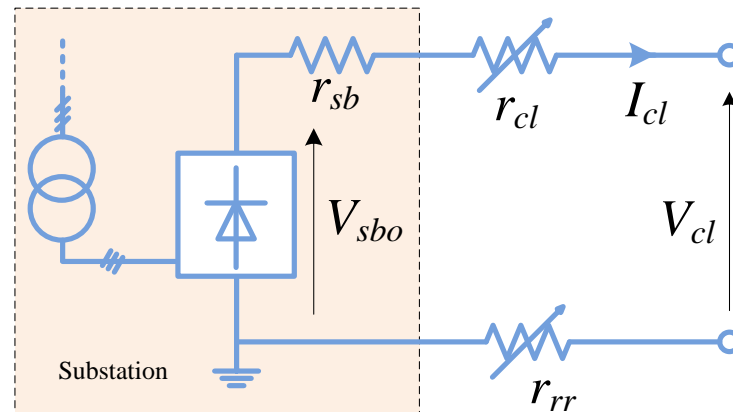


Figure 3.4 Contact line model

A contact line means an ACL for the proposed cap-ACL-Tram system and, a charging bar for a conventional supercapacitor tram (cap-Tram) system. Since there is a substation at every stopping station, in case of the cap-ACL-Tram system, tram distance from a previous stopping station is considered the same to tram distance from a feeding substation.

#### 3.4.1 Contact line constructor

A contact line class has default properties' values. Thus, a contact line constructor can take zero to four inputs which are: - i) contact line data, if it is empty default values are used, ii) contact line length, iii) contact line clearance, and iv) a boolean value "setForSim" (optional).

If "setForSim" is given as true, storage for power ("powerArray"), current ("currentArray"), and voltage ("voltageArray") will be initiated.

#### 3.4.2 Update state method

One of the methods of the contact line (Line) class is updateState method, which needs two inputs, power demand and distance from substation (position where power is demanded). Briefly, the method does the following: -

- a) computes current using instance voltage value,
- b) computes line resistance to the point of contact, and
- c) computes voltage at a point where power is demanded (point of contact between tram current collector and the line).



Equations encapsulated in the updateState method are expressed in Equation (3.4) (Xiao, Sun, Wang, Zhu, and Feng, 2018).

$$\begin{cases} I_{cl}(i) = \frac{P_{cl}(i)}{V_{cl}(i-1)} \\ r_{mcl}(i) = r_{sb} + r_{mcl}s_{sb}(i) \\ V_{cl}(i) = V_{sbo} - I_{cl}(i)r_{mcl}(i) \end{cases} \quad (3.4)$$

Where,  $I_{cl}$  is contact line current (A),  $P_{cl}$  is contact line power (W) at point of contact with tram current collector,  $V_{cl}$  is contact line voltage at point of contact with tram current collector,  $V_{sbo}$  is contact line (substation) no-load voltage (V),  $r_{sb}$  is substation resistance ( $\Omega$ ),  $r_{mcl}$  is contact line resistance per meter ( $\Omega.m^{-1}$ ), and  $s_{sb}$  is tram distance from a feeding substation (m).

For more information on contact line model the read is referred to the appendices section.

### 3.5 Contact line length

The length of an ACL for a given interstation section depends on the distance (from a stopping station) a tram covers to reach desired (cruising) speed, as illustrated in Figure 3.5. In the study, cruising speed was set to 50 kph, resulting to the ACL length of 150 m (approximately) of which 6 m is the total clearance, for all sections.

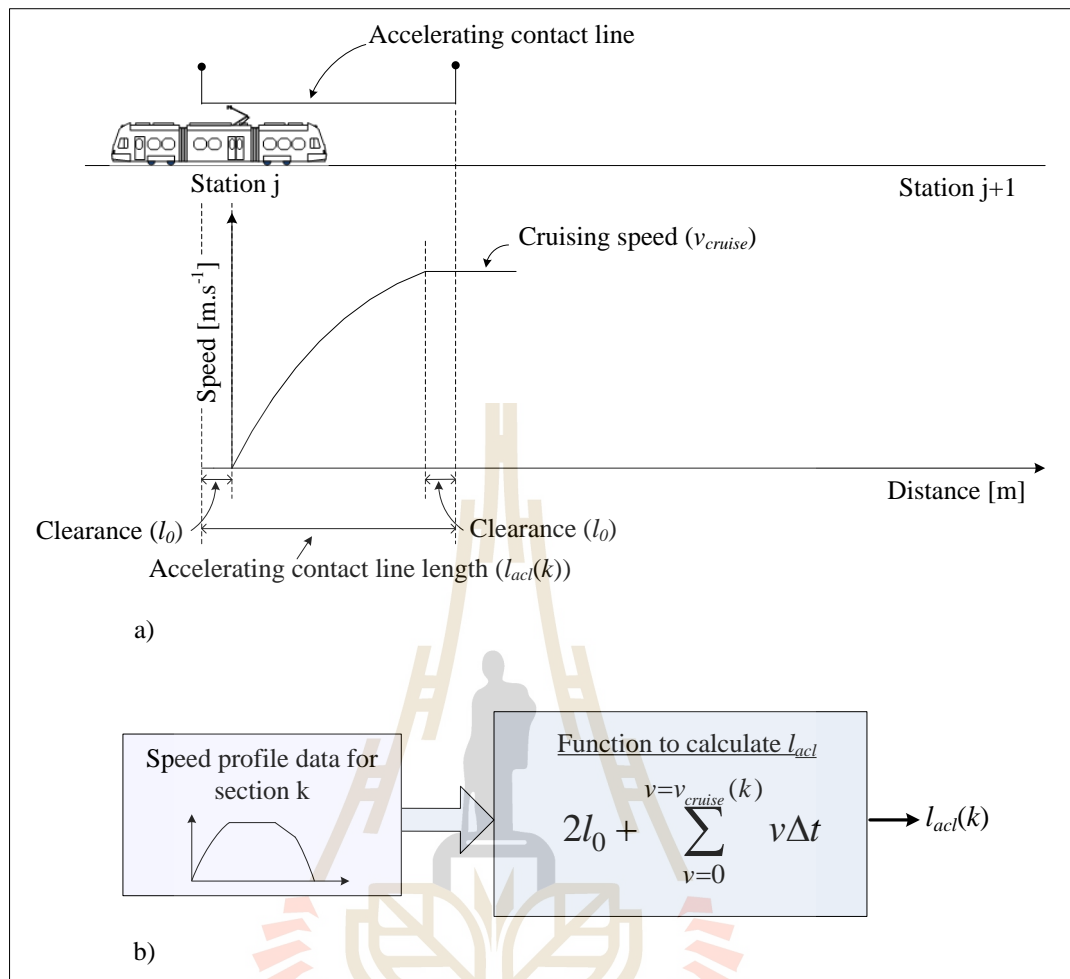


Figure 3.5 Accelerating contact line length, a) description b) computing function

### 3.6 Tram movement model

A tram is modeled as a point mass (a typical tram is not very long), and tram motion is modeled using effect-cause approach. A summary of a general tram move algorithm is given in Table 3.2.

Table 3.2 Tram movement algorithm

---

**Tram move algorithm**

---

*Load tram simulation data*  
*Load route data*  
*Load capacitor bank simulation data*  
*Load contact line data*

*Initiate simulation results storage (interstation storage and trip storage)*

*start for \_loop : interstation index = starting index to stopping index*  
     *start while \_loop : distance to next stop > 0*  
         *Determine speed mode*  
         *Compute tractive effort force  $F_{tr}$  and acceleration*  
         *If  $F_{tr}$  is outside of boundary*  
             *set  $F_{tr}$  to boundary value*  
             *recalculate acceleration*  
         *end\_if*  
         *Compute tractive power demand*  
         *Dispatch power*  
         *Update capacitor bank state (call capacitor bank model)*  
         *Update contact line state (call contact line model)*  
         *Update tram position*  
         *Store interstation results*  
     *end while \_loop*

*Enter dwell mode*

*end for \_loop*

---

### 3.6.1 Tram speed modes

A tram has five speed modes namely i) accelerating speed mode, ii) cruising speed mode, iii) coasting speed mode, iv) braking speed mode, and v) dwelling speed mode. For programming purpose, these speed modes have enumerated integer values ranging from 1 to 5 as shown in Figure 3.6 and expressed in Equation (3.5).

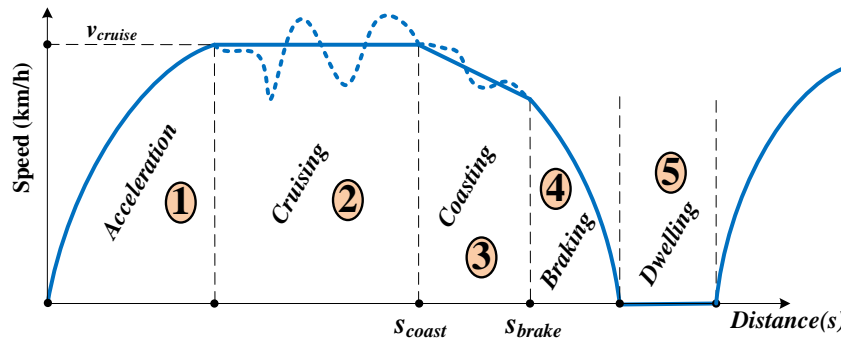
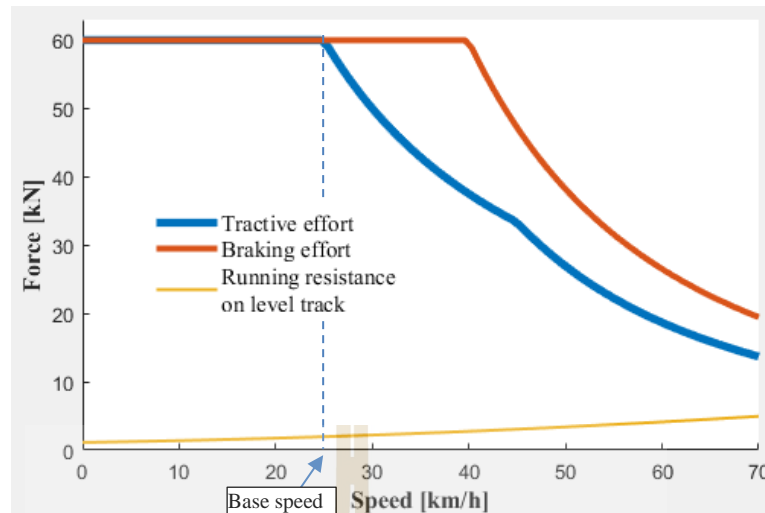


Figure 3.6 Tram speed modes.

$$v_{mode} = \begin{cases} 1, & v < v_{cruise}(k) \text{ and } s_{trs}(k) < s_{coast}(k) \\ 2, & s_{trs}(k) < s_{coast}(k) \\ 3, & s_{coast}(k) \leq s_{trs}(k) < s_{brake}(k) \\ 4, & s_{brake}(k) \leq s_{trs}(k) < s_{stm}(k) \\ 5, & \text{Otherwise} \end{cases} \quad (3.5)$$

Where,  $v_{cruise}$  is cruising speed (set to 50 kph in this study,  $\forall k$ ),  $k$  is an integer representing an interstation section, its value ranges from 1 to  $n_{stm} - 1$ , where  $n_{stm}$  is total number of stations in a given route,  $s_{trs}$  is distance travelled from a previous station,  $s_{coast}$  is coasting point (a distance after which tram speed mode should change to coasting),  $s_{brake}$  is braking point (a distance after which tram speed mode should change to braking), and  $s_{stm}$  is an interstation distance (distance between two adjacent stations).

Tram speed modes as defined in Equation (3.5) and explained in Chapter II (2.3 Tram motion), and tram tractive effort curves as shown in Figure 3.7 (reproduced here just for convenience) also shown in Chapter II (2.3 Tram motion) are the ones used to generate speed profiles used in the study (see Chapter IV, section 4.2: Route and speed profile details).



**Figure 3.7** Tram tractive effort, braking effort, and running resistance curves.

There is a distinction between tram speed mode and tram operation mode. For example, brakes may be applied during cruising speed mode or coasting speed mode (to reinforce speed limit). The application of brakes is tram operation mode, it does not change tram speed mode from cruising speed mode or coasting speed mode to braking speed mode. Tram speed modes are exactly as defined in Equation (3.5).

### 3.6.2 Speed profile generation

As mentioned in Chapter I (Section 1.7 Scope and limitation of the study) detailed speed profile generation is out of scope of the study. However, it is important (for a cap-ACL-Tram system) that, the tram accelerates with high acceleration when it is on ACL section (power mode ACL) so that it reaches the desired (cruising) speed within a short (available) ACL. Briefly, speed profile is generated as follows: -

- i) Speed profile generation, acceleration speed mode ( $v_{mode} = 1$ )

In acceleration speed mode  $v_{mode} = 1$  a tram accelerates using allowable maximum tractive effort. Therefore, tram acceleration  $\alpha$  and consequently speed  $v$ , are determined as expressed in Equation (3.6) (Chymera and Goodman, 2014), (Nicholson, 2014), and Mwambeleko, Kulworawanichpong, and Greyson, 2015).

$$\left\{ \begin{array}{l} F_{trt}(i) = \begin{cases} F_{trt}^{max}, & v \leq v_{base} \\ tramTractiveEffortFunction(v(i)), & otherwise \end{cases} \\ F_{acc}(i) = F_{trt}(i) - (F_{curv}(i) + F_{frdr}(i) + F_{grad}(i)) \\ \alpha(i) = \frac{F_{acc}(i)}{m_{eff}} \\ v(i+1) = v(i) + \alpha(i)\Delta t \end{array} \right. \quad (3.6)$$

Where,  $F_{trt}$  is tractive effort force (N),  $F_{trt}^{max}$  is maximum tractive effort (N),  $v$  is speed (m/s),  $v_{base}$  is base speed (m/s),  $F_{acc}$  is acceleration force (N),  $F_{curv}$  is curvature resistance force (N),  $F_{frdr}$  is frictional drag force (N),  $F_{grad}$  is gradient force (N),  $a$  is acceleration (m/s<sup>2</sup>),  $m_{eff}$  is tram effective mass (kg),  $\Delta t$  is change in time (s) from simulation step index  $i$  to  $i+1$ , and  $i$  is simulation step index number.

As previously mentioned, the allowable maximum tractive effort is a function of tram speed as shown in Figure 3.7 For more details about Equation (3.6) refer to Chapter II (Section 2.6: Tram motion).

ii) Speed profile generation, cruising speed mode ( $v_{mode} = 2$ )

In cruising speed mode ( $v_{mode} = 2$ ), the objective is to balance tractive effort with the motion opposing forces so as to maintain speed (to set acceleration force  $F_{acc}$  to zero). However, speed may not be maintained for reasons explained in Chapter II (Section 2.6: Tram motion). If no constrain is violated, tram acceleration  $\alpha$  and consequently speed  $v$  are determined as expressed in Equation (3.7).

$$\left\{ \begin{array}{l} F_{acc}(i) = 0 \\ F_{trt}(i) = (F_{curv}(i) + F_{frdr}(i) + F_{grad}(i)) \\ \alpha(i) = 0 \\ v(i+1) = v(i) + \alpha(i)\Delta t \end{array} \right. \quad (3.7)$$

Where,  $F_{acc}$  is acceleration force (N),  $F_{trt}$  is tractive effort force (N),  $F_{curv}$  is curvature resistance force (N),  $F_{frdr}$  is frictional drag force (N),  $F_{grad}$  is gradient force (N),  $a$  is acceleration ( $m/s^2$ ),  $v$  is speed (m/s),  $\Delta t$  is change in time (s) from simulation step index  $i$  to  $i+1$ , and  $i$  is simulation step index number.

If tram tractive effort force  $F_{trt}$  is violated, then acceleration  $a$  and speed  $v$  are determined using Equation (3.6). If capacitor bank power  $P_{cb}$  or current  $I_{cb}$  is violated, the corresponding is fixed to its maximum limit, and a backward process is done to recalculate (reduce) tractive effort  $F_{trt}$ .

iii) Speed profile generation, coasting speed mode

In coasting speed mode  $v_{mode} = 3$ , tractive effort is set to zero, and tram speed is expected to be decreasing gradually, as explained in Chapter II. Again, the same Equation (3.6) is used to generate speed profile. Coasting point distance per unit, that is,  $\frac{s_{coast}(k)}{s_{sm}(k)}$  is a random number between 0.5 and 0.6. Through several trials the range was found to suffice.

iv) Speed profile generation, braking speed mode

In braking speed mode  $v_{mode} = 4$ , critical braking distance is used to determine braking acceleration (deceleration), and then braking effort is calculated as expressed in Equation (3.8). If calculated braking effort is greater than allowable maximum braking effort, the braking effort will be set to maximum, and deceleration (negative acceleration) will be re-calculated (Chymera and Goodman, 2014)..

$$\begin{cases} \alpha(i) = \frac{-v^2}{2(s_{sm}(k) - s_{trs}(i,k))} \\ F_{acc}(i) = (m + \lambda m_{tare}) \alpha(i) \\ F_{trt}(i) = F_{acc}(i) + (F_{curv}(i) + F_{frdr}(i) + F_{grad}(i)) \\ v(i+1) = v(i) + \alpha(i) \Delta t \end{cases} \quad (3.8)$$

Where,  $a$  is acceleration ( $m/s^2$ ),  $v$  is tram speed (m/s),  $s_{sm}$  is interstation distance (m),  $k$  is interstation section index number,  $s_{trs}$  is interstation travelled distance (m)  $F_{acc}$

is acceleration force (N),  $m$  is tram total mass (kg),  $\lambda$  is a unitless rotary allowance,  $m_{tare}$  is tram tare mass (kg),  $F_{trt}$  is tractive effort force (N),  $F_{curv}$  is curvature resistance force (N),  $F_{frdr}$  is frictional drag force (N),  $F_{grad}$  is gradient force (N),  $\mathbf{Dt}$  is change in time (s) from simulation step index  $i$  to  $i + 1$ , and  $i$  is simulation step index number.

For more details about Equation (3.8), the reader is referred to Chapter II (Section 2.6: Tram motion)

Since it is not known beforehand (although it could have been set) at what speed will the tram start braking, braking point distance per unit, that is,  $\frac{s_{brake(k)}}{s_{stm(k)}}$  is a random number varying between 0.8 and 0.9. Through several trials the range was found to suffice.

v) *Peek view of a speed profile example*

A peek view of a speed profile example is shown in Table 3.3, the header line starts with a % symbol because the same data is saved in text file (.txt format), and it is from the text file where the data will be later retrieved, the % symbol is used for a line comment in MATLAB language, hence it is used so as to ignore the header line when the file contents are (read) retrieved starting from the very top.

The speed profile was generated using tractive effort curves shown in Figure 3.7. It is shown in Table 3.3 that the tram accelerates with the maximum allowable tractive effort, as the tram approaches cruising speed (13.3 m/s (approx. 48 kph)) the maximum allowable tractive effort is about 30.5 kN, see line 39 of Table 3.3. The value of the tractive effort (at 48 kph) can be roughly confirmed from the tractive effort curves in Figure 3.7. Interestingly (as aforementioned), in cruising mode, when speed is maintained at approx. 48 kph, tractive effort needed is just to counterbalance motion opposing forces, the tractive effort drops dramatically to only about 3.2 kN, see line 40 to line 44 of Table 3.3.



Table 3.3 A peek view of tram speed profile

	A	B	C	D
1				
2	% time[sec]	s [m]	v [m/s]	F_trt [kN]
3	0	0.0	0.0	0.0000
4	0.5	0.1	0.5	60.0000
5	1	0.5	0.9	60.0000
6	1.5	1.0	1.4	60.0000
7	2	1.8	1.8	60.0000
8	2.5	2.9	2.3	60.0000
9	3	4.1	2.8	60.0000
10	3.5	5.6	3.2	60.0000
11	4	7.3	3.7	60.0000
12	4.5	9.3	4.1	60.0000
13	5	11.5	4.6	60.0000
14	5.5	13.9	5.0	60.0000
15	6	16.5	5.5	60.0000
16	6.5	19.3	5.9	60.0000
17	7	22.4	6.4	60.0000
18	7.5	25.7	6.8	60.0000
19	8	29.3	7.3	60.0000
20	8.5	33.0	7.7	57.0590
21	9	37.0	8.1	53.8906
22	9.5	41.2	8.5	51.2143
23	10	45.5	8.9	48.9140
24	10.5	50.0	9.2	46.9088
25	11	54.7	9.6	45.1405
26	11.5	59.6	9.9	43.5657
27	12	64.6	10.2	42.1515
28	12.5	69.8	10.5	40.8724
29	13	75.1	10.8	39.7083
30	13.5	80.6	11.1	38.6428
31	14	86.2	11.3	37.6629
32	14.5	91.9	11.6	36.7577
33	15	97.8	11.9	35.9182
34	15.5	103.8	12.1	35.1370
35	16	109.9	12.4	34.4076
36	16.5	116.1	12.6	33.7246
37	17	122.5	12.8	32.7771
38	17.5	129.0	13.0	31.5980
39	18	135.5	13.3	30.5265
40	18.5	142.2	13.3	3.2370
41	19	148.8	13.3	3.2370
42	19.5	155.4	13.3	3.2370
43	20	162.1	13.3	3.2370
44	20.5	168.7	13.3	3.2370

### 3.6.3 Tram power and energy demand

General tram power flow diagram is shown in

**Figure 3.8** Figure 3.8 It consists of two main parts, ii) power supply section which is on-board supercapacitor bank and contact line, and load section which is tram auxiliary load and tractive load. This illustrates that, when supercapacitor bank is being charged (for example during dwell time) power to charge the supercapacitor bank is not considered as tram power demand (Mwambeleko, Hayasaka and Kulworawanichpong, 2020)

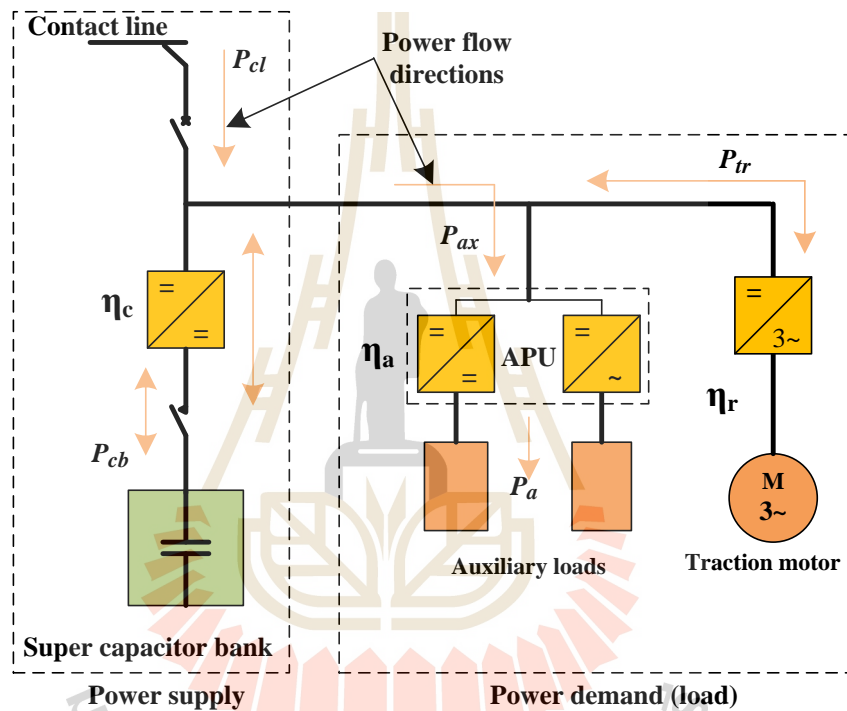


Figure 3.8 Tram general power flow diagram.

Tram power demand is computed following diagram shown in Figure 3.9, using bottom-up (effect-cause) approach.

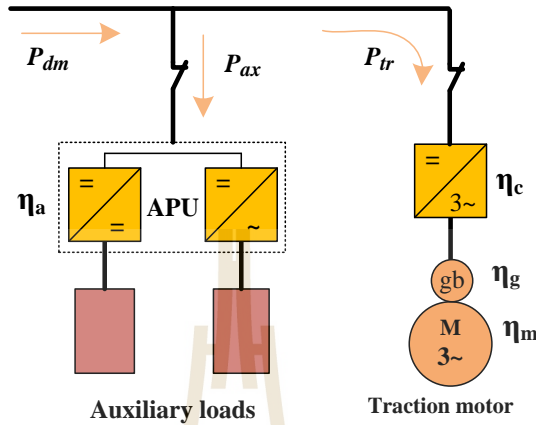


Figure 3.9 Tram power demand diagram.

Given acceptable tractive effort force  $F_{trt}$ , tram tractive power demand is computed using Equation (3.9) (Mwambeleko, Hayasaka and Kulworawanichpong, 2020) and (Chymera and Goodman, 2014).

$$P_{tr}(i) = \begin{cases} \frac{F_{trt}(i)v(i)}{\eta_{trt}}, & F_{trt}(i) > 0 \\ F_{trt}(i)v(i)\eta_{trt}, & F_{trt}(i) < 0 \text{ and } v(i) \geq v_{gmin} \\ 0 & \text{otherwise} \end{cases} \quad (3.9)$$

Where,  $P_{tr}$  is tram traction power demand (kW),  $F_{trt}$  is tractive effort force (kN),  $v$  is tram speed (m/s),  $v_{gmin}$  is minimum regenerative braking speed, and  $\eta_{trt}$  is traction system efficiency, it is a product of traction motor driver (converter) efficiency  $\eta_c$ , gearbox efficiency  $\eta_g$ , and traction motor efficiency  $\eta_m$ . That is,  $\eta_{trt} = \eta_c \eta_g \eta_m$ .

Tram total power demand  $P_{dm}$  is thus a sum of tram auxiliary power demand  $P_{ax}$  and traction power demand  $P_{tr}$  as expressed in Equation (3.10) (Mwambeleko, Hayasaka and Kulworawanichpong, 2020).

$$P_{dm}(i) = P_{ax} + P_{tr}(i) \quad (3.10)$$

Where,  $P_{dm}$  is total tram power demand (kW),  $P_{ax}$  is auxiliary (average) power demand (kW),  $P_{tr}$  is tram traction power demand (kW), and  $i$  is simulation index number (counter)

Net energy consumption between consecutive stations  $E_{sm}$  is computed using Equation (3.11) (Mwambeleko, Hayasaka and Kulworawanichpong, 2020) and (Chymera and Goodman, 2014).

$$E_{sm}(k) = \tau_{sh} \sum_{t=0}^{t=T_{sm}(k)} P_{dm} \Delta t \quad (3.11)$$

Where,  $E_{sm}$  is net energy consumption between consecutive stations (kWh),  $T_{sm}$  is interstation travel time (s),  $\Delta t$  is simulation time step, and  $\tau_{sh}$  is a constant used to convert energy from watt-second to watt-hour.

Total energy consumption on a route section  $k$  is a sum of tram's net energy consumption between consecutive stations and energy consumption during dwell time  $t_{dw}$  (s). It is computed using Equation (3.12). Dwell time in this study is 30 seconds (Mwambeleko, Hayasaka and Kulworawanichpong, 2020) and (Chymera and Goodman, 2014).

$$E_{smd}(k) = E_{sm}(k) + \tau_{sh} \sum_{t=0}^{t=t_{dw}} P_{ax} \Delta t \quad (3.12)$$

Where,  $E_{smd}$  is a sum of energy consumption between consecutive stations and energy consumption during dwell (kWh),  $E_{sm}$  is net energy consumption between consecutive stations (kWh), and  $P_{ax}$  is auxiliary (average) power demand (kW).

### 3.7 Power dispatcher

In this study, a contact line is assumed to be fed by a diode rectifier, unidirectional converter, substation. Thus, energy (such as regenerative braking energy) cannot be sent back to the substation. Moreover, when a tram is braking (to stop at a station), it will not be on a section that has a contact line. Therefore, regenerative energy is stored in the OBESD (the capacitor bank in this case) of the same tram. If regenerative energy/power is more than what the capacitor bank can take, the extra is wasted as heat in the braking resistor bank.

Power dispatcher is used to dispatch tram power demand  $P_{dm}$  to capacitor bank and contact line, given tram position from supplying substation  $s_{sb}$ , and accelerating contact line length on a given section  $L_{acl}(k)$  as shown in Figure 3.10.

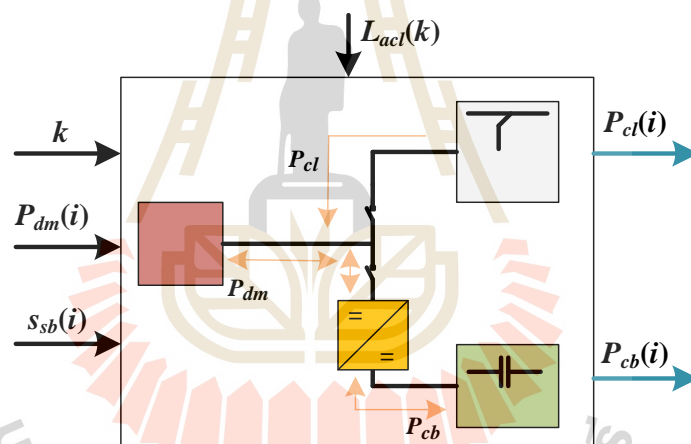
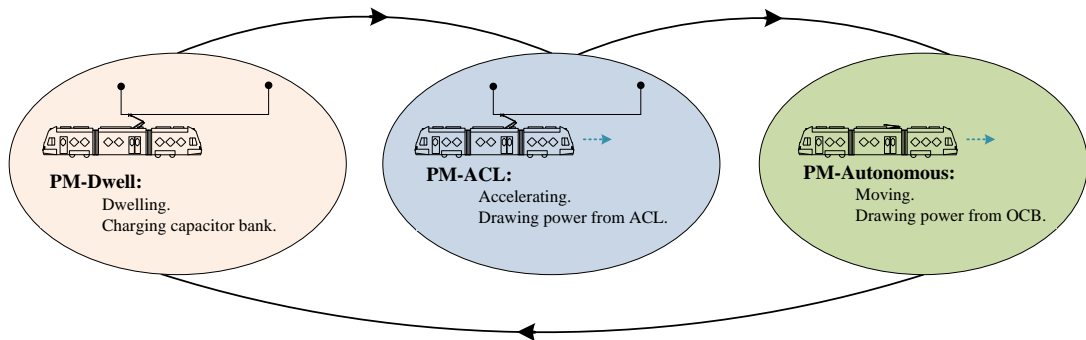
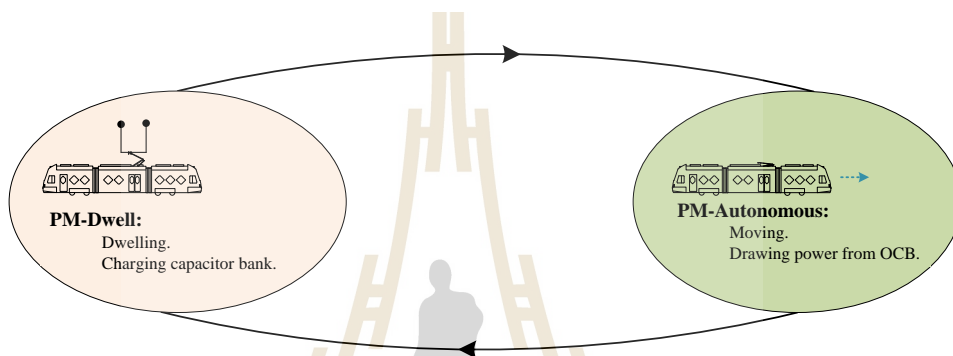


Figure 3.10 Power dispatcher inputs and outputs

A power dispatcher used in this study operates in three modes, namely i) power mode dwell (PM-Dwell), ii) power mode ACL (PM-ACL) and, iii) power mode autonomous (PM-Autonomous) as shown in Figure 3.11 and summarized in Table 3.4.



a) Power modes for a cap-ACL-Tram system



b) Power modes for a cap-Tram system

Figure 3.11 Power dispatcher modes a) cap-ACL-Tram system b) cap-Tram system

Table 3.4 Power dispatcher modes summary

Power mode	Description
PM-Dwell	A tram is dwelling (stopped at a station, passengers are boarding and deboarding). Power from contact line is used to charge on-board capacitor bank and supply tram auxiliary load.
PM-ACL	A tram is leaving its current station (accelerating to the next station) drawing power from accelerating contact line (ACL). Capacitor bank is neither charged nor discharged.
PM-Autonomous	A tram does not have access to ACL power, it draws all its power demand from the on-board capacitor bank.

### 3.7.1 Power mode dwell

In power mode dwell (PM-Dwell), a tram is dwelling (stopped at a station, for passengers to deboard and board). Power from contact line is used to charge on-board capacitor bank and supply tram auxiliary load as shown in Figure 3.12.

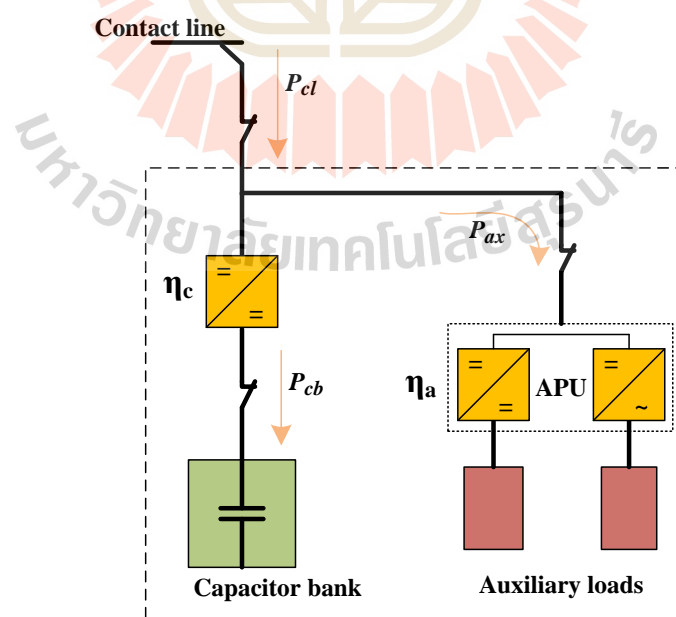


Figure 3.12 Power flow in PM-Dwell

The capacitor bank is charged at a constant power  $P_{cb}$ , which is a function of its state of charge (SoC) when a tram arrives at a station  $\beta_{cb}^{arr}$ , its energy storage capacity  $\Upsilon_{cb}$ , and dwell time  $t_{dw}$ . The objective is to avoid unnecessary high charging current, but rather utilize the entire dwell time to full charge the capacitor bank (or charge the capacitor bank such that it has enough energy to get to the next station). That is  $P_{cb}$ , is such that  $\sum_{t=0}^{t=t_{dw}} P_{cb} \Delta t = \Upsilon_{cb} (1 - \beta_{cb}^{arr}) \tau_{hs}$ . Power equation during PM-Dwell is expressed in Equation (3.13).

$$\begin{cases} P_{cb} = \begin{cases} \frac{-1.25 \tau_{hs} (1 - \beta_{cb}^{arr}) \Upsilon_{cb}}{t_{dw}}, & \beta_{cb} < 1 \\ 0, & \text{Otherwise} \end{cases} \\ P_{cl} = \left| \frac{P_{cb}}{\eta_c} \right| + P_{ax} \end{cases} \quad (3.13)$$

Where,  $P_{ax}$  is tram auxiliary power demand (kW),  $P_{cb}$  is power at capacitor bank terminal (injected power in this case) (kW),  $P_{cl}$  is power at a point of contact between tram power collector and contact line (kW),  $\eta_c$  is converter efficiency (a converter linking contact line and capacitor bank in this case),  $t_{dw}$  is dwell time (s),  $\beta_{cb}^{arr}$  is capacitor bank SoC as the tram arrives at a station (a unitless parameter ranging from 0 to 1),  $\Upsilon_{cb}$  is capacitor bank storage capacity (kWh), and  $\tau_{hs}$  is a constant used to convert hour to seconds, its value is 3600.

A factor of 1.25 is added in Equation (3.13) to account for energy loss due to capacitor bank internal resistance, and the negative sign implies energy is injected into a capacitor bank.

### 3.7.2 Power mode ACL

Power mode ACL (PM-ACL) is only applicable for a supercapacitor and ACL hybrid tram (cap-ACL-Tram) system. In PM-ACL a tram is leaving its current station, it is accelerating going to the next station, drawing power from ACL (a tram is within ACL section).



It is not necessary to charge capacitor bank during acceleration, since supercapacitors can be charged very fast, normally dwell time is more than enough to fully charge a supercapacitor bank. Therefore, in PM-ACL, capacitor bank is disconnected, it is neither charged nor discharged for i) simplicity, and ii) not to overload ACL. Power flow in PM-ACL is shown in Figure 3.13.

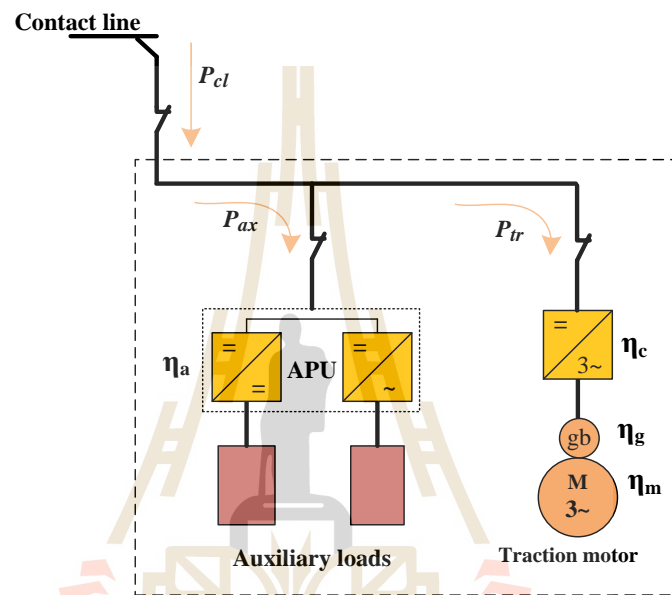


Figure 3.13 Power flow in PM-ACL (applicable only for a cap-ACL-Tram)

Capacitor bank and ACL power equation for a cap-ACL-Tram during PM2 is expressed in Equation (3.13).

$$\begin{cases} P_{cb} = 0 \\ P_{cl}(i) = \begin{cases} P_{ax} + P_{tr}(i), & P_{ax} + P_{tr}(i) > 0 \\ 0, & \text{Otherwise} \end{cases} \end{cases} \quad (3.14)$$

Where,  $P_{cb}$  is power at capacitor bank terminal (kW),  $P_{cl}$  is power at a point of contact between tram power collector and contact line (kW),  $P_{ax}$  is tram auxiliary power demand, and  $P_{tr}$  is tram tractive power demand (kW).

Power mode ACL (PM-ACL) corresponds to speed mode 1 ( $v_{mode} = 1$ ). Brakes are never applied in PM-ACL, if speed reaches cruising speed, then speed mode will change and so will power mode. That is why capacitor bank power is zero (constant)  $P_{cb} = 0$ .

### 3.7.3 Power mode autonomous

In power mode autonomous (PM-Autonomous), a tram is moving powered solely by on-board supercapacitor bank (it has no access to ACL) as shown in Figure 3.14, power from contact line is zero.

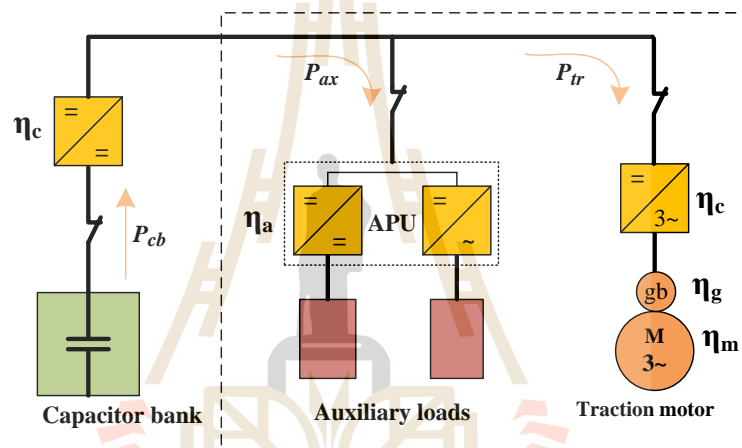


Figure 3.14 Powers flows in PM-Autonomous.

Capacitor bank and ACL power equation during PM-Autonomous is expressed in Equation (3.13).

$$\begin{cases} P_{cl} = 0 \\ P_{cb}(i) = \begin{cases} \frac{P_{ax} + P_{tr}(i)}{\eta_c}, & P_{ax} + P_{tr}(i) \geq 0 \\ (P_{ax} + P_{tr}(i))\eta_c, & \text{Otherwise} \end{cases} \end{cases} \quad (3.15)$$

Where,  $P_{cl}$  is power at a point of contact between tram power collector and contact line (kW),  $P_{cb}$  is power at capacitor bank terminal (kW),  $P_{ax}$  is tram auxiliary power

demand (kW),  $P_{tr}$  is tram tractive power demand (kW), and  $\eta_c$  is a general voltage converter efficiency (a converter linking contact line and capacitor bank)



## CHAPTER IV

### SIMULATION RESULTS AND DISCUSSION

#### 4.1 Introduction

A tram that is powered solely by supercapacitors is also known as a cap-Tram, and the proposed tram system (a supercapacitor – ACL hybrid tram) is also known as cap-ACL-Tram. For both tram systems (cap-Tram system and cap-ACL-Tram system), performance evaluation was done using simulation. The simulation was implemented using MATLAB M-files. In this chapter, the following are presented: -

- i. data used in tram movement simulation and evaluation (that is, the tram systems, route, and speed profile),
- ii. simulation results for both tram systems, and
- iii. discussion on-board capacitor bank reduction, effect of gradient, and significance of the ACLs.

#### 4.2 Route and speed profile

As previously mentioned, the on-board capacitor bank is fully charged at every stopping station. Thus, total route distance is insignificant, but route interstation sections are. That is, as long as a tram can travel from one station to the next for all interstation sections, it can theoretically, complete any route distance. A route can therefore be abstracted by just a single interstation section that has the highest energy (power) demand. It can be recalled that, since supercapacitors have high power density, maximum power demand is normally not a problem given a capacitor bank that meets energy demand. For this reason, an imaginary route shown in Figure 4.1 is carefully chosen to be used in the study. The route is 12 km long with nine (9) stopping stations. As presented in Table 4.1 each interstation section has elevation trajectory that is of interest for the study.

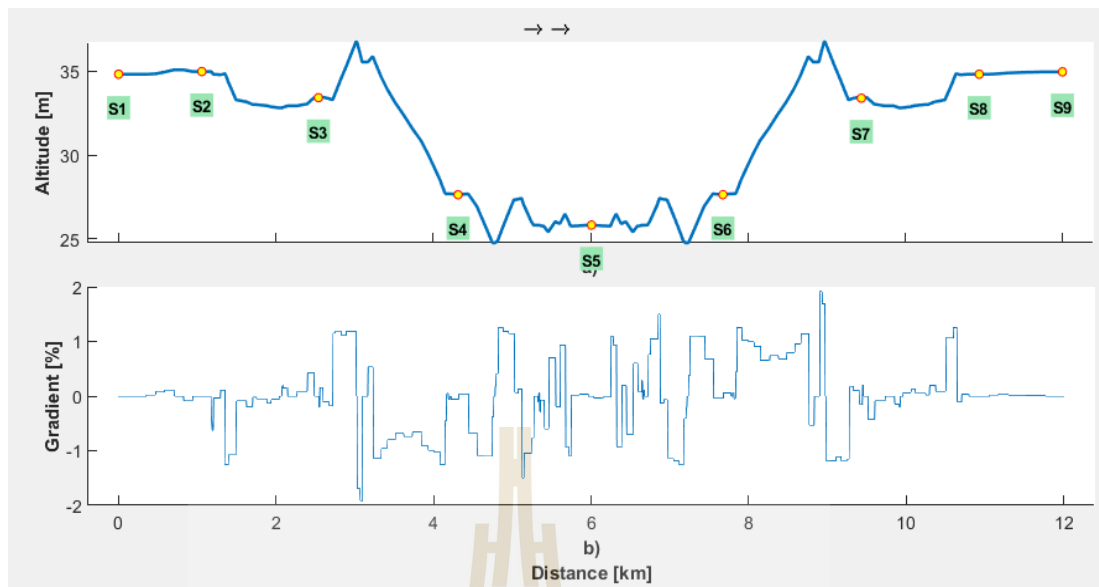


Figure 4.1 Tram route used in the study a) route profile, b) gradient.

Table 4.1 Route sections' elevation trajectory of interest for the study

Section	Elevation trajectory
S1 – S2	Fairly flat
S2 – S3	Fairly flat and down slope
S3 – S4	A short uphill, then long downhill
S4 – S6	Rough sections, up and down slopes.
S6 – S7	A long uphill, then short downhill (mirroring section S3 – S4)
S7 – S8	A long fairly flat, then uphill (mirroring section S2 – S3)
S8 – S9	Fairly flat (mirroring section S1 – S2)

The source (originality) of the route shown in Figure 4.1 is a non-electrified Karasuyama line in Japan. It has been modified to fit the purpose of this study (Shiraki, Tokito, and Yokozutsumi, 2015).

As previously mentioned, total route distance is insignificant, but interstation distance is. The route shown in Figure 4.1 could be represented by only a single section (S6 – S7, in this case), in a sense, the route's eight (8) sections represent

eight (8) routes where each section is the highest energy demand in the respective route. For the comparison purpose, both trams used similar speed profiles as shown in Figure 4.2 The speed profiles are generated as explained in chapter III

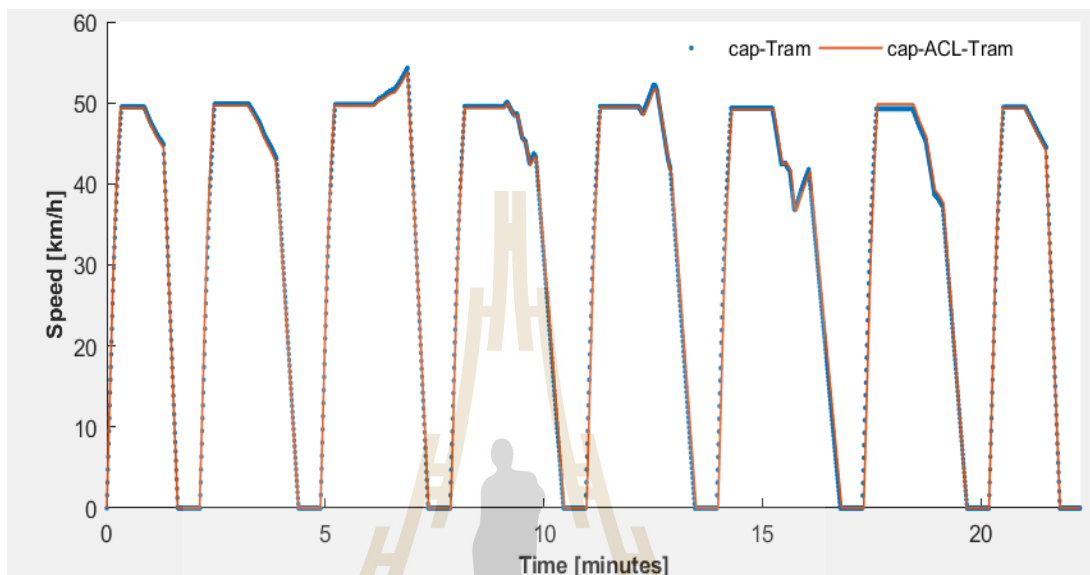


Figure 4.2 Trams' speed profile used in the study.

### 4.3 Results for a cap-Tram

Inputs of the cap-Tram as echoed back by the simulator are shown in Figure 4.3 and Figure 4.4 respectively.

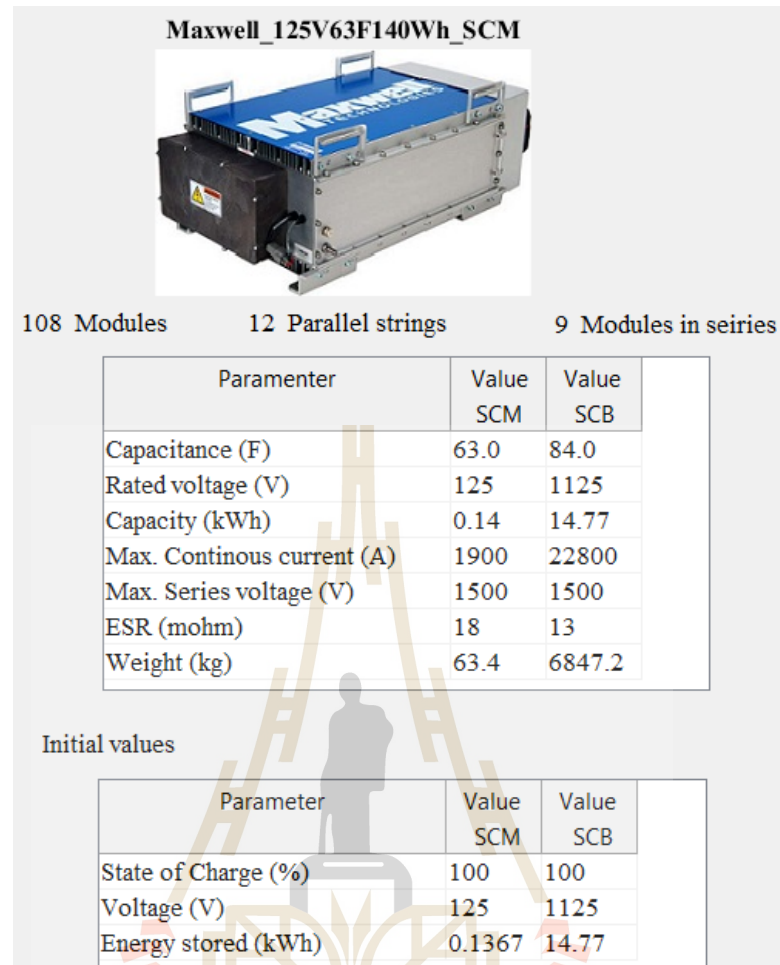


Figure 4.3 Capacitor bank echoed input for a cap-Tram



Figure 4.4 Tram echoed input for a cap-Tram

Simulation results for a cap-Tram are shown in Figure 4.5 through Figure 4.8, and results summary is presented in Table 4.2. Tractive effort and speed profiles are shown in Figure 4.5. Tram power demand, power from contact line (charging bar) and power from capacitor bank profiles are shown in Figure 4.6. Capacitor bank SOE, capacitor bank voltage, and capacitor bank current profiles are shown in Figure 4.7. Distance covered (travelled), net energy consumption, and capacitor bank SOE simulation results for a cap-Tram are shown in Figure 4.8.



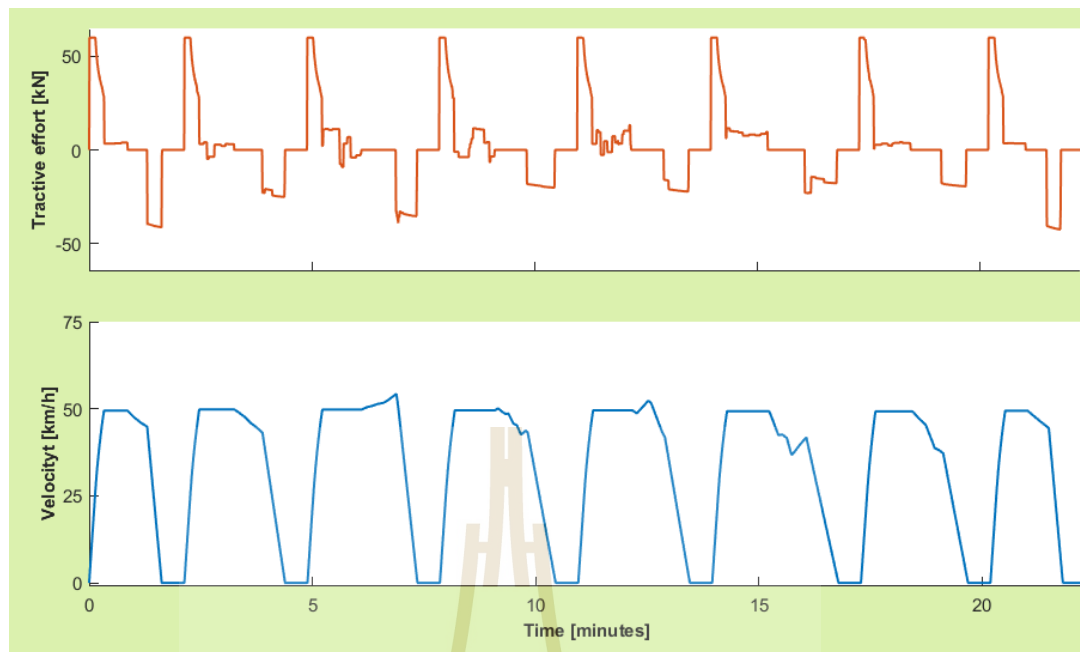


Figure 4.5 Tractive effort and speed profile results for a cap-Tram



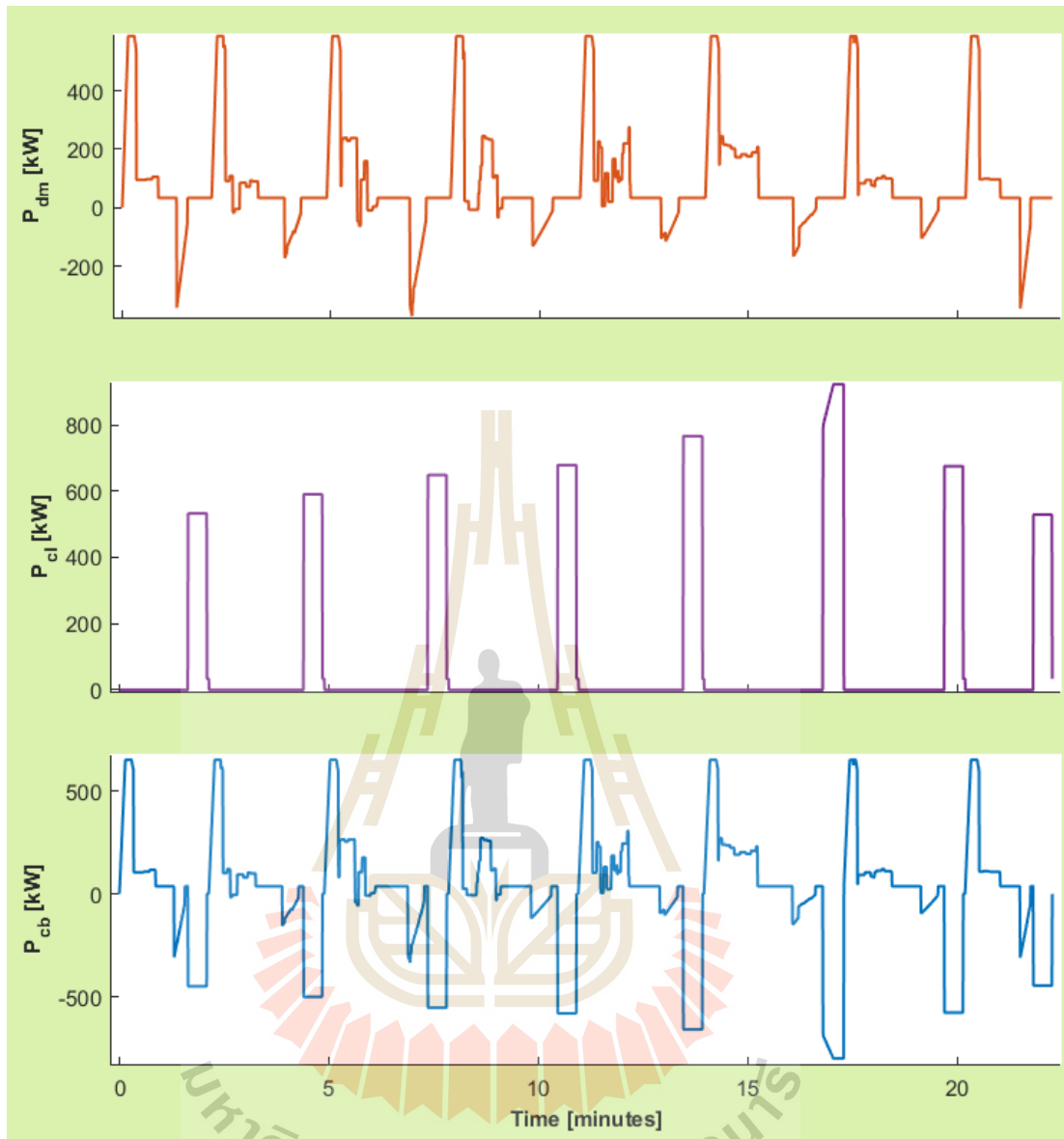


Figure 4.6 Power demand, power from contact line (charging bar), and power from capacitor bank results for a cap-Tram.

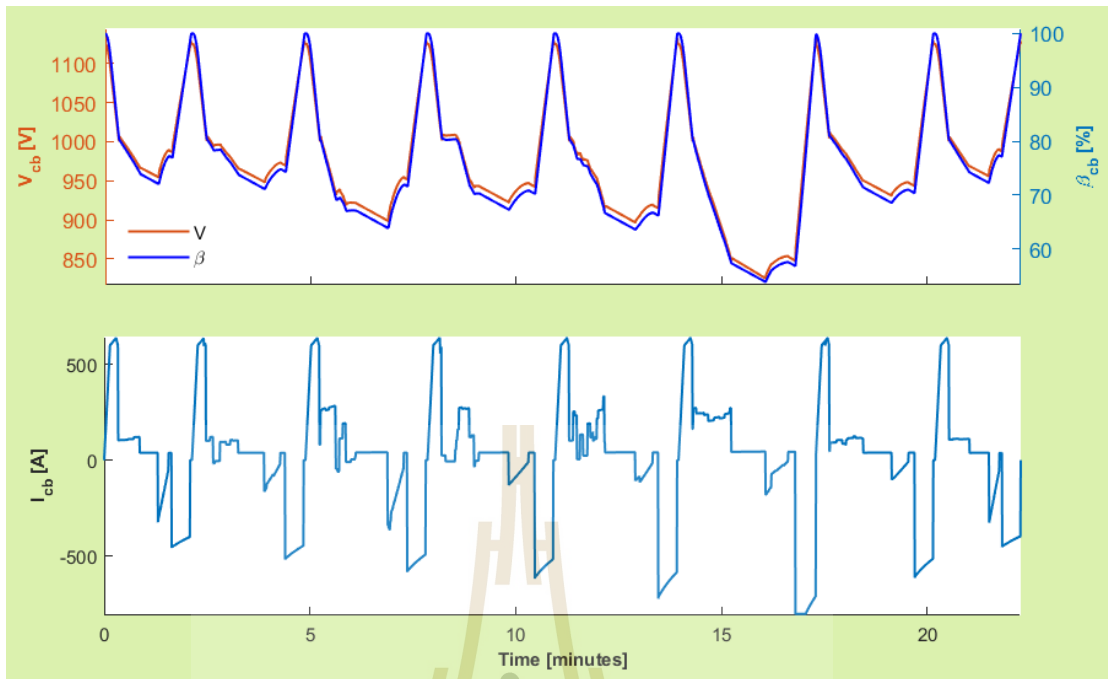


Figure 4.7 Capacitor bank SOE, voltage, and current results for a cap-Tram

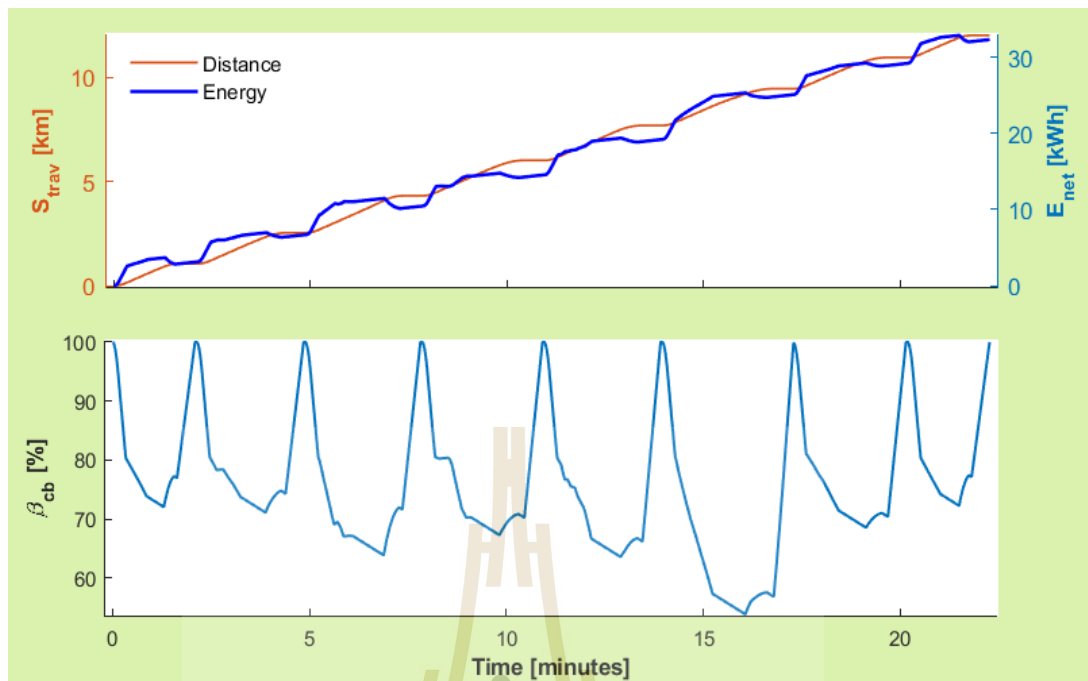


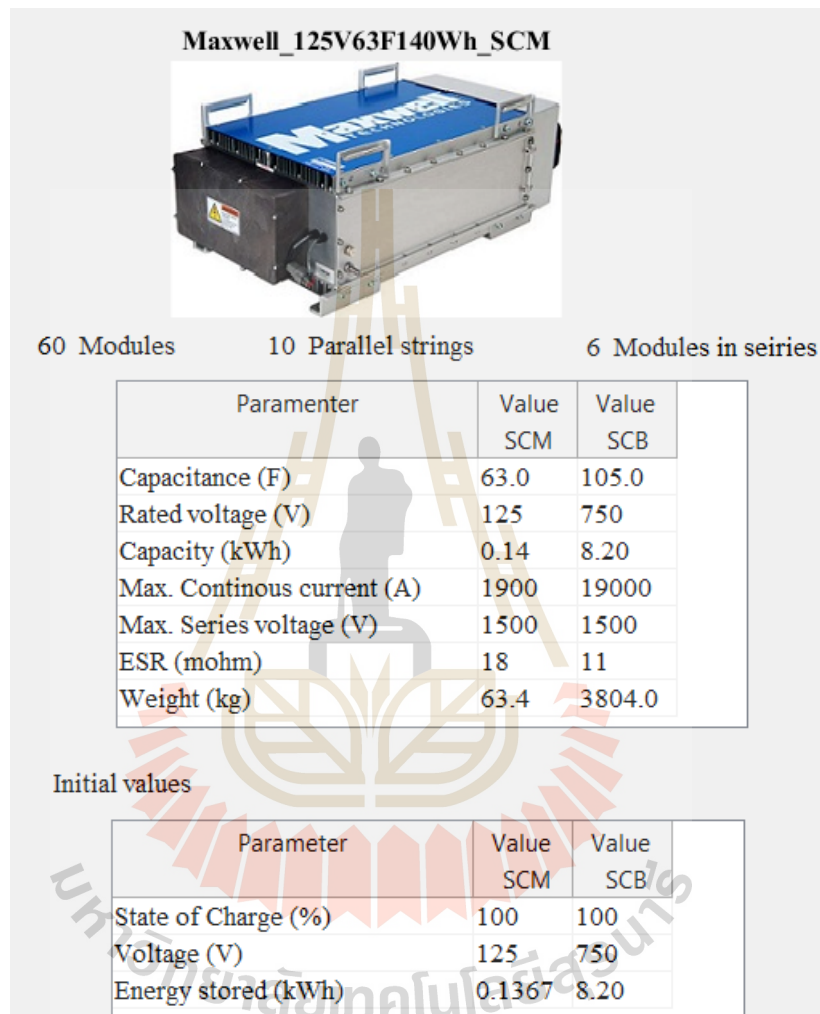
Figure 4.8 Distance travelled, net energy consumption, and capacitor bank SOE results for a cap-Tram.

Table 4.2 Simulation results summary for cap-Tram

Section	$S_{stn}$ [m]	$S_{stn}^{trv}$ [m]	$T_{stn}$ [sec]	$T_{stn}^{d}$ [sec]	$E_{stn}$ [kWh]	$E_{stn}^{d}$ [kWh]	$E_{cl}^{trv}$ [kWh]	$E_{cb}^{trv}$ [kWh]	$E_{cl}^{dw}$ [kWh]	$E_{cb}^{dw}$ [kWh]	$\beta_{cb}^{arv}$ [%]	$\beta_{cb}^{dep}$ [%]
S1 - S2	1058	1058	98	128	2.88	3.16	0	3.38	4.02	-3.41	76.9	100
S2 - S3	1482	1482	136	166	3.28	3.55	0	3.77	4.45	-3.8	74.3	100
S3 - S4	1776	1776	149	179	3.47	3.75	0	4.17	4.89	-4.2	71.6	100
S4 - S5	1697	1697	157	187	3.82	4.09	0	4.37	5.12	-4.4	70.2	100
S5 - S6	1671	1671	151	181	4.37	4.65	0	4.97	5.87	-5.08	66.2	100
S6 - S7	1760	1760	170	200	5.59	5.87	0	6.34	7.42	-6.36	56.8	100
S7 - S8	1498	1498	142	172	3.82	4.1	0	4.33	5.09	-4.38	70.4	100
S8 - S9	1058	1058	98	126	2.86	3.11	0	3.36	3.97	-3.39	77.1	100

#### 4.4 Results for a cap-ACL-Tram

Inputs of the cap-ACL-Tram as echoed back by the simulator are shown in Figure 4.9 and Figure 4.10 respectively.



**Figure 4.9** Capacitor bank echoed input for a cap-ACL-Tram

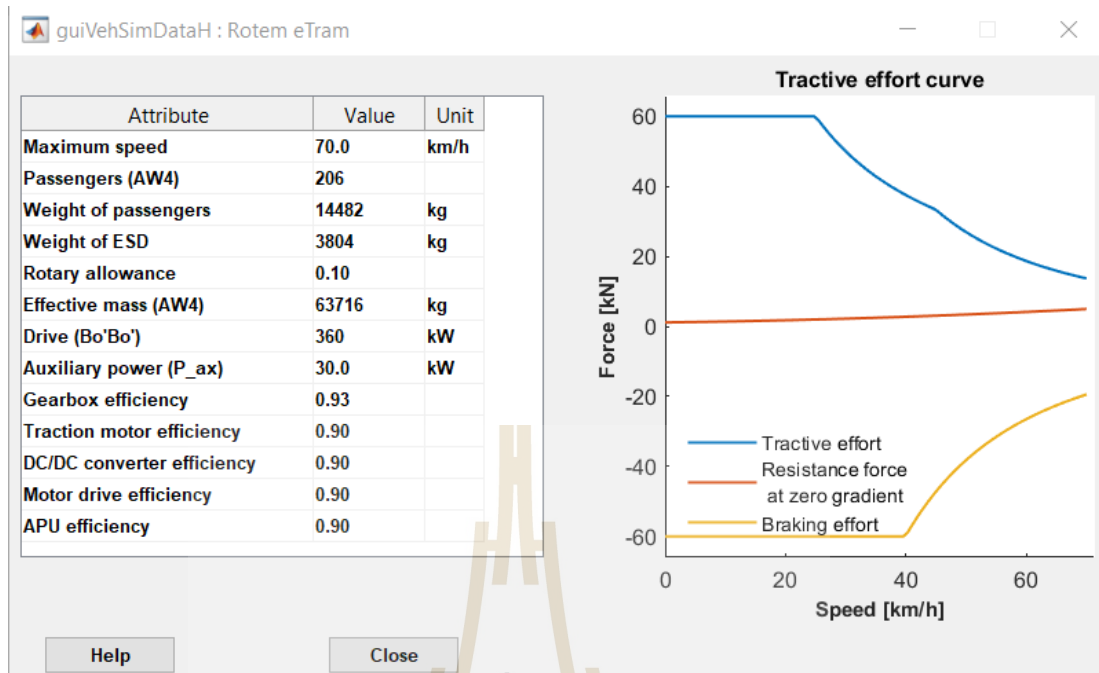


Figure 4.10 Tram echoed input for a cap-ACL-Tram

Simulation results for a cap-ACL-Tram are shown in Figure 4.11 through Figure 4.14, and results summary is presented in Table 4.3.

Tractive effort and speed profiles are shown in Figure 4.11. Tram power demand  $P_{dm}$ , power from contact line (accelerating contact line)  $P_{cl}$  and power from capacitor bank  $P_{cb}$  profiles are shown in Figure 4.12.

Capacitor bank SOE  $\beta_{cb}$ , capacitor bank voltage  $V_{cb}$ , and capacitor bank current  $I_{cb}$  profiles are shown in Figure 4.13. Distance covered (travelled), net energy consumption, and capacitor bank state of charge  $\beta_{cb}$  simulation results for a cap-ACL-Tram are shown in Figure 4.14.

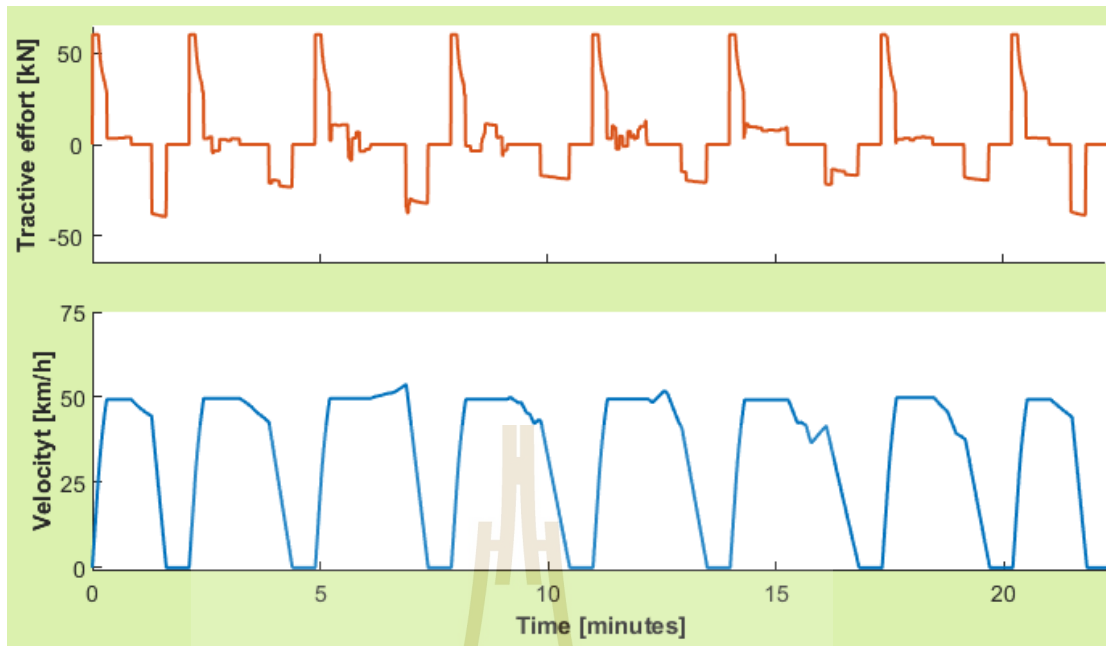


Figure 4.11 Tractive effort and speed profile results for a cap-ACL-Tram



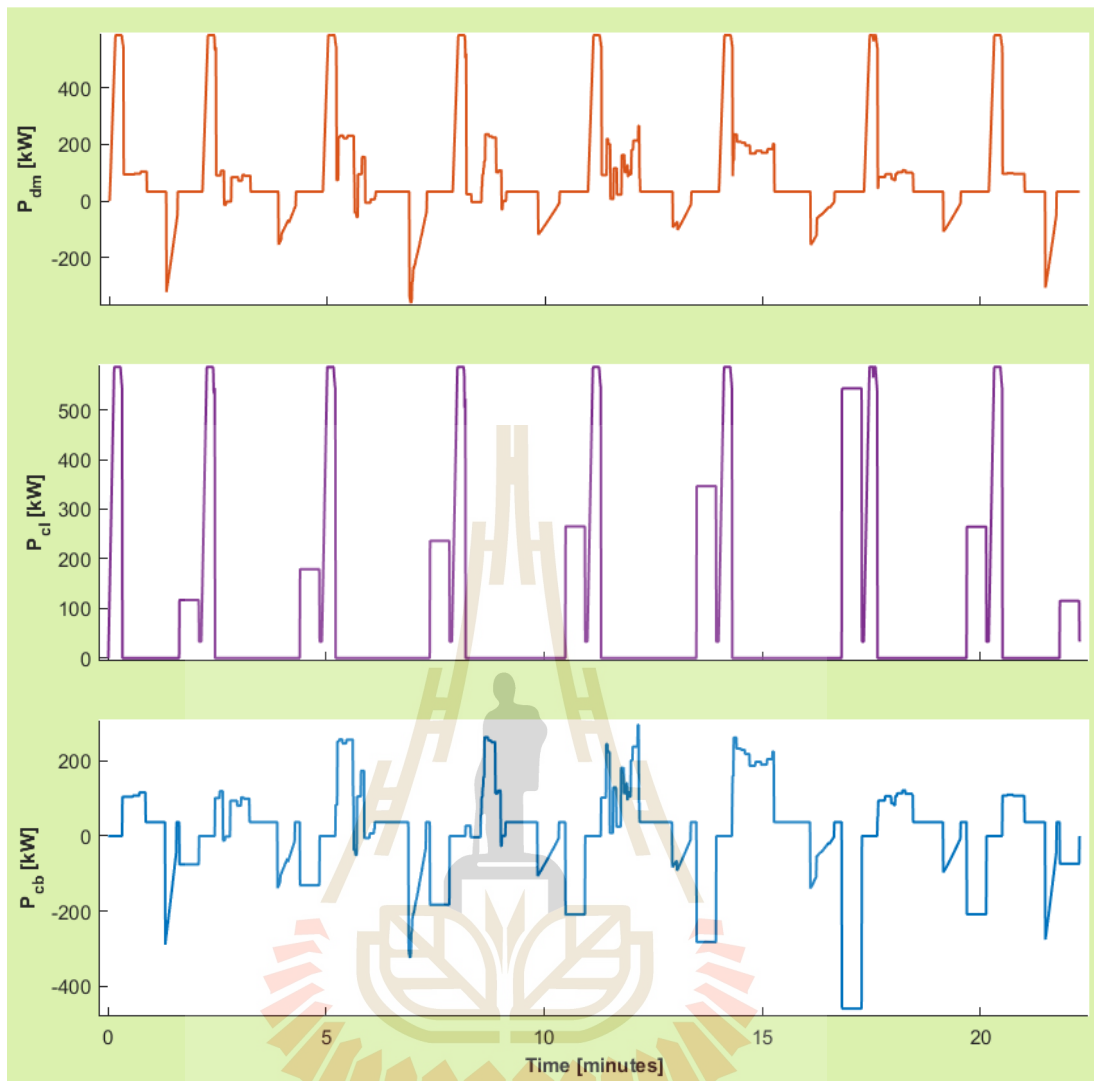


Figure 4.12 Power demand, power from contact line (ACL), and power from capacitor bank results for a cap-ACL-Tram.



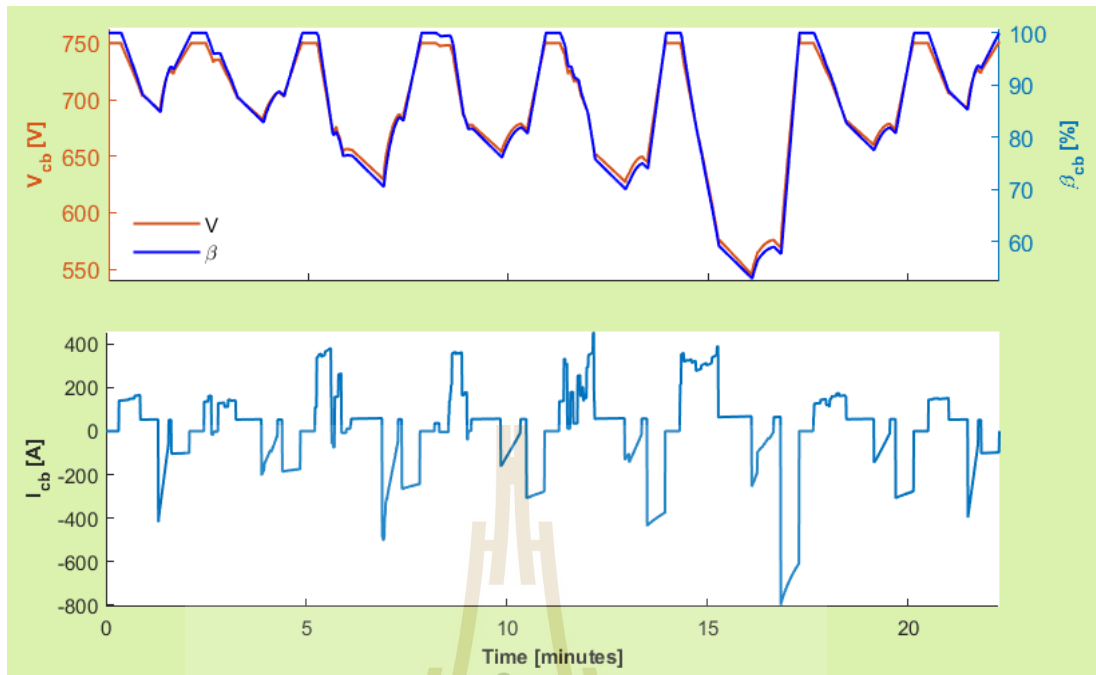


Figure 4.13 Capacitor bank SOE, voltage, and current results for a cap-ACL-Tram

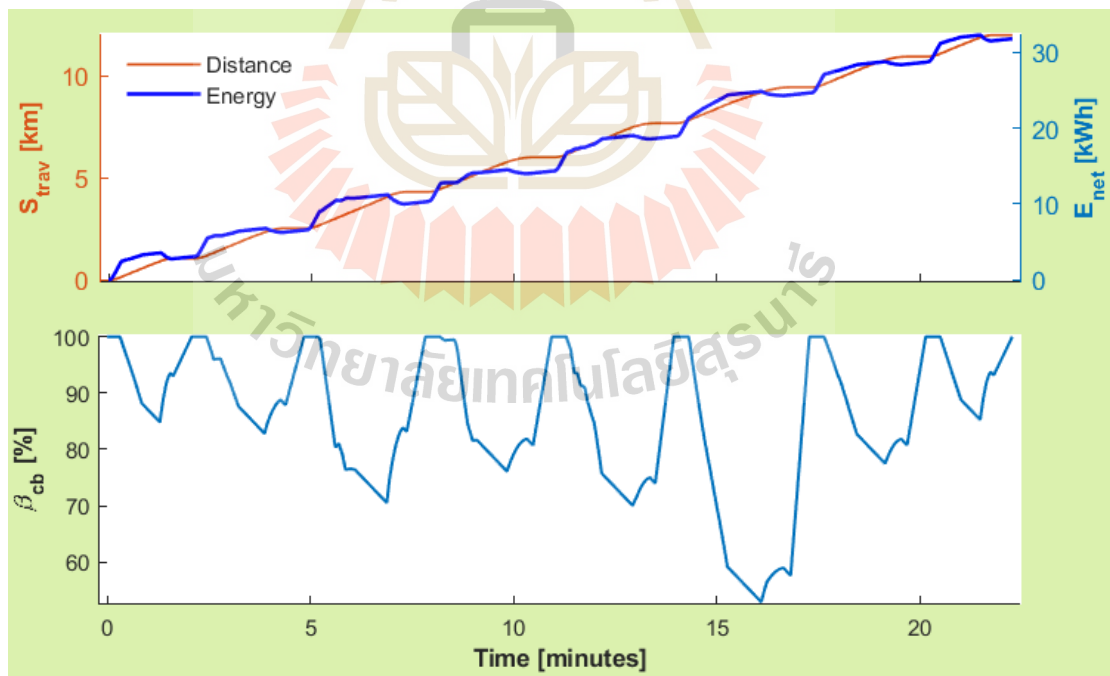


Figure 4.14 Distance travelled, net energy consumption, and capacitor bank SOE results for a cap-ACL-Tram.

**Table 4.3** Simulation results summary for cap-ACL-Tram

Section	$S_{stn}$ [m]	$S_{stn}^{trv}$ [m]	$T_{stn}$ [sec]	$T_{std}$ [sec]	$E_{stn}$ [kWh]	$E_{std}$ [kWh]	$E_{cl}^{trv}$ [kWh]	$E_{cb}^{trv}$ [kWh]	$E_{cl}^{dw}$ [kWh]	$E_{cb}^{dw}$ [kWh]	$\beta_{cb}^{arv}$ [%]	$\beta_{cb}^{dep}$ [%]
S1 - S2	1058	1058	98	128	2.82	3.09	2.46	0.57	0.91	-0.58	93	100
S2 - S3	1482	1482	136	166	3.23	3.51	2.45	0.99	1.37	-1	87.9	100
S3 - S4	1776	1776	149	179	3.45	3.73	2.47	1.37	1.8	-1.39	83.2	100
S4 - S5	1697	1697	157	187	3.75	4.03	2.44	1.57	2.02	-1.59	80.7	100
S5 - S6	1671	1671	151	181	4.28	4.56	2.46	2.13	2.63	-2.14	74	100
S6 - S7	1760	1760	170	200	5.46	5.74	2.46	3.46	4.17	-3.53	57.6	100
S7 - S8	1498	1498	142	172	3.78	4.05	2.44	1.57	2.01	-1.58	80.8	100
S8 - S9	1058	1058	98	126	2.81	3.06	2.46	0.56	0.87	-0.56	93.2	100

#### 4.5 Discussion

Simulation results summary for both trams (cap-Tram and cap-ACL-Tram) is presented in Table 4.4. Both trams have equivalent performances with regard to net energy consumption, trip time and, minimum capacitor bank SOE during travel. However, the cap-ACL-Tram system promises significant capacitor bank size reduction.

**Table 4.4.** Trams performance comparison summary

	Capacitor bank size [modules]	Capacitor bank size [kWh]	$m_{total}$ [metric tons]	$E_{trp}$ [kWh]	$T_{trp}$ [minutes]
cap-Tram	108	14.77	62.63	32.29	22.28
cap-ACL-Tram	60	8.2	59.59	31.79	22.28

##### 4.5.1 Capacitor bank reduction

The cap-ACL-Tram system reduces capacitor bank size by 44.44%. That is, from 108 supercapacitor modules to 60. This reveals a significant reduction in capacitor bank cost. Considering a capacitor module (Maxwell 125V, 63F) cost of 5,000

USD, capacitor bank cost is reduced by 240,000 USD (Mouser Electronics, Inc., 2018) and (Arrow Electronics, Inc, 2018).

As previously mentioned, conventional cap-Tram system (usually) needs a charging infrastructure at every stopping station, as it is the case with the supercapacitor tram in China. Assuming there is a charging infrastructure at every stopping station as needed by cap-Tram system, then, the proposed cap-ACL-Tram system does not add cost on traction substations. The only added cost is to extend the charging feeder. That is, having a short contact line extending from a station.

Having 9 stations (8 interstation sections), the route's total electrified distance is 1.2 km. That is, 150 m for each interstation section. Considering electrification cost of £45,000 (approximately 62,100 USD) per track km, the added cost (for ACLs) is 74,520 USD. This assumes a single wire trolley type ACL arrangement (because of low speed) and not the catenary type (DeltaRail Group Limited, 2010).

The capacitor bank cost reduction is 240,000 USD, whereas added cost for the ACLs is 74,520 USD. This considers only one tram operation on the route. Thus, with just one tram, the reduced cost is more than three times the added cost. It is noteworthy that, the reduced cost is proportional to the number of trams on the route, but the added ACLs cost is approximately fixed. That means, the reduced cost will double (becoming 480,000 USD) for two trams, and triple (becoming 720,000 USD) for three trams, and so forth. Whereas the added ACL cost will be fixed at 74,520 USD. This is very interesting, it shows significant cost reduction, especially with multiple trams operation on the route.

#### 4.5.2 Effect of gradient

Despite the route having small gradients (2% to -2%), effect of gradient is evident on sections S3 - S4 (downhill) and S6 - S7 (uphill). These sections' distances are almost the same (1.776 km and 1.76 km respectively), but both trams consume more energy on section S6 - S7 (uphill) than on section S3 - S4 (downhill).

Effect of gradient on power and current demand can also be noticed on sections S1 – S2, (fairly flat), S2 - S3 (fairly flat and downhill), and S4 – S6 (rough, ups and downs) as shown in Figure 4.15 (for a cap-ACL-Tram).

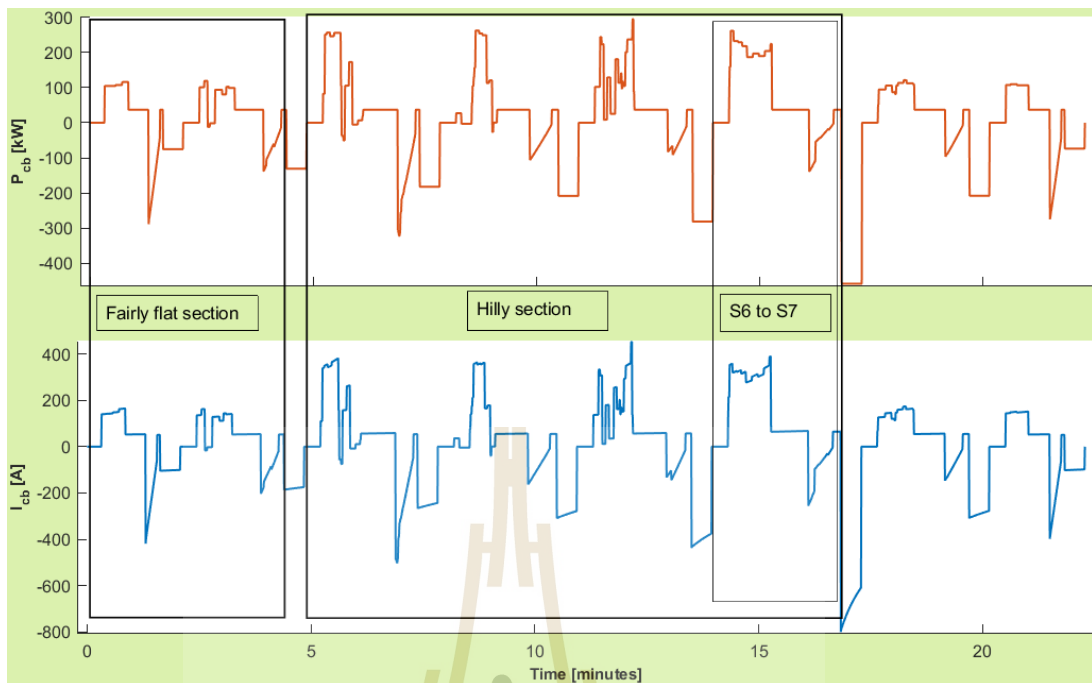


**Figure 4.15** Effect of gradient on power and current demand (cap-ACL-Tram)

Even with the small gradients (2% to -2%), gradient effect on power and current demand is huge as shown in Figure 4.15 above (a cap-ACL-Tram). Therefore, both tram systems are not recommended on hilly routes. With the proposed tram system, a hilly route offsets the advantage of the ACL. That is, what was avoided during acceleration is encountered on uphill.

Supercapacitors have low energy density (unlike other ESDs like batteries), if they are the sole energy storage devices, they are preferred on routes that do not require high energy consumption between any two stations. This can be seen on section S6 – S7 (uphill), see the results summary table.

If a capacitor bank is fully charged during dwell time, then its needed size is just to move a tram to the next stop. This means, for a given route, an interstation section with the highest energy consumption (gradients play significant role) will determine the size of the capacitor bank.

### 4.5.3 Significance of ACLs

It is appealing to note that, with the cap-ACL-Tram system, energy from ACL during interstation travel  $E_{cl}^{trv}$  is more than that from capacitor bank  $E_{cb}^{trv}$  for all interstation sections except section S6 – S7, the uphill section. This agrees with what was mentioned in chapter I. That is, attributed to their high inertial and low rolling friction, trams consume more energy during acceleration, and much less energy thereafter. This also shows the significance of the ACLs.

### 4.5.4 Supercapacitors and ACL

Both trams arrive at station S7 with capacitor bank SOE of around half (50%), the minimum limit. Station S7 comes after an uphill section S6 – S7. Both trams leave station S7 with capacitor bank fully charged. The ACL delivers 7.42 kWh and 4.17 kWh to the cap-Tram capacitor bank and the cap-ACL-Tram capacitor bank respectively. This significant amount of recharge within 30 seconds is possible with supercapacitors since they can be charged quickly (they have high power densities), unlike batteries. This shows a good match between supercapacitors and ACLs, it also shows a good utilization of the charging infrastructure.



## CHAPTER V

### CONCLUSION AND FUTURE WORKS

#### 5.1 Conclusion

On-board storage system in trams is enhanced using Accelerating Contact Lines (ACLs). An ACL is a short extension of a conventional charging bar (at a tram station) that supplies accelerating power as the tram leaves a station. Since trams demand high energy during acceleration, the ACLs are expected to significantly (depending on interstation distances) reduce the needed capacity (size) of the on-board storage device. Hence, cost reduction for the on-board storage device, and reduction in tram effective weight. The latter further reduces tram energy consumption.

One of the scenarios where ACLs prove useful is when a railway route cannot be fully electrified, for reasons such as i) aesthetic in city centers and historical sites, ii) electrification complexity due to crossings, bridges, and not enough right of way, and iii) electrification cost on idle routes.

In this study, a supercapacitor tram system, that is, a tram powered solely by supercapacitors (cap-Tram) and the proposed supercapacitor and accelerating contact line hybrid tram system (cap-ACL-Tram) are modelled and simulated using MATLAB (m-files). Simulation results indicate that, comparatively, the cap-ACL-Tram system reduces the required size of the on-board energy storage device by 44%, tram effective weight by 4.8%, and tram energy consumption by 1.5%.

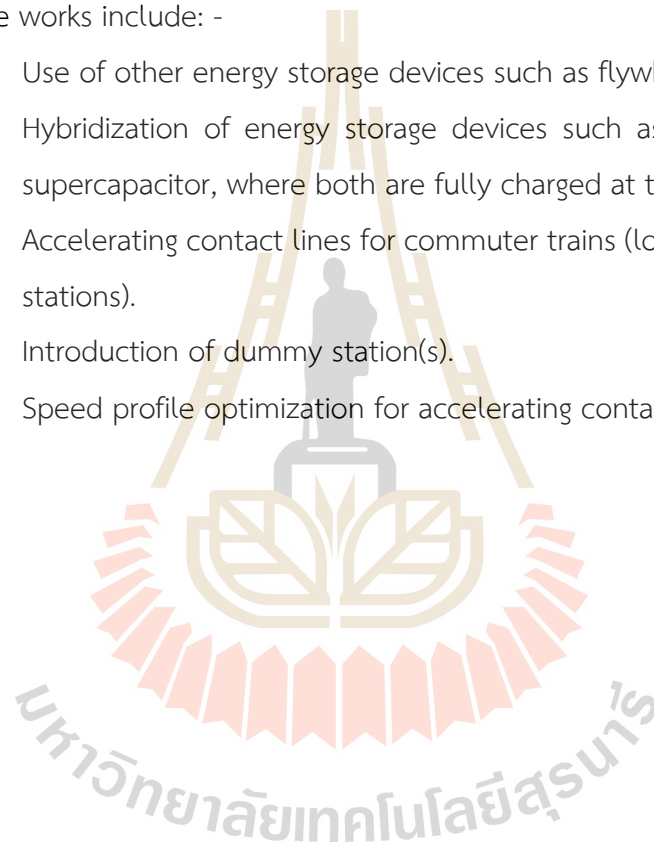
The reduction in OBESD is significant, considering the current supercapacitor cost (a Maxwell 125V, 63F supercapacitor module costing 5,000 USD). Moreover, such a reduction considers only one tram case. Doubling the number of trams (operating on a route) will double the cost reduction in on-board energy storage device while the cost of ACLs stays the same. Therefore, cost reduction in on-board energy storage device is proportional to the number of trams, whereas ACLs cost is constant.

A tram system that already has charging infrastructure installed at every station, for example, the supercapacitor tram in China, can easily be modified to incorporate ACLs by extending the charging bar. Considering the tram system used in the study, with only one tram, the cost reduction in on-board energy storage device outweighs the ACLs cost.

## 5.2 Future works

Future works include: -

- (i) Use of other energy storage devices such as flywheel.
- (ii) Hybridization of energy storage devices such as lithium battery and supercapacitor, where both are fully charged at terminal stations.
- (iii) Accelerating contact lines for commuter trains (long distances between stations).
- (iv) Introduction of dummy station(s).
- (v) Speed profile optimization for accelerating contact lines tram systems.



## REFERENCES

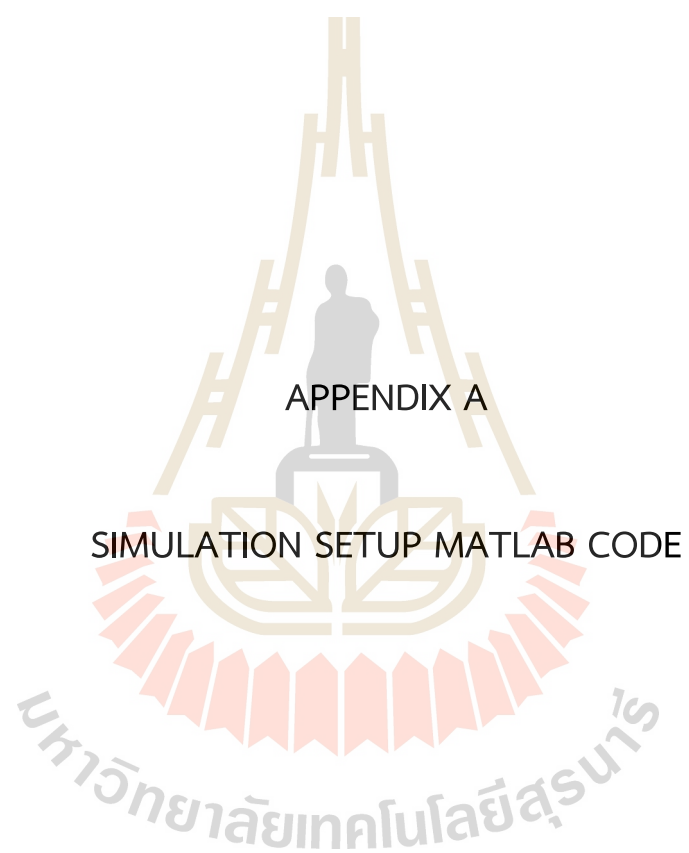
- Ahmadi, S., Dastfan, A., & Assili, M. (2017). Improving energy-efficient train operation in urban railways: employing the variation of regenerative energy recovery rate. *IET Intelligent Transport Systems*, 11(6), 349-357.
- Altairnano. (2021). *70 Amps Hour Cell*. (Altairnano) Retrieved February 4, 2021, from altairnano.com/: <https://altairnano.com/products/70-amp-hour-cell/>
- Arboleya, P., Bidaguren, P., & Armendariz, U. (2016). Energy is On-Board : Energy storage and other alternatives in modern light railways. *IEEE Electrification Magazine* , 30-41.
- Arrow Electronics, Inc. (2018). *BMOD0063P125B08 Maxwell Technologies*. Retrieved June 3, 2018, from richardsonrfpd.com: <http://www.richardsonrfpd.com/Pages/Product-Details.aspx?productId=1015022>
- Barrow, K. (2014, May 29). *CSR unveils 100% supercapacitor-powered tram*. (railjournal.com) Retrieved July 18, 2020, from <https://www.railjournal.com/passenger/light-rail/csr-unveils-100-supercapacitor-powered-tram/>
- Boicea, V. A. (2014). Energy Storage Technologies: The Past and the Present. *Proceedings of the IEEE*, 102(11), 1777-1794, doi: 10.1109/JPROC.2014.2359545.
- Cheng, L., Wang, W., Wei, S., Lin, H., & Jia, Z. (2018). An Improved Energy Management Strategy for Hybrid Energy Storage System in Light Rail Vehicles. *Energies*, 11(2), 423. <https://doi.org/10.3390/en11020423>.
- DeltaRail Group Limited. (2010, July). *Low Cost Electrification for Branch Lines*. Retrieved February 14, 2021, from [https://assets.publishing.service.gov.uk/government/uploads/system/uploads/attachment\\_data/file/3872/low-cost-electrification-report.pdf](https://assets.publishing.service.gov.uk/government/uploads/system/uploads/attachment_data/file/3872/low-cost-electrification-report.pdf)
- Farhadi, M., & Mohammed, O. (2016). Energy Storage Technologies for High-Power Applications. *IEEE Transactions on Industry Applications*, 52(3), 1953-1961, doi: 10.1109/TIA.2015.2511096.



- Golchoubian, P., & Azad, N. L. (2017). Real-Time Nonlinear Model Predictive Control of a Battery–Supercapacitor Hybrid Energy Storage System in Electric Vehicles. *IEEE Transactions on Vehicular Technology*, 66(11), 9678-9688, doi: 10.1109/TVT.2017.2725307.
- Hyundai Rotem; Hyundai Motor Group. (2014). *Project Record : Catenary-free Low-floor tram*. (Hyundai Rotem Company) Retrieved July 5, 2020, from [hyundai-rotem.co.kr: https://www.hyundai-rotem.co.kr/Eng/Business/Rail/Business\\_Record\\_View.asp?brid=68](https://www.hyundai-rotem.co.kr/Eng/Business/Rail/Business_Record_View.asp?brid=68)
- ITCgroup. (2014, April). *Hybrid Low Floor Tram*. Retrieved May 31, 2018, from [itcgroup.cz/: http://www.itcgroup.cz/download.php?id=732](http://www.itcgroup.cz/download.php?id=732)
- Iwase, T., Kawamura, J., Tokai, K., & Kageyama, M. (2015). Development of battery system for railway vehicle. *2015 International Conference on Electrical Systems for Aircraft, Railway, Ship Propulsion and Road Vehicles (ESARS)* (pp. 1-6). Aachen, Germany: IEEE.
- Kermani, M., Parise, G., Chavdarian, B., & Martirano, L. (2020). Ultracapacitors for port crane applications: Sizing and techno-economic analysis. *Energies*, doi: 10.3390/en13082091.
- Liu, S., Jiang, J., Shi, W., Ma, Z., Wang, L. Y., & Guo, H. (2015). Butler–Volmer–Equation–Based Electrical Model for High-Power Lithium Titanate Batteries Used in Electric Vehicles. *IEEE Transactions on Industrial Electronics*, 62(12), 7557-7568, doi: 10.1109/TIE.2015.2449776.
- Maxwell Technologies. (2021). *All Ultracapacitor Documents*. Retrieved July 25, 2021, from [maxwell.com: https://maxwell.com/products/ultracapacitors/downloads/](https://maxwell.com/products/ultracapacitors/downloads/)
- Moghbeli, H., Hajisadeghian, H., & Asadi, M. (2016). Design and simulation of hybrid electrical energy storage (HEES) for Esfahan urban railway to store regenerative braking energy. *2016 7th Power Electronics and Drive Systems Technologies Conference (PEDSTC)* (pp. 93-98). Tehran, Iran: IEEE.
- Mouser Electronics, Inc. (2018). *Maxwell Technologies BMOD0063 P125 B08*. Retrieved June 3, 2018, from [th.mouser.com: https://th.mouser.com/c/passive-components/capacitors/supercapacitors-ultracapacitors/?m=Maxwell+Technologies](https://th.mouser.com/c/passive-components/capacitors/supercapacitors-ultracapacitors/?m=Maxwell+Technologies)

- Mwambeleko, J. J. (2015). *Reducing passenger travel fuel cost and emission: A case study of Tanzania commuter trains*. Nakhon Ratchasima, Thailand: Suranaree University of Technology (SUT).
- Mwambeleko, J. J., & Kulworawanichpong, T. (2017). Battery and accelerating-catenary hybrid system for light rail vehicles and trams. *2017 International Electrical Engineering Congress (iEECON)*. Pattaya, Thailand.
- Mwambeleko, J. J., & Kulworawanichpong, T. (2017). Battery electric multiple units to replace diesel commuter trains serving short and idle routes. *Journal of Energy Storage*, 7-15, doi : 10.1016/j.est.2017.01.004.
- Mwambeleko, J. J., Hayasaka, T., & Kulworawanichpong, T. (2020). Enhancing conventional battery and contact line hybrid tram system with accelerating contact lines. *IET Electrical Systems in Transportation*, 105-115.
- Mwambeleko, J. J., Kulworawanichpong, T., & Greyson, K. A. (2015). Tram and trolleybus net traction energy consumption comparison. *2015 18th International Conference on Electrical Machines and Systems (ICEMS)*. Pattaya, Thailand.
- Nicholson, T. J. (2014). DC & AC traction motors. *IET 13th Professional Development Course on Electric Traction Systems* (pp. 1-14). London, UK: IET.
- Raghavendra, K. V., Vinoth, R., Zeb, K., Gopi, C. V., Sambasivam, S., Kummara, M. R., . . . H. J. (2020). An intuitive review of supercapacitors with recent progress and novel device applications. *Journal of Energy Storage*, 31, 1 - 34.
- Saracco, R. (2016, November 2). *Supercapacitor Tram*. Retrieved from IEEE Future Directions: <https://cmt.ee.org/futuredirections/2016/11/02/supercapacitor-tram/>
- Schmid, F., & Goodman, C. (2014). The calculation of train performance. *IET 13th Professional Development Course on Electric Traction Systems* (pp. 1 - 13). London, UK: IET.
- Sengupta, A. S., Satpathy, S., Mohanty, S. P., Baral, D., & Bhattacharyya, B. K. (2018). Supercapacitors Outperform Conventional Batteries [Energy and Security]. *IEEE Consumer Electronics Magazine*, 7(5), 50-53, doi: 10.1109/MCE.2018.2835958.

- Shiraki, N., Tokito, K., & Yokozutsumi, R. (2015). Propulsion system for catenary and storage battery hybrid electric railcar series EV-E301. *2015 International Conference on Electrical Systems for Aircraft, Railway, Ship Propulsion and Road Vehicles (ESARS)* (pp. 1-7). Aachen, Germany: IEEE.
- Sumpavakup, C., Ratniyomchai, T., & Kulworawanichpong, T. (2017). Optimal energy saving in DC railway system with on-board energy storage system by using peak demand cutting strategy. *Journal of Modern Transportation*, *25*(4), 223–235.
- Wang, L., Guo, J., Xu, C., Wu, T., & Lin, H. (2019). Hybrid model predictive control strategy of supercapacitor energy storage system based on double active bridge. *Energies*, doi: 10.3390/en12112134.
- Wang, Y., Yang, Z., & Li, F. (2018). Optimization of energy management strategy and sizing in hybrid storage system for tram. *Energies*, doi: 10.3390/en11040752.
- Wang, Y., Yang, Z., & Lin, F. (2020). A Hybrid Energy Management Strategy based on Line Prediction and Condition Analysis for the Hybrid Energy Storage System of Tram. *IEEE Transactions on Industry Applications*, *6*(2), 1793 - 1803.
- Yihui Wang, B. N. (2011). A Survey on Optimal Trajectory Planning for Train Operations. *Proceedings of 2011 IEEE International Conference on Service Operations, Logistics and Informatics* (pp. 589-594). Beijing, China: IEEE.



The system simulation ground is setup using two classes, namely, CounterTimer class and SimulationGround class. The latter contains a *constant* handle to the object of the former. Other classes inherit from the SimulationGround class. Therefore, they share the CounterTimer object. CounterClass is presented in Algorithm A-1 and SimulationGround class is presented in Algorithm A-2.

Algorithm A-1 Counter and timer class

---



---

CounterTimer class MATLAB code

---



---

```

% Written by Joachim J. Mwambeleko
classdef CounterTimer < handle
    % Object of this class will be shared
    % in order to share time and counter data.
    % Use class that has a constant handle to
    % this class object e.g. SimulationGround
    % to update properties of this class.
    properties
        dt = 0.5;
        k = 0;    % Simulation counter
        time = 0;
        timeArray = ones(1, 100) * NaN;
        countArray = ones(1, 100) * NaN;
    end
end
end

```

---



---

## Algorithm A-2 Simulation ground class

## simulationGround class MATLAB code

---

```
% Written by Joachim J. Mwambeleko
```

```
% To set the ground for simulation
```

```
% This class will be inherited by almost all other classes
```

```
% MAKE SURE, its constructor can accept zero arguments
```

```
classdef SimulationGround < matlab.mixin.SetGet
```

```
    properties (Constant, Hidden)
```

```
        g = 9.8;
```

```
        mps2kph = 3.6;
```

```
        kph2mps = 1/3.6;
```

```
        h2s = 3600;
```

```
        s2h = 1/3600;
```

```
        RISE_ERRORS = true;
```

```
        ct = CounterTimer; % Constant handle
```

```
    end
```

```
    properties (SetAccess = immutable)
```

```
        DAS; % Used to clear reset arrays of the CounterTimer
```

```
        % It will be empty in other subclass objects
```

```
    end
```

```
    methods
```

```
        function obj = SimulationGround(dt, DAS)
```

```
            if nargin > 0
```

```
                mustBeNonempty(dt)
```

```
                mustBeNumeric(dt)
```

```
                obj.ct.dt = dt;
```

```
            end
```

---

---

simulationGround class MATLAB code

---

```
if nargin > 1
    mustBeInteger(DAS)
    obj.DAS = DAS;
    obj.ct.timeArray = ones(1, DAS) * NaN;
    obj.ct.countArray = ones(1, DAS) * NaN;
end
end
end

methods
function x = initiateStorage(obj)
    x = obj.ct.timeArray * NaN;
end

function up(obj)
    % Ups (updates) CounterTimer

    % Increment counter,
    obj.ct.k = obj.ct.k + 1;
    % Store current time,
    obj.ct.countArray(obj.ct.k) = obj.ct.k;
    obj.ct.timeArray(obj.ct.k) = obj.ct.time;
    % Then increment time.
    obj.ct.time = obj.ct.time + obj.ct.dt;
end

function clearCT(obj)
    %Clears CounterTimer
    obj.ct.k = 0;
    obj.ct.time = 0;
```

---

---

simulationGround class MATLAB code

---

```
obj.ct.timeArray = ones(1, obj.DAS) * NaN;  
obj.ct.countArray = ones(1, obj.DAS) * NaN;
```

```
end
```

```
end
```

```
end
```

---







APPENDIX B

CAPACITOR MODULE AND CAPACITOR BANK MATLAB CODE

มหาวิทยาลัยเทคโนโลยีสุรนารี

This section presents MATLAB code used to create capacitor bank object. Capacitor module class is presented in Algorithm B 1, capacitor module data function is presented in Algorithm B 2, and a function to create capacitor bank object and display its information is presented in Algorithm B 3. Capacitor bank class is presented in Algorithm B 4. A function to display capacitor bank data in GUI is presented in Algorithm B 5. The GUI figure is developed using GUIDE.

Algorithm B-1 Capacitor module class

---



---

CapModule class MATLAB code

---



---

% Written by Joachim J. Mwambeleko

`classdef` CapModule < SimulationGround

`properties`

    % Will be inherited and modified in CapBank

    name

    image

    voltageRated

    voltageFullCharge

    voltageMaxSeries

    capacitance

    energyFullCharge

    currentMax

    ESR

    mass

    soelInitial

    voltageInitial

`end`

`properties` (Hidden) % For Simulation

    simRemarks

---

---

 CapModule class MATLAB code
 

---

```

soe
voltage {mustBeReal}
powerArray
currentArray
soeArray
voltageArray {mustBeReal}
end
methods % Constructor
function obj = CapModule(data, SoE, setForSim)
    obj.name = data.name;
    obj.image = data.image;
    obj.voltageRated = data.voltageRated;
    obj.voltageFullCharge = data.voltageFullCharge;
    obj.voltageMaxSeries = data.voltageMaxSeries;
    obj.currentMax = data.currentMaxContinous;
    obj.capacitance = data.capacitance;
    obj.ESR = data.ESR;
    obj.mass = data.mass;
    obj.energyFullCharge = (0.5 * obj.capacitance * ...
        obj.voltageFullCharge ^ 2)*obj.s2h; % [Wh]

    % If SoE is given use it to compute voltage (initial)
    if nargin > 1 && not(isempty(SoE))
        mustBeGreaterThanOrEqual(SoE, 0)
        mustBeLessThanOrEqual(SoE, 1)
        [obj.soe, obj.soeInitial] = deal(SoE);
        [obj.voltage, obj.voltageInitial] = ...
            deal(sqrt(obj.soe) * obj.voltageFullCharge);
    end
end

```

---

---

 CapModule class MATLAB code
 

---

```

if nargin > 2 && setForSim == true
    [obj.powerArray,...
     obj.currentArray,...
     obj.soeArray,...
     obj.voltageArray] = deal(obj.initiateStorage());
end
end
end
methods % APIs
function chargeDischarge(obj, P)
    % P : power at cap module terminals

    pMAX = 0.12 * obj.voltage ^2 / obj.ESR; % per IEC 62391-2
    if abs(P) > pMAX
        error('Power %.1f [W] beyond max %.1f [W]',...
             P, pMAX)
    end

    I = P/obj.voltage;

    if abs(I) > obj.currentMax
        error('Current %.1f [A] beyond max %.1f [A]', ...
             I, obj.currentMax)
    end

    dE_Wh = ((P + I^2 * obj.ESR) * obj.ct.dt)* obj.s2h;
    dSoE = dE_Wh/obj.energyFullCharge;
    nextSoE = obj.soe - dSoE;

    if nextSoE >= 1.01 || nextSoE < 0

```

---

---

CapModule class MATLAB code

---

```
[P, I] = deal(0, 0);  
[SoE, V] = deal(obj.soe, obj.voltage); % Retain  
else  
    SoE = nextSoE;  
    if SoE > 1, SoE = 1; end  
    Vo = sqrt(SoE) * obj.voltageFullCharge;  
    V = Vo - I * obj.ESR;  
end  
  
% NOTE: obj.soe and obj.voltage are instantiated  
obj.powerArray(obj.ct.k) = P;  
obj.currentArray(obj.ct.k) = I;  
obj.soeArray(obj.ct.k) = obj.soe;  
obj.voltageArray(obj.ct.k) = obj.voltage;  
  
% Update state variables  
obj.soe = SoE;  
obj.voltage = V;  
end  
function plotChargeDischarge(obj)  
    ResultsCap(obj).plotChargeDisCharge()  
end  
end  
end
```

---

## Algorithm B-2 Capacitor module data function

## Capacitor Module Data MATLAB code

---

```

% **** CAPACITOR MODULE DATA ****

% Maxwell 125V, 63F

function cap = data_capModule_Maxwell_125V_63F()
cap.name = "Maxwell_125V_63F";
cap.manufacturer = "Maxwell Technologies";
cap.image = imread('Image_Supercap_Maxwell_125V_63F_380x200.png');

cap.voltageRated = 125;
cap.voltageFullCharge = 125;
cap.voltageMaxSeries = 1500;
cap.capacitance = 63 ; % [Farads]

cap.currentMaxContinous = 1900;
cap.currentMax = 1900;

cap.ESR = 18e-3; % [ohms]
% cap.ESR = 18e; % See effect of ESR

% Physical properties
cap.mass = 63.4;
cap.massRemarks = "Including cooling fan [kg]";

% *** Projected Life ***
cap.cycleLife = 1e6 ; % [Cycles]
cap.dcLife = 10 ; % [years], Stored at rated voltage
cap.shelfLife = 4 ; % [years], Stored full discharged

% *** Cost ***

```

---

---

```

cap.cost = 5000;      % USD
cap.costRemarks = "As of 2021. Source : email";

cap.reference = ...
    "https://maxwell.com/products/ultracapacitors/modules/";

```

---

Algorithm B-3 Capacitor bank object create function

---

createCapBank function MATLAB code

---

```

% Written by Joachim J. Mwambeleko

function capBank = createCapBank(ts)
% Creates capacitor bank object and
% calls gui function to display capBank info

% INPUTS
% ts : Tram System (from TramSystem)

% The function can be run without inputs (easy debugging)
if nargin == 0
    [nms, nps] = deal(2);
else
    [nms, nps] = deal(ts.nms, ts.nps);
end

SoE = 1;

moduleData = data_capModule_Maxwell_125V_63F();
capSimData = struct(...
    'SoE', SoE,...
    'converter_voltageMin',500,...

```

---

---

```
'converter_voltageMax', 1200);

capBank = CapBank(moduleData, nms, nps, capSimData);
moduleObject = CapModule(moduleData, capSimData.SoE);
capBank.guiCapSimData(moduleObject);
```

---

Algorithm B-4 Capacitor bank class

---

CapBank class MATLAB code

---

% Written by Joachim J. Mwambeleko

```
classdef CapBank < CapModule
    % NOTE: CapModule(superclass) constructor needs
    %   i) capacitor module data (md)
    %   ii) Initial SOE, (optional) for simulation purpose, and
    %   iii) setForSim (Optional, boolean) for simulation purpose
    % If setForSim is true, CapModule will initiate storage for
    % variables needed for simulation
    properties (SetAccess = immutable)
        voltageMinLimit
        voltageMaxLimit
        numModules {mustBeInteger}
        numModulesSeries {mustBeInteger}
        numParallelStrings {mustBeInteger}
    end

    methods % Constructor
        function obj = CapBank(md, nms, nps, simData)
            %md : module data

            % CapModule object set for simulation
```

---



---

 CapBank class MATLAB code
 

---

```

obj@CapModule(md, simData.SoE, true);

obj.numModulesSeries = nms;
obj.numParallelStrings = nps;
obj.numModules = nms * nps;

% Modify values inherited from CapModule
obj.ESR = obj.ESR * nms / nps;
obj.capacitance = obj.capacitance * nps / nms;
obj.energyFullCharge = obj.energyFullCharge * nms * nps;
obj.mass = obj.mass * obj.numModules;
obj.currentMax = obj.currentMax * nps;
obj.voltageFullCharge = obj.voltageFullCharge * nms;
obj.voltage = sqrt(obj.soe) * obj.voltageFullCharge;
obj.voltageInitial = obj.voltage;

obj.name = sprintf('%d V capBank_from_%s',...
  obj.voltageFullCharge, obj.name);

% Assign CapBnk voltage limit properties
obj.voltageMinLimit = simData.converter_voltageMin;
obj.voltageMaxLimit = min(...
  simData.converter_voltageMax, obj.voltageMaxSeries);
%Check voltage_fullcharge Vs voltageMaxLimit
mustBeLessThanOrEqualTo(obj.voltageFullCharge,...
  obj.voltageMaxLimit)

end
end

methods % capBank State Update API

```

---

---

 CapBank class MATLAB code
 

---

```

function updateState(obj, power)
    chargeDischarge(obj, power)
    if obj.voltage < obj.voltageMinLimit
        error('Voltage [V] below min: %.1f < %.1f ',...
            obj.voltage, obj.voltageMinLimit)
    end
end

function p = getPowerToFullCharge(obj, time)
    % energy needed [Watt-sec] / time [sec]
    p = 1.1 * (1 - obj.soe) * ...
        obj.energyFullCharge * obj.h2s / time;
end

function varsTable = tableVariables(obj)
    varNames = {'Index', 'Time_S', 'SOE', 'Voltage_V',...
        'Power_W', 'Current_A'};
    varsTable = table(...
        obj.ct.countArray',... % Note :
        obj.ct.timeArray',... % vars are transposed
        obj.soeArray' * 100,...
        obj.voltageArray', ...
        obj.powerArray', ...
        obj.currentArray', ...
        'VariableNames', varNames);
end

function trimArrays(obj)

```

```

%NOTE

```

---

---

 CapBank class MATLAB code
 

---

```

% The class has to be a handle class
if length(obj.soeArray) > obj.ct.k
    obj.soeArray = obj.soeArray(1 : obj.ct.k);
    obj.powerArray = obj.powerArray (1 : obj.ct.k);
    obj.currentArray = obj.currentArray (1 : obj.ct.k);
    obj.voltageArray = obj.voltageArray (1 : obj.ct.k);
end

if length(obj.ct.timeArray) > obj.ct.k
    obj.ct.timeArray = obj.ct.timeArray(1 : obj.ct.k);
    obj.ct.countArray = obj.ct.countArray(1 : obj.ct.k);
end
end

function guiCapSimData(obj, Module)
    % Module : Module Object
    guiCapBankSimData(obj, Module);
end
end
end
  
```

---

 Algorithm B-5 Function to display capacitor bank data in GUI
 

---

 guiCapBankSimData function MATLAB code
 

---

```

function varargout = guiCapBankSimData(varargin)
% Begin initialization code - DO NOT EDIT
gui_Singleton = 1;
gui_State = struct('gui_Name',    mfilename, ...
                  'gui_Singleton', gui_Singleton, ...
                  'gui_OpeningFcn', @guiCapBankSimData_OpeningFcn, ...
  
```

---

---

 guiCapBankSimData function MATLAB code
 

---

```

    'gui_OutputFcn', @guiCapBankSimData_OutputFcn, ...
    'gui_LayoutFcn', [], ...
    'gui_Callback', []);
if nargin && ischar(varargin{1})
    gui_State.gui_Callback = str2func(varargin{1});
end

if nargin
    [varargout{1:nargout}] = gui_mainfcn(gui_State, varargin{:});
else
    gui_mainfcn(gui_State, varargin{:});
end
% End initialization code - DO NOT EDIT

% --- Executes just before guiCapBankSimData is made visible.
function guiCapBankSimData_OpeningFcn(hObject, ~, handles, varargin)
% This function has no output args, see OutputFcn.
% hObject    handle to figure
% eventdata  reserved - to be defined in a future version of MATLAB
% handles    structure with handles and user data (see GUIDATA)
% varargin   command line arguments to guiCapBankSimData (see VARARGIN)

fontName = 'Times New Roman';
fontSize = 10 ;
%----- Inputs -----
cb = varargin{1};
cm = varargin{2};

%----- Main Figure -----

```

---

---

 guiCapBankSimData function MATLAB code
 

---

```

% set(handles.mainFigure, 'menubar', 'figure')

%----- Supercap Image -----
axes(handles.Image)
imshow(cb.image);
title(cb.name,...
      'FontName',fontName, 'fontSize', fontSize, 'interpreter', 'none')

%----- nModules & nPS(Parallel strings) -----
set(handles.nModules, 'String',...
      [num2str(cb.numModules), ' modules (total)']);
set(handles.nPS, 'String', ...
      [num2str(cb.numParallelStrings), ' parallel strings']);
set(handles.nSeries, 'String',...
      [num2str(cb.numModulesSeries), ' modules in series'])

%- - - Table 1 Data - - - 7 Rows x 3 Columns
dataTable1 = {
  'Voltage full charge [V]', ...
  sprintf('%0f', cm.voltageFullCharge), ...
  sprintf('%0f', cb.voltageFullCharge);...      % Row 1 End
  'Capacitance [F]', ...
  sprintf('%4g', cm.capacitance),...
  sprintf('%4g', cb.capacitance);...          % Row 2 End
  'Energy full charge [kWh]',...
  sprintf('%2f', cm.energyFullCharge/1e3),...
  sprintf('%2f', cb.energyFullCharge/1e3);... % Row 3 End
  sprintf('ESR [m $\times$ 2126]'),...
  sprintf('%0f', cm.ESR * 1e3),...

```

---

---

 guiCapBankSimData function MATLAB code
 

---

```

sprintf('%0f', cb.ESR * 1e3);...           % Row 4 End
'Current max continous [A]',...
sprintf('%0f', cm.currentMax),...
sprintf('%0f', cb.currentMax);...
'Voltage max series [V]', ...
sprintf('%0f', cm.voltageMaxSeries),...
sprintf('%0f', cm.voltageMaxSeries);...
'Mass [kg]',...
sprintf('%0f', cm.mass),...
sprintf('%0f', cb.mass);...
};
set(handles.Table1, 'Data', dataTable1)

%----- Table 2 Data -----
if not(isempty(cb.soelInitial))
dataTable2 = {
    'State of Charge [%]',...
    sprintf('%0.3g', cm.soelInitial * 100),...
    sprintf('%0.3g', cb.soelInitial * 100);...
    'Voltage [V]', ...
    sprintf('%0f', cm.voltageInitial),...
    sprintf('%0f', cb.voltageInitial);...
    'Energy stored [kWh]',...
    sprintf('%0.2f', cm.soe * cm.energyFullCharge /1e3),...
    sprintf('%0.2f', cb.soe * cb.energyFullCharge /1e3);...
};

else
dataTable2 = {
    'State of Charge [%]', 'NaN', 'NaN';...

```

---

---

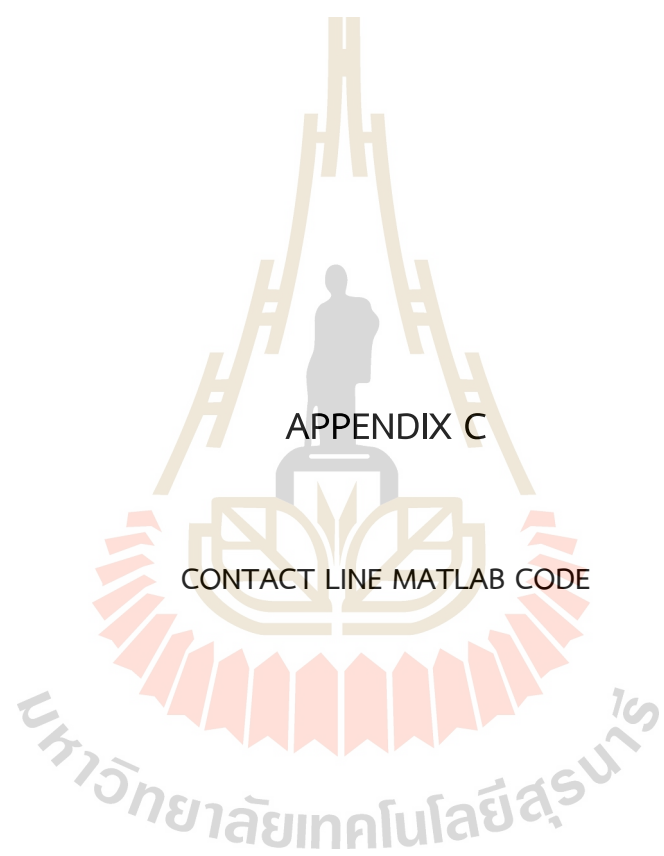
guiCapBankSimData function MATLAB code

---

```
'Voltage [V]', 'NaN', 'NaN';...  
'Energy stored [kWh]', 'NaN', 'NaN';...  
};  
end  
  
set(handles.Table2, 'Data', dataTable2)  
  
% Choose default command line output for guiCapBankSimData  
handles.output = hObject;  
  
% Update handles structure  
guidata(hObject, handles);  
  
% --- Outputs from this function are returned to the command line.  
function varargout = guiCapBankSimData_OutputFcn(~, ~, handles)  
varargout{1} = handles.output;
```

---

มหาวิทยาลัยเทคโนโลยีสุรนารี



APPENDIX C

CONTACT LINE MATLAB CODE

มหาวิทยาลัยเทคโนโลยีสุรนารี



Contact line MATLAB code is presented in this section. The contact line class is presented in Algorithm C-1. The class can be easily tested using the test function presented in Algorithm C-2. Test results are shown in Figure C.1

Algorithm C-1 Contact line class

---

Line class MATLAB code

---

```

% Accelerating Contact Line Class
% Written by Joachim J. Mwambeleko
% Last update : 2021, June, 11
% Use      : Thesis

classdef Line < SimulationGround
    properties(SetAccess = immutable)
        % Contact line default values
        name = 'Overhead DC line'
        voltageNoLoad = 900;
        subR = 30 * 1e-3; % Substation resistance [Ohms]
        lineRPM = 170 * 1e-6; % line resistance per meter [Ohms]
        railRPM = 17.2 * 1e-6; % rail RPM [Ohms]
        len = 150; % ACL length [m]
        clearance = 6;
    end
    properties(Hidden) % For simulation
        voltage % at point of contact to the Tram
        voltageArray
        powerArray
        currentArray
    end

    methods % Constructor
        function obj = Line(data, len, clearance, setForSim)

```

---

---

 Line class MATLAB code
 

---

```

if nargin > 0 && not(isempty(data))
    obj.name = name;
    obj.voltageNoLoad = data.voltageNoLoad;
    obj.subR = data.subR;
    obj.lineRPM = data.lineRPM;
    obj.railRPM = data.railRPM;
end
if nargin > 1 && isPositive(len)
    %isPositive is in supportFuncs folder
    obj.len = len;
end
if nargin > 2 && isPositive(clearance)
    obj.clearance = clearance;
end
if nargin > 3 && setForSim == true
    obj.voltage = obj.voltageNoLoad;
    [obj.powerArray,...
    obj.currentArray,...
    obj.voltageArray]= ...
    deal(obj.initiateStorage());
end
end
end
methods

```

```

function updateState(obj, power, dfs)
    % power tram power demand [W]
    % dfs: tram distance from feeding substation
    if dfs > obj.len - obj.clearance
        power = 0;
    end
end

```

---

---

 Line class MATLAB code
 

---

```

end

if power < 0
    error(['Negative power [kW] %.0f : ',...
        'The line is unidirectional.'], power/1e3)
end

I = power/obj.voltage;
R = obj.lineRPM * dfs;
V = obj.voltageNoLoad - (I * (R + obj.subR));

% obj.voltage has to be initiated
% obj.voltage is the voltage before(at which)
% power was demanded (numerical approach)
obj.powerArray(obj.ct.k) = power;
obj.currentArray(obj.ct.k) = I;
obj.voltageArray(obj.ct.k) = obj.voltage;

%- What's the voltage change after time dt;
%- Voltage taken as a state variable
obj.voltage = V;
end

function plotLineProfile(obj)
    ResultsLine(obj).plotProfile();
end

function varsTable = tableVariables(obj)
    varNames = {'Index', 'Time',...
        'Power_kW','Current_A', 'Voltage_V'};
    % If DAS > k, don't include the NaNs
  
```

---

---

Line class MATLAB code

---

```
varsTable = table(...
    row2col(obj.ct.countArray(1 : obj.ct.k)),...
    row2col(obj.ct.timeArray(1 : obj.ct.k)),...
    row2col(obj.powerArray(1 : obj.ct.k)/1e3),...
    row2col(obj.currentArray(1 : obj.ct.k)), ...
    row2col(obj.voltageArray(1 : obj.ct.k)), ...
    'VariableNames', varNames);
end

function trimArrays(obj)
    % If length(initiated_array_storage) > counter vaule k
    % Trim arrays to counter vaule k (remove the NaNs)

    %Usefulness
    % table and displayTablePortion
    % Results: passing data by value

    %NOTE: plot needs equal length
    if length(obj.soeArray) > obj.ct.k
        obj.soeArray = obj.soeArray(1 : obj.ct.k);
        obj.powerArray = obj.powerArray (1 : obj.ct.k);
        obj.currentArray = obj.currentArray (1 : obj.ct.k);
        obj.voltageArray = obj.voltageArray (1 : obj.ct.k);
    end

    % time and count Arrays might have been trimmed elsewhere
    if length(obj.ct.timeArray) > obj.ct.k
        obj.ct.timeArray = obj.ct.timeArray(1 : obj.ct.k);
        obj.ct.countArray = obj.ct.countArray(1 : obj.ct.k);
    end
end
```

---

---

Line class MATLAB code

---

end

end

end

%{

References

[1]: Energy Saving in Public Transport [IEEE Magazine, 2008]

Network:-

Contact line structure : Overhead contact line

Contact line material : Copper

Contact line crosssectional area : 100 mm<sup>2</sup>

Overhead line resistance : 170E-3 [Ohm/km] = 170E-6 [Ohm/m]

Rail electric resistance : 17.2E-3 [Ohm/km] = 17.2E-6 [Ohm/km]

Substation internal resistance: 30E-3 Ohm

No load substation voltage: 900 V

%}

---

Algorithm C-2 Contact line test function (object) with constant power

---

Line test function(object)teo\_Line\_cp MATLAB code

---

% Written by Joachim J. Mwambeleko

% \*\* Add path (RUN 'main') before running this file

% teo\_Line\_cp : Test Object Line at Constant Power

% Basic Test

% The Line class has default values for line properties

clc ; clear variables; close all

dt = 0.5;

DAS = 5000;

sg = SimulationGround(dt, DAS);

sg.clearCT %clear couterTimer (IMPORTANT)

%Create line Object set for Simulation

len = 150;

clearance = 6;

setForSim = true;

line = Line([], len, clearance, setForSim);

% Test with constant power demand

maxTE = 60e3;

baseSpd = 25 / 3.6;

efc = 0.75;

power = (maxTE \* baseSpd) / efc;

for dfs = 0 : len - clearance

---

---

Line test function(object)teo\_Line\_cp MATLAB code

---

```
sg.up() %update CounterTimer

% Increasing distance dfs
line.updateState(power, dfs);
end

line.plotLineProfile();
disp('Line variables table(table portion)')
displayTablePortion(line.tableVariables())
```

---



มหาวิทยาลัยเทคโนโลยีสุรนารี

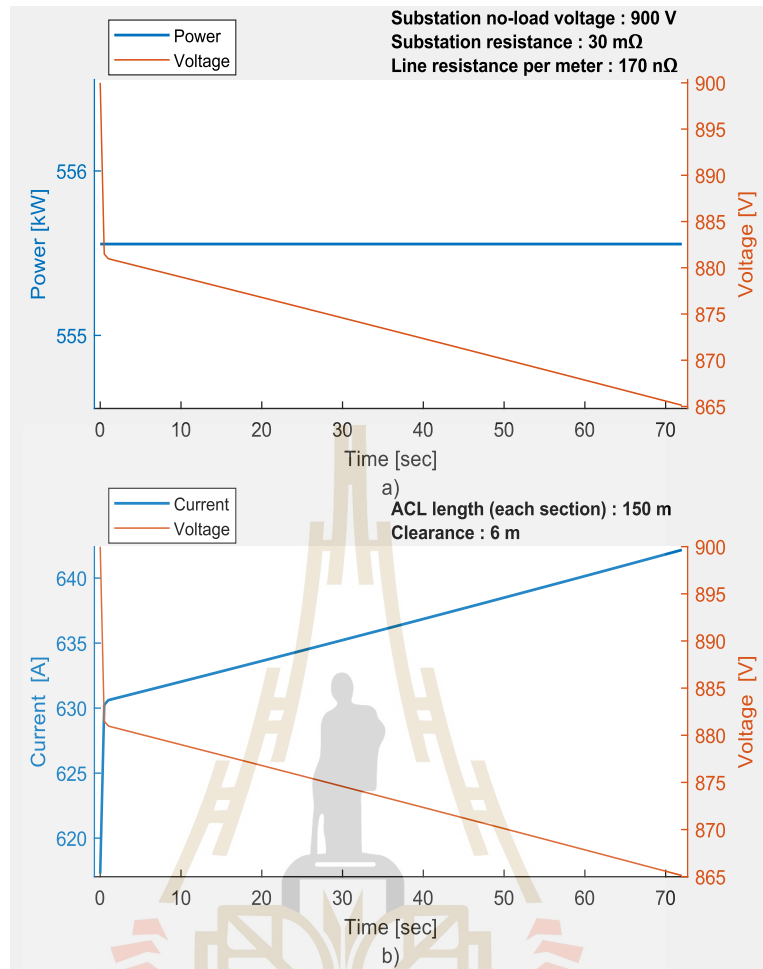
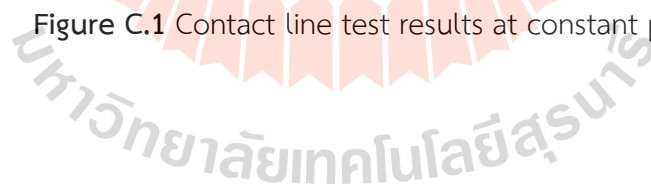
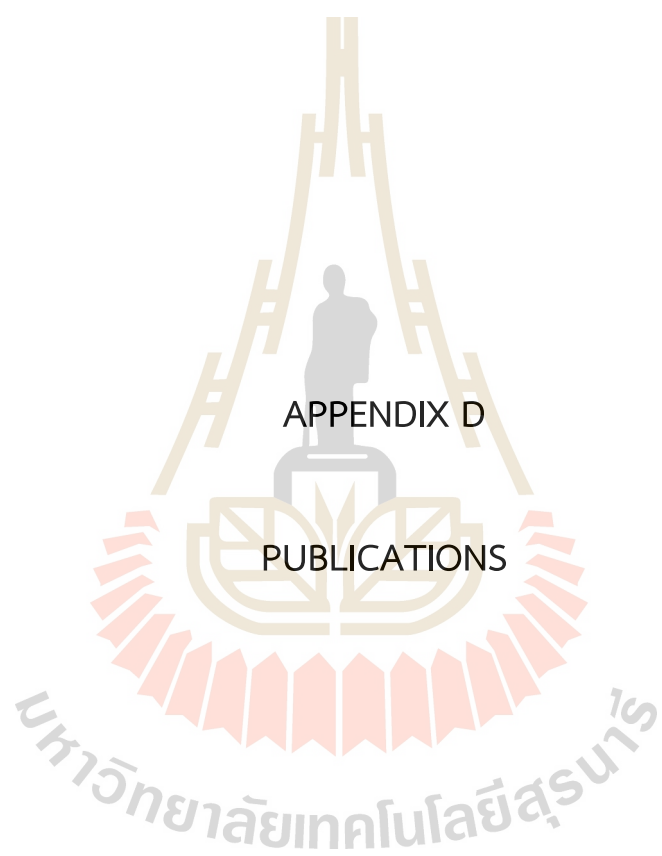


Figure C.1 Contact line test results at constant power







The following section contains copies of publications done during PhD study time. Only publications that are closely related to this work are included.

- 1 J. J. Mwambeleko, T. Hayasaka and T. Kulworawanichpong, "Enhancing conventional battery and contact line hybrid tram system with accelerating contact lines," *IET Electrical Systems in Transportation*, pp. 105-115, 2020.
- 2 J. J. Mwambeleko and T. Kulworawanichpong, "Battery and accelerating-catenary hybrid system for light rail vehicles and trams," in *2017 International Electrical Engineering Congress (IEECON)*, Pattaya, Thailand, 2017
- 3 K. Thanatchai and M. Joachim, "Development of a battery and catenary hybrid light rail vehicle simulator for vehicle and battery performance analysis: Version\_01," [D] *Industrial Application Division Transportation and Electric Railway Study Group* (<http://id.nii.ac.jp/1031/00112802/>), 2018
- 4 J. J. Mwambeleko, U. Leeton and T. Kulworawanichpong, "Effect of partial charging at intermediate stations in reducing the required battery pack capacity for a battery powered tram," in *IEEE/SICE International Symposium on System Integration*, Sapporo, Japan, 2016.

## Enhancing conventional battery and contact line hybrid tram system with accelerating contact lines

 ISSN 2042-9738  
 Received on 27th May 2018  
 Accepted on 3rd September 2019  
 E-First on 7th January 2020  
 doi: 10.1049/iet-est.2018.5033  
 www.ietdl.org

 Joachim J. Mwambeleko<sup>1</sup>, Takamasa Hayasaka<sup>2</sup>, Thanatchai Kulworawanichpong<sup>1</sup>✉

<sup>1</sup>School of Electrical Engineering, Suranaree University of Technology, Nakhon Ratchasima, Thailand

<sup>2</sup>Power Supply Technology Division, Railway Technical Research Institute, Tokyo, Japan

✉ E-mail: thanatchai@gmail.com

**Abstract:** Urban passenger mobility challenges can be sustainably eased with electric trains. However, due to the visual impact, safety and, electrification cost concerns, some routes or section(s) of a route are not electrified. In such cases, battery powered trams present a promising alternative. Rail vehicles are heavy but, they have a low coefficient of rolling friction. Consequently, they draw high power during acceleration as compared to the power demand during cruising. Thus, a high capacity high-voltage traction battery is required to provide accelerating power. To minimise total electrified distance and traction battery size, a battery and accelerating-contact line (BACL) hybrid tram system in which a tram accelerates from a station drawing power from a short contact line and cruises with traction battery is presented. Simulated in MATLAB, the BACL hybrid tram system with 1.8 km total electrified distance has equivalent performance to the conventional battery and contact line hybrid tram system with 12.2 km total electrified distance. Compared to independently battery powered tram, battery size is reduced by 62.5%. Suggested applications for the BACL tram system are on short, fairly flat, idle lines with few stops.

### Nomenclature

$\beta$	traction battery pack state of charge
$T_E$	tractive effort
$P_t$	power supplied to the traction system
$P_a$	power supplied to the auxiliary power unit
$P_{cl}$	power supplied from the contact line
$P_{bp}$	power supplied from the traction battery pack
$E_{net}$	net energy consumed
$S_{bs}$	distance between two successive stations
$S_{tvbs}$	distance travelled between two successive stations
$T_{bs}$	travel time between two successive stations
$T_{bsd}$	$T_{bs}$ plus dwell time
$T_{cmd}$	cumulative $T_{bsd}$
$E_{bs}$	net energy consumed between two successive stations
$E_{bsd}$	$E_{bs}$ plus energy consumed during the dwelling
$E_{cmd}$	cumulative $E_{bsd}$
$E_{cltv}$	energy supplied from contact line during travel between two successive stations
$E_{bptv}$	energy supplied from traction battery pack during travel between two successive stations
$E_{clid}$	energy supplied from the contact line during the dwelling
$E_{bpid}$	energy supplied from traction battery pack during the dwelling
$\beta_{start}$	$\beta$ when a tram left a previous station
$\beta_{arrival}$	$\beta$ when a tram arrives at a current station
$\beta_{depart}$	$\beta$ when a tram leaves the current station

### 1 Introduction

Owing to the petroleum energy price and security concerns, growing mobility demand and its associated traffic congestion and air pollution in urban areas, efficient and clean urban transportation systems have drawn the attention of authorities, companies, and researchers [1, 2, 3]. Urban transportation is among the highest energy-consuming industries, its associated air pollution caused by petroleum fuelled vehicles is on the rise [4, 5].

Mass transportation helps in minimising traffic congestion and energy consumption per passenger kilometre. Compared to

petroleum fuelled vehicles, electric vehicles are not only cleaner but have much higher energy efficiency and low running cost [6, 7]. Electric mass transportation, therefore, significantly reduced energy consumption and air pollution per passenger kilometre. An electric train is currently one of the best electric mass transportation options, owing to its low rolling friction, high passenger capacity and regenerative braking capability [8, 9, 10]. However, for various reasons, such as electrification cost, the unsightliness of overhead lines on areas such as historical sites and city centres, and electrification complexity (safety concerns), some railway routes are either partially electrified or not electrified at all [11, 12]. Electrification cost is particularly true for lightly used routes on which the density of traffic is insufficient to justify the high railway electrification fixed costs. Tunnels, bridges, and route crossings impose complexity and safety concerns when a railway route is to be electrified, particularly an old route which was constructed without electrification consideration [13, 14]. Under such circumstances, light rail vehicles with on-board energy storage bring one of the alternatives that some railway operators have been opting for, even during the age of lead acid battery. Strikingly, Deutsche Bahn (DB) railway operator successfully operated lead acid battery powered trains class ETA 150 (later 515) from 1955 to 1995 [13, 15]. With on-board energy storage, regenerative braking energy that would otherwise be dissipated as heat if a line is non-receptive and there is no other tram in vicinity that demands power, is stored and reused (Fig. 1).

Over the past two decades, battery technology has greatly improved with a significant drop in cost; the trend is expected to be the same in the future [4]. Lithium-ion (Li-ion) is currently a battery technology that features the best characteristics for electric traction, particularly, robustness, low life-cycle cost, absence of memory effect, and high power and energy densities [16, 17]. Common Li-ion batteries used in electric traction include lithium manganese oxide, lithium nickel manganese cobalt oxide, lithium nickel cobalt aluminium oxide, lithium iron phosphate and lithium titanate (LTO) [6]. Among these Li-ion battery chemistries, LTO battery has emerged as a leading candidate for fast charging and vehicular applications [18]. Allowing ultrafast-charging (as fast as 6 min to full charge), LTO battery technology is already broadly in use in electric buses and family cars. In railway sector, LTO battery technology has been reported to be used in Škoda's ForCity Classic



(28 T) trams (in Konya, Turkey) and Vossloh's tramlink v4 (in Santos, Brazil) to link the electrified and non-electrified lines (or parts of a line) or to be used in case of emergency (e.g. power outage) [15].

Li-ion battery trains have shown the potential to replace diesel trains serving short and idle routes in several countries [13, 19]. In Japan, for instance, railway operators (JR East and JR Kyushu) have recently started replacing diesel multiple units (DMUs) which were used to link non-electrified and electrified lines, with battery and catenary hybrid trams. As presented in Table 1, more than ten battery and catenary hybrid light rail vehicles are now in revenue earning service in Japan. The train sets use battery power on non-electrified sections and draw power from catenary on electrified sections. The traction battery pack is recharged while a train is under electrified section and at terminal stations [20–23]. With such a battery and catenary hybrid tram system, traction battery has to meet peak power demand during acceleration (when a train is leaving a station) on non-electrified section as illustrated in Fig. 2a. Thus, a high capacity high-voltage traction battery is needed. Depending on train weight, the needed battery capacity can be significantly large.

It is very interesting that, attributable to the low rolling resistance and high capacity, rail transport consumes less energy per passenger kilometre than road transport. Thus, as LTO batteries have proven success powering electric buses, it is expected that they will prove even more success powering trams [13, 14]. However, unlike buses, rail vehicles are heavy and require high power to accelerate, but little power to cruise due to low rolling friction. Consequently, a high capacity high-voltage traction battery is needed to meet acceleration (peak) power demand even if the overall energy consumption does not require such a battery. Furthermore, adding batteries increases vehicle weight.

To address the peak power problem during acceleration, Mwambeleko and Kulworawanichpong [15] present a battery and accelerating catenary hybrid system where a tram accelerates under a short catenary ('accelerating-catenary'), and cruises with

batteries. However, route gradient is not considered, the authors assume that the route is fairly flat and therefore ignore route gradient. Practically, tram routes have gradients, the gradients might not be very high but due to high tram inertial (as tram are heavy), even a low gradient has a significant effect on tram power demand and energy consumption. Moreover, no performance comparison is given between the proposed system and conventional system. It is also not explained how an accelerating-contact line (ACL) from each station will be energised. Having a traction substation (transformer, converters, and switch gears) at each station may be costly.

Extending the work presented in [15], this study presents a battery and accelerating-contact line (BACL) hybrid tram system where a tram accelerates drawing power from a short contact line ('ACL'), which can be in the form of a catenary, overhead busbar or third rail. The tram then cruises drawing power from traction battery, as shown in Fig. 2b. The proposed BACL hybrid tram system will have shorter total electrified distance than a typical conventional battery and contact line (CBCL) hybrid tram system with equivalent performance. Additionally, with the proposed BACL system, the electrified sections extend from a stopping station (i.e. just a short distance from a stopping station is electrified), these make the proposed system more convenient as far as visual impact and electrification cost especially on routes that are idle and difficulty to electrify (e.g. where two routes cross, a route passing under a bridge or in a tunnel with insufficient clearance and routes passing in congested areas with insufficient right of way for electrification). Moreover, the proposed BACL hybrid tram system is expected to reduce required battery size and increase tram performance (due to reduction in battery weight) as compared to independently battery powered (IBP) tram. Suggested applications are, on short, lightly used lines with few stops. Such lines may include non-electrified line linking with a main electrified line, line from a city centre to a suburban where the tram is available only during rush hours, and line from the city centre to

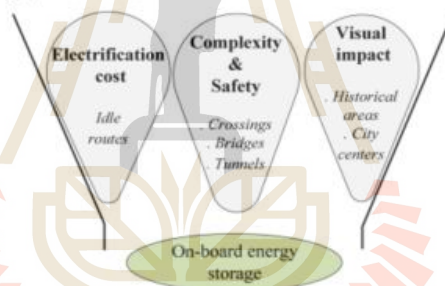
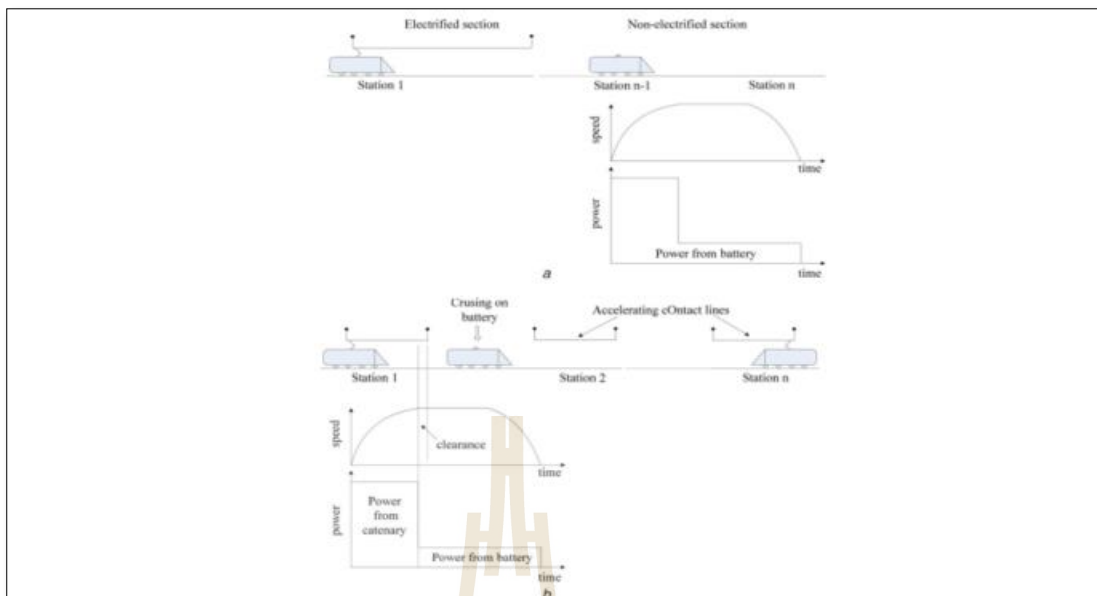


Fig. 1 Need for on-board energy storage

Table 1 Battery catenary hybrid trams operating commercially in Japan [15, 22, 23]

Manufacturer	J-TREC	Hitachi	Hitachi
family name	Accum	Hitachi A-train	Accum
series	EV-E301	BEC819	EV-E801
Formation	two cars per train set	two cars per train set	two cars per train set
weight, ton	77.9	72.1	75.6
length/width, m	20/2.8	20/2.95	-
passenger capacity	266	264	256
battery capacity, kWh	190	-	360
entered service	March 2014	October 2016	March 2017
replaced DMU	KiHa 40 series	-	KiHa 40 series
operator	JR East	JR Kyushu	JR East
number in operation	four train sets	seven train sets	one train set
distance served, km	non-electrified 20.4 electrified 11.7	10.8	26.6 13

Data not currently available.



**Fig. 2** Battery and catenary hybrid tram systems  
(a) CBCL hybrid tram system,  
(b) Proposed BACL hybrid tram system

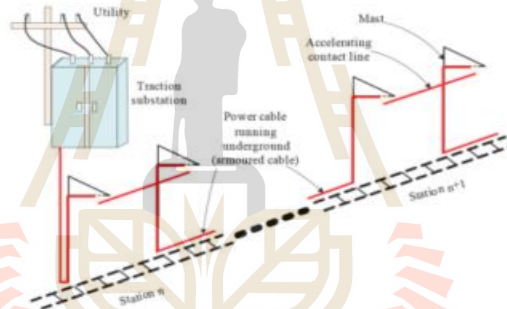


**Fig. 3** ACLs feeding scheme

a location such as a stadium, where the tram is available only on particular days or during a particular time of the day.

The rest of the paper is organised as follows: ACL feeding scheme is presented in Section 2. Tram and battery models are presented in Section 3, the route used in the study, system design, and simulation details are presented in Section 4, simulation results are presented and discussed in Section 5, and finally Section 6 concludes the paper.

## 2 ACL feeding scheme

As aforementioned, having a traction substation (transformer, converters and switch gears) at each station to supply the ACL sections is costly. It is proposed in this study not to have a traction substation at each stopping station and instead, feeding ACL sections using the underground cable as illustrated in Fig. 3. At the end of an ACL section, power is transferred to the next station (the beginning of the ACL) using underground (armoured) cable. Thus, one traction substation supplies multiple ACL sections. The same concept applies to both catenary and third rail systems. The number of traction substations can be one, at the middle of the route; or

two, one at each terminal station or station near terminal station; or more than two at appropriate locations. Establishing the number of traction substations and their locations is out of the scope of this study.

## 3 Tram and battery models

Modelled as a point mass, tram's mechanical driving power ( $P_m$ ) is given by a product of its tractive effort ( $T_E$ ) and velocity ( $v$ ), where  $T_E$  (kN) is calculated as in (1), neglecting curve resistance which is usually very low (negligible) [24, 25]. In (1), the first term accounts for acceleration resistance, the second term accounts for gradient resistance, and rest account for friction and drag resistance

$$T_E = \hat{m} \frac{\Delta v}{\Delta t} + mg \sin \theta + A + Bv + Cv^2 \quad (1)$$

where  $\hat{m}$  and  $m$  are tram effective and normal masses given as  $\hat{m} = m_{tare}(1 + \lambda) + m_{load}$  and  $m = m_{tare} + m_{load}$ , respectively, where  $m_{tare}$  is the vehicle tare mass (tonne),  $\lambda$  is rotary allowance accounting for angular acceleration of the rotating parts (motor

rotors, gears, and wheel sets), and  $m_{load}$  is the mass of the vehicle load (tonne).  $\Delta v/\Delta t$  is a change in velocity per change in time ( $ms^{-2}$ ),  $g$  is the gravitational acceleration constant ( $9.81 ms^{-2}$ ),  $\theta$  is a slope angle,  $A$ ,  $B$  and  $C$  are constants, and  $v$  is tram's velocity (km/h) [14, 24].

Following (1), tram's tractive electric power ( $P_t$ ) and net energy consumption ( $E_{net}$ ) are given by (2) and (3), respectively

$$P_t = \begin{cases} T_E v / (\eta_{mg} \eta_d) & \text{if } T_E > 0 \\ \eta_{mg} \eta_d T_E v & \text{if } T_E < 0 \text{ and } v > 10 \text{ km/h} \\ 0 & \text{otherwise} \end{cases} \quad (2)$$

$$E_{net} = \int_{t_{start}}^{t_{stop}} (P_t(t) + P_{ax} / \eta_{ax}) dt \quad (3)$$

where  $T_E$  is the tractive effort (N) as given in (1),  $\eta_{tr}$  is the electrical-mechanical tractive power conversion efficiency,  $v$  is the velocity (m/s),  $t_{start}$  is the time at which the tram starts moving from its current station,  $t_{stop}$  is the time at which the tram stops at the next station,  $P_{ax}$  is the auxiliary power,  $\eta_{ax}$  is the efficiency of the auxiliary system and  $dt$  is the change in time (s).

A tram manufactured by Hyundai Rotem Company was used in this study; its details as used in the simulation are given in Table 2 and in Fig. 4b. State of charge (SoC) of a battery charged or discharged from time  $t_0$  to  $t_1$  is given by (4) or alternatively by (5),

**Table 2** Tram details used in the simulation [13, 26–29]

Attribute	Value	
maximum desired speed	60 km/h	
passenger capacity (52 seats, 152 standees)	204	
vehicle effective weight ( $\hat{m}$ ) (70.3 kg per person, $\lambda = 0.1$ )	62,104 kg	
resistance coefficients	A	1.125
	B	0.0218
	C	0.00047
gearbox and motor efficiency ( $\eta_{gm}$ )	0.83	
converter efficiency ( $\eta_c$ )	0.9	
auxiliary power unit efficiency ( $\eta_a$ )	0.85	
motor drive (VVVF) efficiency ( $\eta_d$ )	0.91	
auxiliary power ( $P_a$ )	25 kVA	
drive	8 × 45 kW	

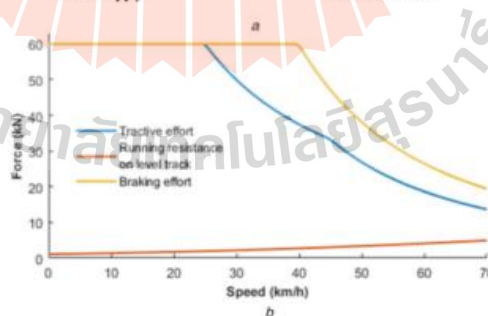
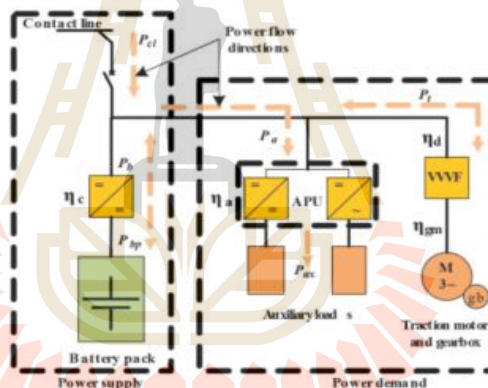


**Fig. 4** Battery and contact line hybrid tram  
(a) Block diagram,  
(b) Tractive effort, running resistance and, braking effort



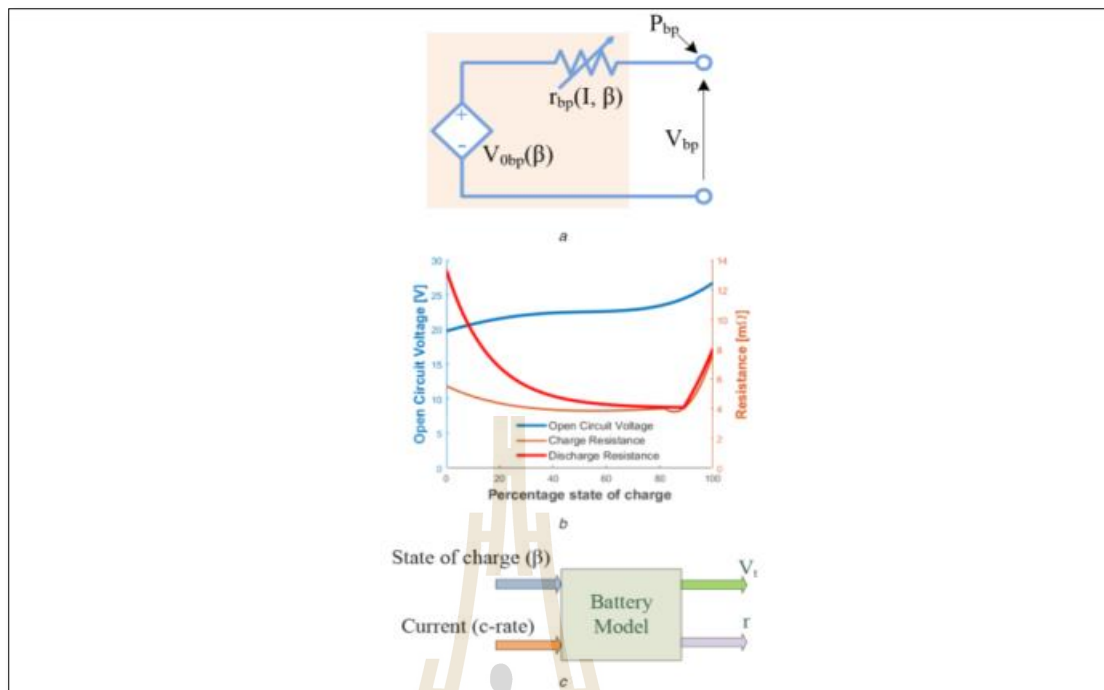


**Fig. 5** Battery model  
(a) Equivalent circuit,  
(b) Voltage and resistance curves,  
(c) Model inputs and outputs

**Table 3** Battery module details [30]

Attribute	Battery value	Battery pack value
nominal voltage	24 V	480 V
nominal capacity	60 Ah	240 Ah
maximum continuous charge	360 A	1440 A
maximum continuous discharge	360 A	1440 A
maximum pulse-charge (10 s)	600 A	2400 A
maximum pulse-discharge (10 s)	600 A	2400 A
weight	27.4 kg	2192 kg

where  $\beta^{(t_0)}$  is the SoC at time  $t_0$ ,  $\beta^{(t)}$  is the SoC at time  $t$ ,  $I_b$  is the battery current (A),  $V_b$  is the battery terminal voltage (V),  $r_b$  is the battery internal resistance ( $\Omega$ ),  $C$  is the battery capacity (Amps-seconds),  $V_{bet}$  is the battery rated voltage (V) and,  $dt$  is the change in time (s). Battery current ( $I_b$ ) is taken as negative during charging and as positive during discharging

$$\beta^{(t)} = \begin{cases} \beta^{(t_0)} - \frac{1}{C} \int_{t_0}^t \left(1 - \frac{I_b r_b}{V_b}\right) I_b dt, & \text{charging} \\ \beta^{(t_0)} - \frac{1}{C} \int_{t_0}^t \left(\frac{V_b}{V_b - I_b r_b}\right) I_b dt, & \text{discharging} \end{cases} \quad (4)$$

$$\beta^{(t)} = \beta^{(t_0)} - \frac{1}{C} \int_{t_0}^t \left(\frac{V_b + I_b r_b}{V_{bet}}\right) I_b dt \quad (5)$$

A 24 V, 60 Ah LTO battery manufactured by Altairmano was used and it was modelled as a varying voltage source in series with a varying resistor as in Fig. 5. The battery pack (80 batteries, 40 in series) details are given in Table 3. Converters, motors, and motor drives are presented by their respective efficiency parameters as

given in Table 2. The battery electric multiple unit (BEMU) block diagram consisting of a battery pack, bidirectional DC-DC converter, variable voltage variable frequency (VVVF) converter, traction motor, and gear box is shown in Fig. 4. The BEMU is assumed to be capable of regenerative braking.

#### 4 Route, system design, and simulation details

A 25 km route with nine intermediate stations as shown in Fig. 6 is used in this study. From station 3 (S3) to station 10 (S10) of the route is an actual non-electrified line (known as Karasuyama line) linking with a main (electrified) line in Japan. Station (S1) and station (S2) have been added for the purpose of this study. Travelling from S10 to S1, the direction is called down direction, while from S1 to S10; the direction is called up direction. Six cases are considered as explained in Table 4.

For cases 1Up, 1Down, 2Up, and 2Down, when a tram is in the electrified zone (a zone with contact line), all tram power demands are drawn from the contact line, and also a battery pack is recharged. A contact line is assumed to be fed using rectified diode substations, and therefore it is non-receptive. Thus, regenerative braking energy is supplied to tram auxiliaries and the remaining is stored in the battery pack. If the remaining regenerative energy is

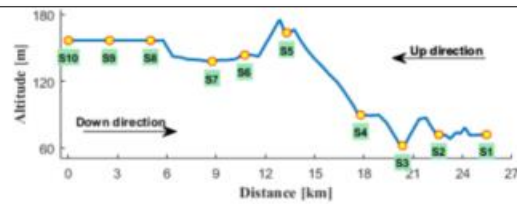


Fig. 6 Tram route used in the study

Table 4 Cases considered in the study

Case	Tram system	Direction	Remarks
1Up 1Down	BACL	up down	it is assumed that an ACL runs for 200 m from each stopping station and a tram stops at a station with its pantograph or collector shoe at the beginning of the ACL. Out of the 200 m, the effective length is 185 m, 15 m are left as clearance as shown in Fig. 2b.
2Up 2Down	CBCL		section S6 to S10 of the route is assumed to be electrified
3Up 3Down	IBP	down up	the entire route is not electrified. A battery pack is the sole tram power supply and there is no battery charging at intermediate stations.

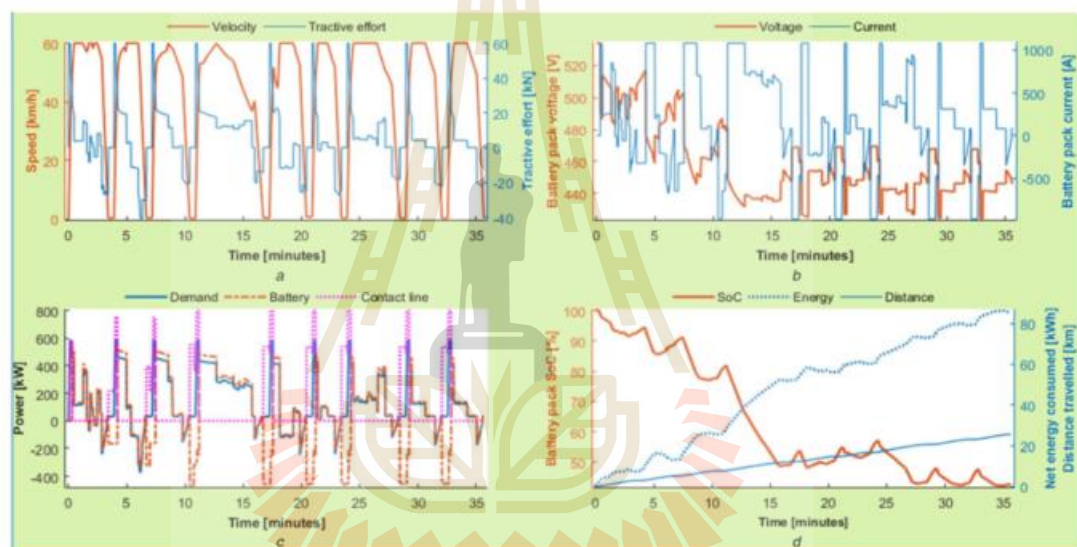


Fig. 7 Results for case 1Up (BACL hybrid tram system, a tram going up)

- (a) Velocity and tractive effort.  
 (b) Power.  
 (c) Battery pack current and voltage.  
 (d) Distance, energy consumed and battery pack SoC.

more than what a battery pack can absorb, then the extra is dissipated in braking resistor bank. In non-electrified zone (a zone with no contact line) all tram power demand is drawn from a traction battery pack.

Both the contact line and traction battery pack have power limitations. It is assumed that maximum power that can be drawn from a contact line is 800 kW. The maximum continuous charging and discharge C-rate of the battery is 6 C (360 A). In the simulation, however, 5 C (300 A) was taken as the battery maximum charging and discharge C-rate. Charging is done at 5 C to 80% state of charge (SoC) and then at 3.6 C-rate to 90% SoC, and then at 2.4 C-rate to 95% SoC, and finally at 1.2 C-rate to full charge. Also, in the simulation battery minimum SoC is taken as 20%. When the battery SoC at the next time step is below 20%, the tram will stop at the current time step.

The tram dwells for 45 s at an intermediate station, and if there is a battery charging infrastructure (a contact line in this case) at the station, the battery pack is recharged. When the tram reaches the terminal station, the battery pack is to be recharged to full charge.

## 5 Simulation results and discussion

Simulated using MATLAB, simulation results for case 1Up and case 1Down are presented in Figs. 7 and 8, respectively. The results are also summarised in Tables 5 and 6. For case 2Up and case 2Down, the simulation results are presented in Figs. 9 and 10, respectively, and summarised in Tables 7 and 8, respectively. Simulation results for case 3Up and case 3Down are presented in



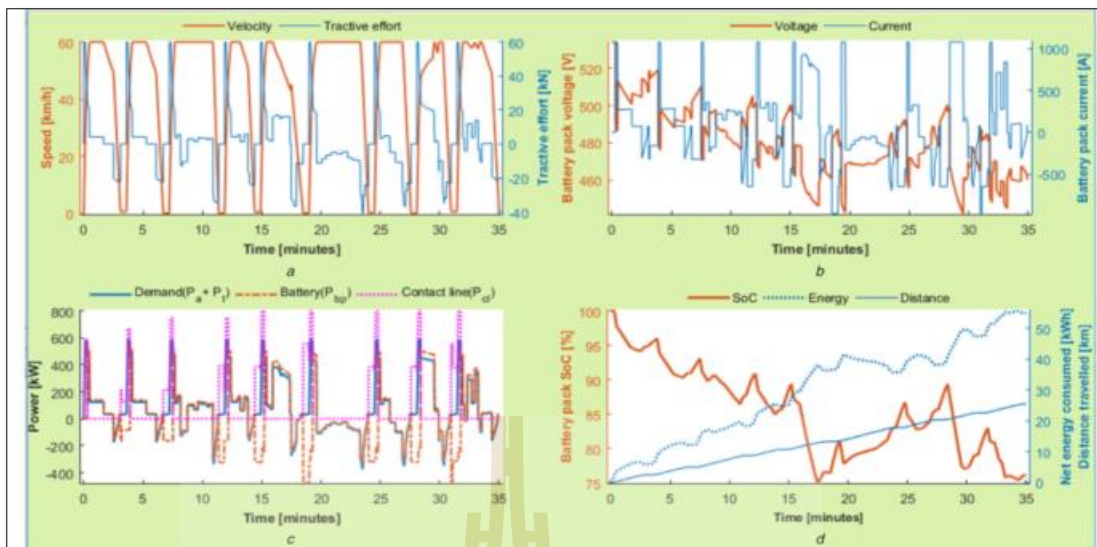


**Fig. 8** Results for case 1Down (BACL hybrid tram system, a tram going down)  
 (a) Velocity and tractive effort,  
 (b) Power,  
 (c) Battery pack current and voltage,  
 (d) Distance, energy consumed and battery pack SoC

**Table 5** Results summary case 1Up

Section	$S_{bs}$ , m	$S_{tvs}$ , m	$T_{bs}$ , s	$T_{bsd}$ , s	$T_{cmd}$ , s	$E_{bs}$ , kWh	$E_{bsd}$ , kWh	$E_{cmd}$ , kWh	$E_{cltv}$ , kWh	$E_{bptv}$ , kWh	$E_{cld}$ , kWh	$E_{bpd}$ , kWh	$\alpha_{initial}$ , %	$\alpha_{arrival}$ , %	$\alpha_{depart}$ , %
S1→S2	2908	2908	205	235	235	7.41	7.69	7.69	2.32	5.94	1.81	-1.38	100	92.4	93.8
S2→S3	2210	2210	165	195	430	5.47	5.75	13.44	3.15	3.39	2.71	-2.19	93.8	88.5	90.6
S3→S4	2550	2550	195	225	654	12.05	12.33	25.76	3.07	10.22	4.2	-3.53	90.6	77.6	80.7
S4→S5	4511	4511	351	381	1035	26.31	26.59	52.35	3.58	25.51	4.49	-3.79	80.7	49	52.3
S5→S6	2557	2557	191	221	1255	3.77	4.05	56.4	3.8	0.81	4.5	-3.8	52.3	50.1	53.5
S6→S7	1983	1983	152	182	1437	3.87	4.15	60.55	3.8	0.45	4.5	-3.8	53.5	52.4	55.7
S7→S8	3751	3751	271	301	1737	12.58	12.86	73.41	3.8	10.05	4.48	-3.79	55.7	43.2	46.6
S8→S9	2500	2500	187	217	1954	5.95	6.23	79.64	3.8	2.72	4.48	-3.78	46.6	42.9	46.3
S9→S10	2500	2500	187	187	2140	5.95	5.95	85.59	3.8	2.72	0	0	46.3	42.6	42.6

**Table 6** Results summary case 1Down

Section	$S_{bs}$ , m	$S_{tvs}$ , m	$T_{bs}$ , s	$T_{bsd}$ , s	$T_{cmd}$ , s	$E_{bs}$ , kWh	$E_{bsd}$ , kWh	$E_{cmd}$ , kWh	$E_{cltv}$ , kWh	$E_{bptv}$ , kWh	$E_{cld}$ , kWh	$E_{bpd}$ , kWh	$\alpha_{initial}$ , %	$\alpha_{arrival}$ , %	$\alpha_{depart}$ , %
S10→S9	2500	2500	186	216	216	5.94	6.22	6.22	2.32	4.2	1.18	-0.81	100	94.8	95.6
S9→S8	2500	2500	187	217	433	5.95	6.23	12.45	2.74	3.78	1.79	-1.36	95.6	90.9	92.3
S8→S7	3751	3751	250	280	713	5.85	6.13	18.58	3.14	3.63	3.16	-2.59	92.3	87.7	90.1
S7→S6	1983	1983	152	182	895	6.19	6.47	25.04	3.13	3.66	3.25	-2.67	90.1	85.6	88.2
S6→S5	2557	2557	215	245	1140	11.36	11.63	36.68	3.61	9.11	4.63	-3.92	88.2	76.4	79.9
S5→S4	4511	4511	301	331	1471	-1.05	-0.77	35.9	3.63	-3.83	3.21	-2.64	79.9	83	85.5
S4→S3	2550	2550	185	215	1685	2.22	2.49	38.4	3.6	-0.72	3.25	-2.67	85.5	85.6	88.1
S3→S2	2210	2210	173	203	1888	8.93	9.21	47.61	3.7	6.46	3.56	-2.96	88.1	79.1	81.8
S2→S1	2908	2908	213	213	2101	7.24	7.24	54.84	3.59	4.43	0	0	81.8	76.1	76.1

Figs. 11 and 12, respectively, and summarised in Tables 9 and 10, respectively. Results summary for all cases is given in Table 11.

In all cases going up is expensive mainly due to the uphill from S3 to S5 and S7 to S8. On these sections, the tram consumes a substantial amount of energy and the battery pack SoC drops considerably. Compared to the up direction, the down direction is an easy one mainly due to the downhill from S5 to S3 and S8 to S7. On these sections, the regenerative energy is significant.

Consequently, the tram consumes less energy on down direction compared to up direction.

As can be seen in Figs. 7–10, Tables 5–8 and 11, the performance of a BACL tram system is comparable to that of the CBCL tram system in terms of net energy consumption, travel time and battery minimum SoC. However, with the BACL tram system, the total electrified distance is only 1.8 km, while with the CBCL tram system, the total electrified distance is 12.18 km. The 1.8 km

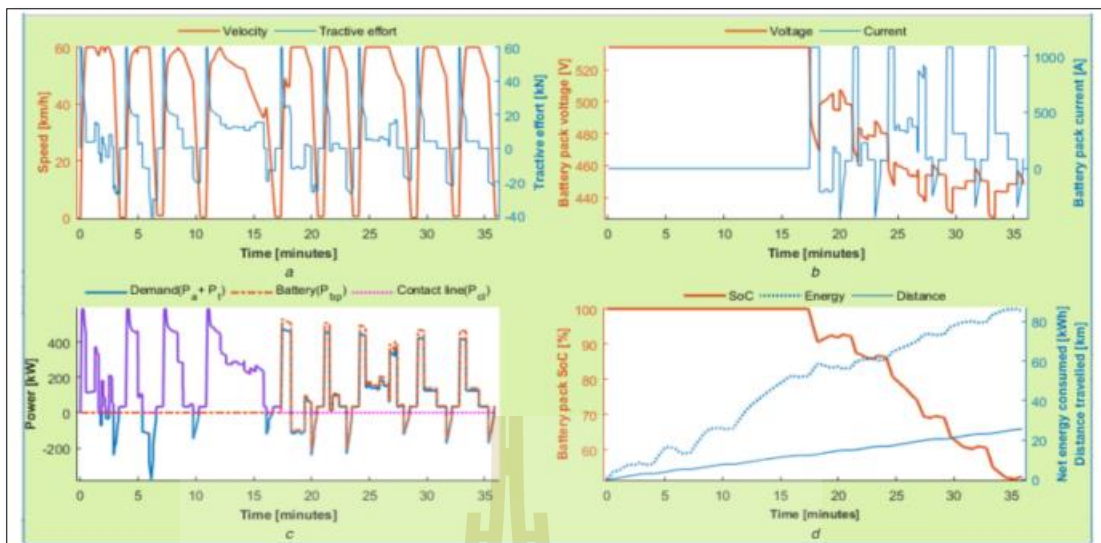


**Fig. 9** Results for case 2Up (CBCL hybrid tram system, a tram going up)

- (a) Velocity and tractive effort,  
 (b) Power,  
 (c) Battery pack current and voltage,  
 (d) Distance, energy consumed and battery pack SoC

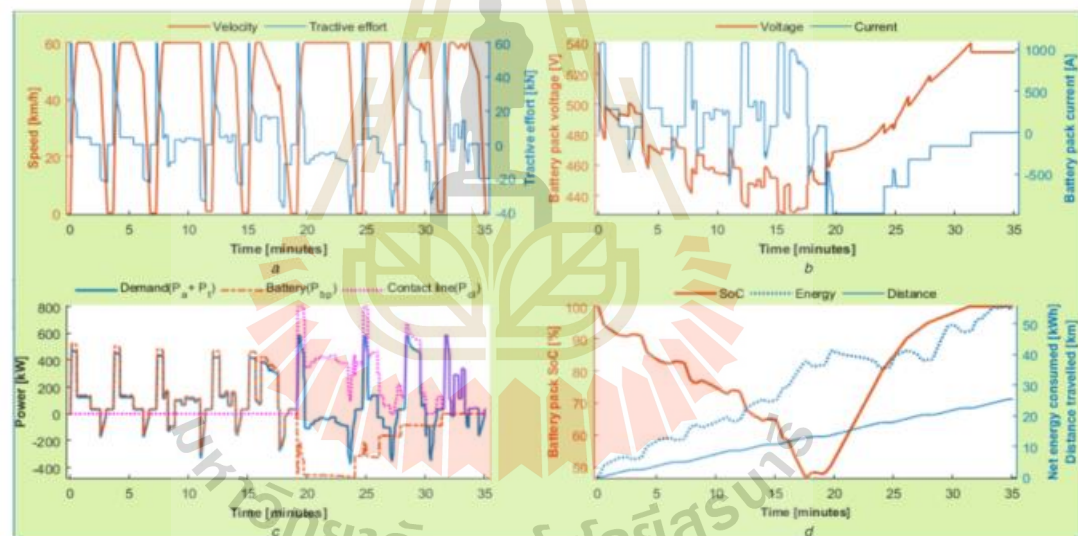


**Fig. 10** Results for case 2Down (CBCL hybrid tram system, a tram going down)

- (a) Velocity and tractive effort,  
 (b) Power,  
 (c) Battery pack current and voltage,  
 (d) Distance travelled, net energy consumed and battery pack SoC

total electrified distance (for the BACL tram system) is divided into short sections extending from a stopping station. This is convenient as far as visual impact, electrification complexity, and safety (such as under bridges and at route crossings), and electrification cost are concerned. The 12.18 km total electrified distance (for the CBCL tram system) covers a mountainous section

of the route; this is of advantage particularly when a tram is going uphill.

For both directions (Up and Down), the IBP tram does not make it to the terminal station due to low battery. As previously mentioned, the minimum battery SoC is set to 20%. Discharging the battery pack below 20% SoC is not recommended, as it can be seen from Fig. 5b, battery internal resistance below 20% SoC may

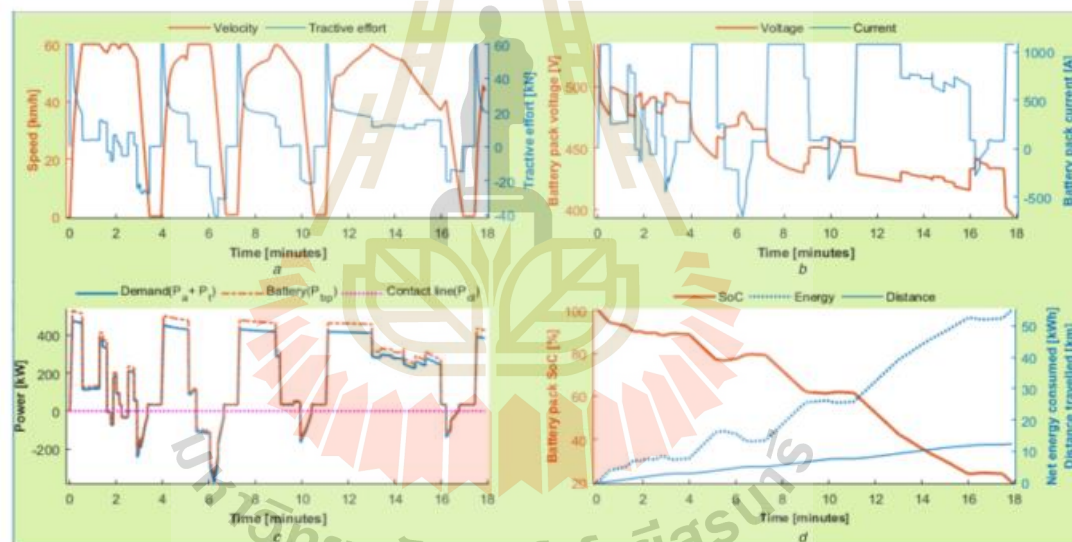


**Table 7** Results summary case 2Up

Section	$S_{DS}$ , m	$S_{tVDS}$ , m	$T_{DS}$ , s	$T_{bSD}$ , s	$T_{cmd}$ , s	$E_{bs}$ , kWh	$E_{bsd}$ , kWh	$E_{cmd}$ , kWh	$E_{cltv}$ , kWh	$E_{bptv}$ , kWh	$E_{cld}$ , kWh	$E_{bpd}$ , kWh	$\alpha_{initial}$ , %	$\alpha_{arrival}$ , %	$\alpha_{depart}$ , %
S1→S2	2908	2908	205	235	235	7.43	7.7	7.7	8.75	0	0.28	0	100	100	100
S2→S3	2210	2210	164	194	429	5.48	5.76	13.46	8.88	0	0.28	0	100	100	100
S3→S4	2550	2550	194	224	653	12.1	12.38	25.84	12.81	0	0.28	0	100	100	100
S4→S5	4511	4511	359	389	1042	26.24	26.52	52.37	26.71	0	0.28	0	100	100	100
S5→S6	2557	2557	192	222	1263	3.86	4.14	56.5	0	4.97	0	0.28	100	92.6	92.3
S6→S7	1983	1983	153	183	1446	3.87	4.15	60.65	0	4.51	0	0.28	92.3	86.6	86.3
S7→S8	3751	3751	272	302	1748	12.57	12.85	73.5	0	14.09	0	0.28	86.3	69.5	69.2
S8→S9	2500	2500	189	219	1967	5.95	6.23	79.73	0	6.78	0	0.28	69.2	60.9	60.6
S9→S10	2500	2500	189	189	2156	5.95	5.95	85.68	0	6.78	0	0	60.6	52.3	52.3

**Table 8** Results summary case 2Down

Section	$S_{DS}$ , m	$S_{tVDS}$ , m	$T_{DS}$ , s	$T_{bSD}$ , s	$T_{cmd}$ , s	$E_{bs}$ , kWh	$E_{bsd}$ , kWh	$E_{cmd}$ , kWh	$E_{cltv}$ , kWh	$E_{bptv}$ , kWh	$E_{cld}$ , kWh	$E_{bpd}$ , kWh	$\alpha_{initial}$ , %	$\alpha_{arrival}$ , %	$\alpha_{depart}$ , %
S10→S9	2500	2500	188	218	218	5.95	6.23	6.23	0	6.78	0	0.28	100	91.3	91
S9→S8	2500	2500	188	218	436	5.95	6.22	12.45	0	6.77	0	0.28	91	82.9	82.6
S8→S7	3751	3751	252	282	718	5.82	6.1	18.55	0	6.99	0	0.28	82.6	73.9	73.6
S7→S6	1983	1983	155	185	903	6.17	6.44	24.99	0	7.02	0	0.28	73.6	65	64.7
S6→S5	2557	2557	217	247	1150	11.33	11.61	36.6	0	12.95	0	0.28	64.7	48.2	47.9
S5→S4	4511	4511	301	331	1481	-1.04	-0.76	35.85	35.75	-36.79	3.18	-2.61	47.9	80.7	83.1
S4→S3	2550	2550	184	214	1695	2.24	2.52	38.36	14.69	-11.76	1.34	-0.95	83.1	94.5	95.5
S3→S2	2210	2210	170	200	1894	8.99	9.27	47.63	14.16	-4.02	0.8	-0.46	95.5	99.5	100
S2→S1	2908	2908	213	213	2107	7.25	7.25	54.88	8.38	0	0	0	100	100	100

**Fig. 11** Results for case 3Up (IBP tram system, a tram going up)

- (a) Velocity and tractive effort,  
 (b) Power,  
 (c) Battery pack current and voltage,  
 (d) Distance travelled, net energy consumed and battery pack SoC.

result in significant heating, which decreases battery life span. Increasing battery size not only increases cost but also tram weight, which will lead to increased energy consumption. In case 3Up, if the IBP tram was to get to a terminal station with a minimum battery SoC not less than 20%, then the battery pack size was to be increased by a factor of 1.6.

With the BACL tram system, the electrified distance increases with the number of stations, that is why it was previously mentioned that the BACL tram system is suggested for a lightly

used route with few stations per kilometre. BACL tram will perform even better on a fairly flat route unlike the one used in this study. A fairly flat section from S1 to S3 was added to emphasise the point, as it can be seen in Figs. 7c and 8c, the power needed for cruising (not accelerating but maintaining the velocity) on a flat section is <200 kW while the peak (accelerating) power is about 600 kW. This highlights the advantage of having a short ACL.

Apart from providing accelerating power, the ACL provides an intermediate charging point during dwell time. This further reduces

the required size of the battery pack. Increasing acceleration will reduce the length of the ACL. However, maximum acceleration is

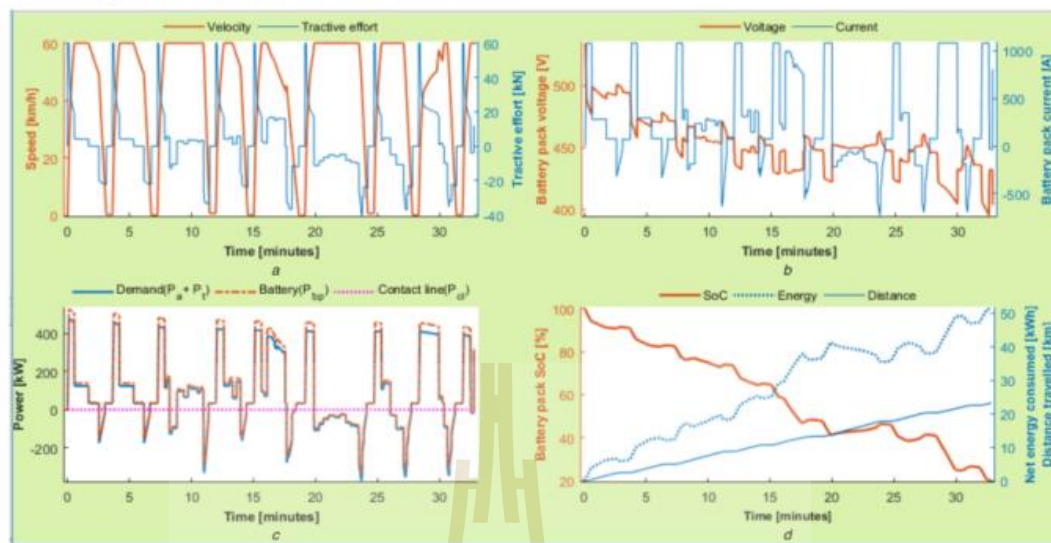


Fig. 12 Results for case 3Down (IBP tram system, a tram going down)

- (a) Velocity and tractive effort,
- (b) Power,
- (c) Battery pack current and voltage,
- (d) Distance travelled, net energy consumed and battery pack SoC

Table 9 Results summary case 3Up

Section	$S_{bs}$ , m	$S_{tvs}$ , m	$T_{bs}$ , s	$T_{bsd}$ , s	$T_{cmd}$ , s	$E_{bs}$ , kWh	$E_{bsd}$ , kWh	$E_{cmd}$ , kWh	$E_{cltv}$ , kWh	$E_{bptv}$ , kWh	$E_{cld}$ , kWh	$E_{bpd}$ , kWh	$\alpha_{initial}$ , %	$\alpha_{arrival}$ , %	$\alpha_{depart}$ , %
S1→S2	2908	2908	206	236	236	7.42	7.69	7.69	0	8.52	0	0.28	100	89.1	88.8
S2→S3	2210	2210	168	198	434	5.49	5.77	13.46	0	6.82	0	0.28	88.8	79.5	79.2
S3→S4	2550	2550	198	228	662	12.07	12.35	25.81	0	13.58	0	0.28	79.2	61.9	61.6
S4→S5	4511	4511	355	385	1047	26.3	26.57	52.39	0	29.33	0	0.28	61.6	24.4	24.1
S5→S6	2557	233	27	27	1074	2.65	2.65	55.04	0	2.94	0	0	24.1	20	NaN

Table 10 Results summary case 3Down

Section	$S_{bs}$ , m	$S_{tvs}$ , m	$T_{bs}$ , s	$T_{bsd}$ , s	$T_{cmd}$ , s	$E_{bs}$ , kWh	$E_{bsd}$ , kWh	$E_{cmd}$ , kWh	$E_{cltv}$ , kWh	$E_{bptv}$ , kWh	$E_{cld}$ , kWh	$E_{bpd}$ , kWh	$\alpha_{initial}$ , %	$\alpha_{arrival}$ , %	$\alpha_{depart}$ , %
S10→S9	2500	2500	188	218	218	5.95	6.23	6.23	0	6.78	0	0.28	100	91.3	91
S9→S8	2500	2500	188	218	436	5.95	6.22	12.45	0	6.77	0	0.28	91	82.9	82.6
S8→S7	3751	3751	252	282	718	5.82	6.1	18.55	0	6.99	0	0.28	82.6	73.9	73.6
S7→S6	1983	1983	155	185	903	6.17	6.44	24.99	0	7.02	0	0.28	73.6	65	64.7
S6→S5	2557	2557	217	247	1150	11.33	11.61	36.6	0	12.95	0	0.28	64.7	48.2	47.9
S5→S4	4511	4511	304	334	1484	-1.09	-0.81	35.79	0	0.01	0	0.28	47.9	46.3	46.1
S4→S3	2550	2550	187	217	1700	2.24	2.51	38.3	0	3.16	0	0.28	46.1	41.3	41
S3→S2	2210	2210	183	213	1913	8.77	9.05	47.36	0	10.23	0	0.28	41	26.6	26.3
S2→S1	2908	742	58	58	1971	4.08	4.08	51.44	0	4.55	0	0	26.3	20	NaN

Table 11 Results summary, all cases

	Case 1Up	Case 1Down	Case 2Up	Case 2Down	Case 3Up	Case 3Down
net energy consumed, kWh	85.59	54.84	85.68	54.88	55.04	51.44
final battery pack SoC	42.6	76.1	52.3	100	20	20
trip time, min	35.7	35	36.9	35.1	18	33
distance travelled, km	25.47	25.47	25.47	25.47	12.41	23.3
reached the terminal station	yes	yes	yes	yes	no	no
electrified (contact line) distance, km	1.8	1.8	12.18	12.18	0	0



limited by tram's maximum tractive effort. Hence, trams that have high acceleration ability are much preferred for a BACL tram system.

While ensuring safety, it is good for a battery driven tram to be constructed in such a way that its weight is minimised while its passenger capacity is maximised. With good (light but strong) materials and good designs, high passenger-capacity to vehicle-weight ratio can be achieved. This will help to reduce the required traction power, energy, and consequently battery capacity. Owing to advancements in battery technology, battery performance has been improving while the cost is going down, this keeps increasing the attractiveness of a battery-driven tram on short and idle routes.

## 6 Conclusion

The need for efficient and sustainable urban transportation system cannot be overemphasised. Despite the advantages of an electric train, for reasons such as electrification cost, the unsightliness of overhead lines on areas such as historical sites and city centres, and electrification complexity (safety concerns); some railway routes are either partially electrified or not electrified at all. This is particularly true for lightly used routes (routes with low-traffic density). To still benefit from electric traction on such routes, trams with on-board energy storage device(s) bring a promising alternative. This study presents a BACL tram system in which a tram accelerates from a station drawing power from a short contact line (ACL) and cruises with battery power. The main aim is to reduce (i) total electrified distance which will, in turn, reduce unsightliness of overhead lines, (ii) electrification cost especially on routes that are difficult to electrify and have a low density of traffic, and (iii) the required size of a traction battery pack. Reducing battery size not only reduces battery cost but also vehicle weight and net energy consumption.

From the simulation results, the performance of a BACL tram system (in terms of net energy consumption, travel time, and minimum battery SoC) with 1.8 km total electrified distance is comparable to that of a CBCL tram system with 12.18 km total electrified distance. Compared to an IBP tram, the BACL tram system reduced the size of a traction battery pack by 62.5%.

BACL tram system is more attractive if the tram has high accelerating ability (this will reduce the length of the ACL), high passenger-capacity to vehicle-weight ratio (this will reduce power demand and energy consumption per passenger) and if the route is fairly flat. Suggested applications for the BACL tram system are on lightly used lines with few stops per kilometre. Owing to advancements in battery technology, battery performance has been increasing while the cost is decreasing; this increases the attractiveness of battery-driven trams on short and lightly used routes.

## 7 References

- [1] Kandasamy, N.K., Kandasamy, K., Tseng, K.J.: 'Loss-of-life investigation of EV batteries used as smart energy storage for commercial building-based solar photovoltaic systems', *IET Electr. Syst. Transp.*, 2017, 7, (3), pp. 223–229
- [2] Weng, C., Sun, J., Peng, H.: 'A unified open-circuit-voltage model of lithium-ion batteries for state-of-charge estimation and state-of-health monitoring', *J. Power Sources*, 2014, 258, pp. 228–237
- [3] Margaritis, D., Anagnostopoulou, A., Tromaras, A., et al.: 'Electric commercial vehicles: practical perspectives and future research directions', *Res. Transp. Bus. Manag.*, 2016, 18, pp. 4–10
- [4] Ghaviha, N., Campillo, J., Bohlin, M., et al.: 'Review of application of energy storage devices in railway transportation', The 9th Int. Conf. on Applied Energy – ICAE2016, Beijing, 2017
- [5] Naik, M.B., Kumar, P., Majhi, S.: 'Small-scale solar plants coupled with smart public transport system and its coordination with the grid', *IET Electr. Syst. Transp.*, 2017, 7, (2), pp. 135–144
- [6] Mwambeleko, J.J.: 'Reducing passenger travel fuel cost and emission: a case study of Tanzania commuter trains' (Soranaree University of Technology, Nakhon Ratchasima, Thailand, 2016)
- [7] Bjerkan, K.Y., Norbeck, T.E., Nordhømme, M.E.: 'Incentives for promoting battery electric vehicle (BEV) adoption in Norway', *Transp. Res. D*, 2016, 43, pp. 169–180
- [8] Ghaviha, N., Bohlin, M., Dahlquist, E.: 'Speed profile optimization of an electric train with on-board energy storage and continuous tractive effort', 2016 Int. Symp. on Power Electronics, Electrical Drives, Automation and Motion (SPEEDAM), Anacapri, 2016
- [9] Arboleya, P., Bidaguren, P., Armendariz, U.: 'Energy is on board: energy storage and other alternatives in modern light railways', *IEEE Electr. Mag.*, 2016, 4, (3), pp. 30–41
- [10] Hillmansen, S., Ellis, R.: 'Electric railway traction systems and techniques for energy saving', IET 13th Professional Development Course on Electric Traction Systems, London, 2014
- [11] Ratniyomchai, T., Hillmansen, S., Tricoli, P.: 'Recent developments and applications of energy storage devices in electrified railways', *IET Electr. Syst. Transp.*, 2013, 4, (1), pp. 9–20
- [12] Herrera, V.I., Gaztanaga, H., Milo, A., et al.: 'Optimal energy management and sizing of a battery-supercapacitor-based light rail vehicle with a multiobjective approach', *IEEE Trans. Ind. Appl.*, 2016, 52, (4), pp. 3367–3377
- [13] Mwambeleko, J.J., Kulworawanichpong, T.: 'Battery electric multiple units to replace diesel commuter trains', *J. Energy Storage*, 2017, XI, pp. 7–15
- [14] Mwambeleko, J.J., Kulworawanichpong, T., Greyson, K.A.: 'Tram and trolleybus net traction energy consumption comparison', 2015 18th Int. Conf. on Electrical Machines and Systems (ICEMS2015), Pattaya, January 2016, pp. 2164–2169
- [15] Mwambeleko, J.J., Kulworawanichpong, T.: 'Battery and accelerating-catenary hybrid system for light rail vehicles and trams', 2017 Int. Electrical Engineering Congress (iEECON), Pattaya, 2017
- [16] Kim, N., Rousseau, A., Rask, E.: 'Parameter estimation for a lithium-ion battery from chassis dynamometer tests', *IEEE Trans. Veh. Technol.*, 2016, 65, (6), pp. 4393–4400
- [17] Shen, P., Ouyang, M., Lu, L., et al.: 'The co-estimation of state of charge, state of health, and state of function for lithium-ion batteries in electric vehicles', *IEEE Trans. Veh. Technol.*, 2018, 67, (1), pp. 92–103
- [18] Liu, S., Jiang, J., Shi, W., et al.: 'Butler-Volmer-equation-based electrical model for high-power lithium titanate batteries used in electric vehicles', *IEEE Trans. Ind. Electron.*, 2015, 62, (12), pp. 7557–7568
- [19] Swanson, J., Smatlak, J.: 'State of the art in light rail alternative power supplies', 13th National Light Rail and Streetcar Conf., Minnesota, September 2016, pp. 47–64
- [20] Masatsuki, I.: 'Development of the battery charging system for the new hybrid train that combines feeder line and the storage battery'. The 2010 Int. Power Electronics Conf. – ECCE ASIA, Sapporo, August 2010, pp. 3128–3135
- [21] Hirose, H., Yoshida, K., Shibamura, K.: 'Development of catenary and storage battery hybrid train system', Electrical Systems for Aircraft, Railway and Ship Propulsion (ESARS), Bologna, December 2012, pp. 1–4
- [22] Kono, Y., Shiraki, N., Yokoyama, H., et al.: 'Catenary and storage battery hybrid system for electric railcar series EV-E301', 2014 Int. Power Electronics Conf. (IPEC-Hiroshima 2014 – ECCE ASIA), Hiroshima, August 2014, pp. 2120–2125
- [23] Shiraki, N., Tokito, K., Yokozutsumi, R.: 'Propulsion system for catenary and storage battery hybrid electric railcar series EV-E301', 2015 Int. Conf. on Electrical Systems for Aircraft, Railway, Ship Propulsion and Road Vehicles (ESARS), Aachen, May 2015, pp. 1–7
- [24] Chymera, M., Goodman, C.J.: 'The calculation of train performance', IET 13th Professional Development Course on Electric Traction Systems, London, 2014
- [25] Ahmadi, S., Dastfan, A., Assili, M.: 'Improving energy-efficient train operation in urban railways: employing the variation of regenerative energy recovery rate', *IET Intell. Transp. Syst.*, 2017, 11, (6), pp. 349–357
- [26] The Institute of Electrical and Electronics Engineers, Inc.: 'IEEE guide for rail transit traction power systems modeling' (IEEE Vehicular Technology Society, New York, 2013)
- [27] Nicholson, T.J.: 'DC & AC traction motors', IET 13th Professional Development Course on Electric Traction Systems, London, UK, 2014
- [28] Hyundai Rotem Company: 'Project record: catenary-free low-floor tram' (Hyundai Rotem Company, Ulsang-si, South Korea, 2014). Available at [https://www.hyundairotem.co.kr/Eng/Business/Rail/Business\\_Record\\_View.asp?brid=68#this](https://www.hyundairotem.co.kr/Eng/Business/Rail/Business_Record_View.asp?brid=68#this), accessed 5 May 2018
- [29] Hyundai Rotem: 'Hybrid low floor tram', April 2014. Available at <http://www.atcgroup.co.uk/download.php?id=732>, accessed 4 March 2018
- [30] Altair Nanotechnology: '24 V 60 Ah battery module', 10 March 2011. Available at <http://www.altairnano.com/wp-content/uploads/2015/11/24V-60Ah-BATTERY-MODULE-Data-Sheet.pdf>, accessed 28 March 2017

# Battery and Accelerating-Catenary Hybrid System for Light Rail Vehicles and Trams

Joachim J. Mwambeleko and Thanatchai Kulworawanichpong\*

School of Electrical Engineering, Institute of Engineering, Suranaree University of Technology  
Nakhon Ratchasima, Thailand.

[jo.mb@outlook.com](mailto:jo.mb@outlook.com), \*[thanatch@sut.ac.th](mailto:thanatch@sut.ac.th)

**Abstract**—An electric train is currently one of the best solutions to urban passenger mobility challenges. However, diesel powered trains are still common in low capacity lines on which the density of traffic is insufficient to justify the high fixed cost of railway electrification. In such cases, battery driven trams present an alternative that some railway operators have been opting for. Since rail vehicles are heavy, a high capacity, high voltage traction battery will be required to provide accelerating power. To minimize the peak power that a traction battery has to supply and subsequently the required battery size, this paper presents a battery-catenary hybrid tram system in which a tram accelerates from a station under a 200-meter-long catenary and cruises with traction battery. The tram was modelled and simulated in MATLAB. The traction battery peak power was reduced from 300 kW to 100 kW. This means a significant reduction in the required battery size with just a short catenary. Suggested applications of such a system are, on shuttle lines with few stops and in countries or regions where full railway electrification would mean dominance of diesel trains.

**Keywords**—electric trains; railway electrification; battery trams; battery-catenary hybrid trams

## I. INTRODUCTION

With the growing traffic congestion and energy security concerns, the need for efficient and sustainable intracity transportation system cannot be overstated. Transportation being among the most energy-consuming industries, there has been a growing effort towards finding an affordable, reliable and sustainable alternative to petroleum traction systems. As a reliable, environmental friendly and efficient traffic mode, an electric train is currently one of the best options that addresses traffic congestion, energy security and pollution concerns in urban areas. Thanks to its low rolling friction and high passenger capacity [1], [2], [3], [4].

While electrified railways benefit from the improved performance offered by electric traction motors and the overall energy transmission system, diesel traction remains common on idle routes where the density of traffic movement is insufficient to justify the high fixed costs of railway electrification [5] [6], [7]. In such cases, battery driven trains bring an alternative that some railway operators have been opting for, even during the age of lead acid traction battery technology. Notably, British Rail operated a lead acid battery driven train from 1958 to 1962 and Deutsche Bahn (DB), a Germany rail operator, operated lead acid battery driven trains class ETA 150 (later 515) from 1955 to 1995 [8], [9]. Battery technology has greatly improved from

lead acid to nickel-based battery, and from nickel-based to Lithium-ion (Li-ion) battery. Li-ion is currently a battery technology with the best performance [8], [10], [11].

Several Li-ion battery driven trams are now in operation, Japan will serve as a good reference. In Japan, there are so many electrified railway lines, but there are a few nonelectrified lines as well. Japanese railway operators (JR East and JR Kyushu) are now replacing diesel multiple units which were used to link electrified and nonelectrified lines, with battery-catenary hybrid (BCH) trams. Two BCH trams are now in commercial operation and seven are scheduled to be introduced this year (2017) [12], [13], [14], [15], [16], [17], [18].

Efforts to promote application of batteries in electric vehicles has resulted into a wide family of Li-ion battery technology. Owing to its high power capability, long circle life and chemical stability; lithium titanate (LTO) battery has emerged as a leading candidate for fast charging and power assist vehicular applications [19], [20], [21], [22]. The LTO battery technology which allows ultrafast-charging, as fast as 6 minutes to full charge, is already widely in use in electric buses and family passenger cars [23], [24], [25], [26], [27], [28]. In railway sector, LTO battery technology has been reported to be used in Škoda's ForCity Classic (28T) trams (in Konya, Turkey) and Vossloh's tramlink v4 (in Santos, Brazil) to link the electrified and nonelectrified lines (or parts of a line) or to be used in case of emergency (e.g. power outage) [29], [30], [31].

Unlike buses, rail vehicles are heavy and require high power to accelerate, but little power to cruise due to low rolling friction. Thus, a high capacity, high voltage traction battery will be needed to meet acceleration (peak) power demand even if the overall energy consumption does not require such a battery. Furthermore, adding batteries increases vehicle weight. This paper therefore, presents a BCH tram system where a tram accelerates under a short catenary ("acceleration-catenary"), and cruises with batteries. In this way, electrification cost, battery cost and train performance will be well optimized. Suggested applications are, on shuttle lines with few stops and in countries or regions where full railway electrification would mean dominance of diesel trains.

The rest of the paper is organized as follows: Battery and catenary hybrid tram model is presented in section II, simulation results are presented and discussed in section III, and finally section IV concludes the paper.



## II. BATTERY AND CATENARY HYBRID TRAM MODEL

### A. Tram Dynamics

Modelled as a point mass, tram's mechanical driving power ( $P_m$ ) is given by a product of its tractive effort ( $T_E$ ) and velocity ( $v$ ), where  $T_E$  is calculated as in (1), neglecting curve resistance which is usually very low (much lower at low speeds)

$$T_E = M'' \frac{\Delta v}{\Delta t} + Mg(\mu + \sin \theta) + 0.5\rho_{air}C_dA_f v_{air}^2 \quad (1)$$

where

$M''$  and  $M$  are tram effective and normal masses given as  $M'' = m_{arc}(1 + \lambda) + m_{load}$  and  $M = m_{arc} + m_{load}$  respectively, where  $m_{arc}$  is the vehicle tare mass,  $\lambda$  is rotary allowance accounting for angular acceleration of the rotating parts (motor rotors, gears and wheel sets) and,  $m_{load}$  is the mass of the vehicle load.

$\frac{\Delta v}{\Delta t}$  is the change in velocity per change in time,  $\mu$  is the rolling resistance coefficient and  $g$  is the gravitational acceleration constant ( $9.81\text{ms}^{-2}$ ),  $\rho_{air}$  is air density ( $1.23\text{kgm}^{-3}$ )  $C_d$  is aerodynamic drag coefficient,  $v_{air}$  is air velocity relative to the tram body,  $A_f$  is the tram frontal area ( $\text{m}^2$ ) and  $\theta$  is a slope angle which is normally very small in urban railways and thus  $\sin \theta$  can be approximated by  $\tan \theta$  (rise/run) [5], [32].

Following (1), tram's tractive electric power ( $P_{te}$ ) and net energy ( $E_E$ ) consumption are given by and (2) and (3) respectively.

$$P_{te} = \begin{cases} T_E v / \eta & \text{if } T_E > 0 \\ \eta T_E v & \text{if } T_E < 0 \text{ and } v > 8 \text{ km/h.} \\ 0 & \text{otherwise} \end{cases} \quad (2)$$

$$E_E = \int_{t_{start}}^{t_{stop}} (P_{te} + Aux) dt \quad (3)$$

where  $T_E$  is the tractive effort (N) as given in (1),  $\eta$  is the electrical – mechanical tractive power conversion efficiency,  $v$  is velocity (m/s),  $t_{start}$  is the time at which the tram starts moving from its current station,  $t_{stop}$  is the time at which the tram stops at the next station,  $Aux$  is the auxiliary load (VA), and  $dt$  is the change in time (s)

For the purpose of this paper, a Stadler-bidirectional tram type Variobahn with technical specifications as given in [33], was chosen. The tram details used in the simulation are given

TABLE I.

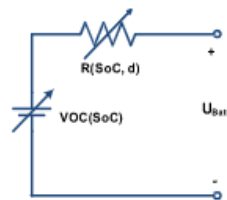


Fig. 1. Battery equivalent circuit

TABLE I. TRAM DETAILS USED IN THE SIMULATION [34], [33], [35], [36]

Attribute	Value
Maximum desired speed ( $v_{md}$ )	40 km/h
Passenger capacity ( $T_{cp}$ )	312
Vehicle effective weight ( $M''$ ) (60.7 kg per person, $\lambda = 1.11$ )	62,883 kg
Rolling resistance coefficient ( $\mu$ )	0.006
Aerodynamic drag coefficient ( $C_d$ )	0.6
Frontal area ( $A_f$ )	7.7 $\text{m}^2$
Gearbox efficiency	0.93
Motors efficiency	0.9
DC/DC converter (bidirectional) efficiency	0.9
DC/AC converter (bidirectional) efficiency	0.9
Motor drive efficiency	0.91
Auxiliary load (Aux)	15 VA
Drive	8 x 45 kW

### B. Traction Battery and other Components

A 24 V, 60 Ah LTO battery manufactured by Altairnano was used and it was modeled as a varying voltage source behind a varying resistor as in Fig. 1 and Fig. 2. The battery pack (16 batteries, in series) details are given in TABLE II. Converters, motors and motor drives are presented by their respective efficiency parameters as given in TABLE I.

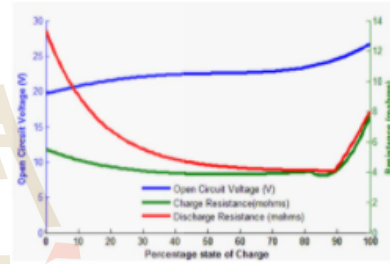


Fig. 2. Battery module curves, plotted from curve fitting functions

TABLE II. ALTAIRNANO 24V, 60 AH BATTERY MODULE DETAILS [37]

Attribute	Battery value	Battery pack value
Nominal Voltage	24 V	384 V
Nominal capacity	60 Ah	60 Ah
Maximum continuous charge	360 A	360 A
Maximum continuous discharge	360 A	360 A
Maximum pulse-charge (10 sec)	600 A	600 A
Maximum pulse-discharge (10 sec)	600 A	600 A
Weight	27.4 kg	438.4 kg

### C. Route and Speed profile

The BCH tram was simulated assuming a route and speed profile as shown in Fig. 3. The route actually exists in Dar es salaam Tanzania, served by a diesel commuter train operated by Tanzania Railways Limited. As the route is fairly flat, in the simulation gradient force was neglected. It is assumed a catenary system runs for 200 m from each station and a tram stops at a station such that its pantograph is at the beginning of the

catenary. Thus, the tram will accelerate drawing power from the catenary.

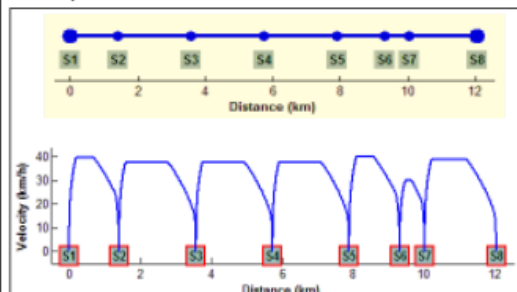


Fig. 3. Route and speed profile

### III. SIMULATION RESULTS AND DISCUSSION

#### A. Simulation Results

The tram speed and tractive force profiles are shown in Fig. 4. At an intermediate station the tram dwells for 30 seconds, and the battery pack is partially recharged (only during the dwell time and not during acceleration). When the tram reaches at the terminal station, the battery pack is recharged to full charge within 15 minutes. Charging is done at 5 C-rate to 80% state of charge (SoC) and then at 2.5 C-rate to 90% SoC, and then at 1 C-rate to 95% SoC, and finally at 0.5 C-rate to full charge as shown in Fig. 6 and Fig. 7.

Tram power demand profile is shown in Fig. 5, and battery-pack current and voltage profiles are shown in Fig. 6. The battery pack provides cruising power (which is about one third of the acceleration power) and auxiliary power when the tram is not under catenary.

Battery pack SoC and distance travelled profiles are shown in Fig. 7, for the purpose of this study, the minimum battery-pack SoC was limited to 60%.

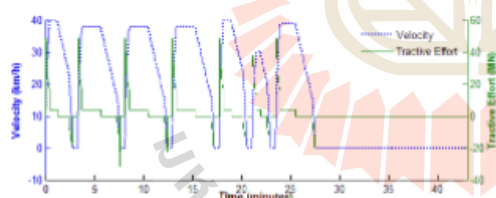


Fig. 4. Tram velocity and tractive force profiles

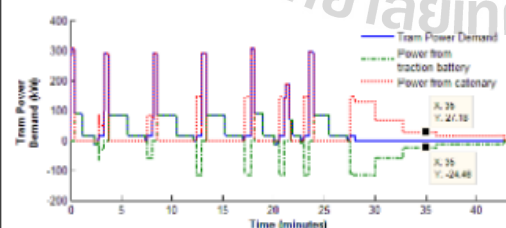


Fig. 5. Tram power demand profile

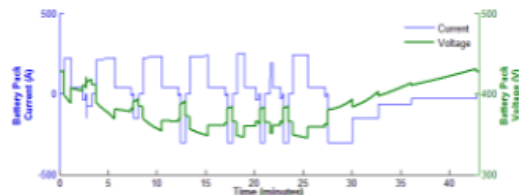


Fig. 6. Tram battery-pack current and voltage profiles

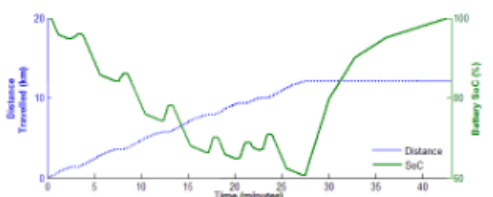


Fig. 7. Distance travelled and battery state of charge profiles

#### B. Discussion

The advantage of having a short acceleration-catenary system (200 m in this case), such that a tram accelerate from a station under catenary is clear in Fig. 5, the peak power demand is around 300 kW. That peak demand is supplied from catenary, and when the tram starts cruising the power demand drops to around 100 kW which is then supplied by a battery pack. Apart from providing acceleration power, the short catenary provides a charging point during dwell time, thus the battery pack is partially recharged at every intermediate station. This further reduces the required size of the battery pack. Increasing acceleration will reduce the length of the acceleration-catenary. However, maximum acceleration is limited by tram's maximum tractive effort. Hence, trams that have high acceleration ability are much preferred in this system.

Charging rate is reduced as the battery gets near full charged as seen in Fig. 6 and Fig. 7. One of the reason is that, near full charge, charging resistance increases considerably as shown in Fig. 2, charging current is therefore reduced to avoid excessive heating of the cells. Even if a battery cooling system is very good, high charging current near full charge will lead to high energy loss. If journey time is limited, a way around is just to charge the battery to near full charge, so the battery SoC can be varying from say 60% to 90%. The same happens during discharging, where discharging resistance start to increase exponentially when the SoC has dropped to 60% (Fig. 2), and for that reason the minimum SoC in this paper was set to 60%.


### IV. CONCLUSION

The paper presents a battery-catenary hybrid tram system in which a tram accelerates from a station under a 200-meter-long catenary and cruises with battery. The battery pack peak power was reduced from 300 kW to 100 kW which means a significant reduction in the required battery size with just a short catenary. The option is more attractive if a tram has high accelerating ability. Suggested applications are, on shuttle lines with few stops and in countries or regions where railway electrification would mean dominance of diesel trains



## REFERENCES

- [1] L. Yang, KepingLi, ZiyuGao and XiangLi, "Optimizing trains movement on a railway network," *Omega*, vol. 40, p. 619-633, 2012.
- [2] M. Samadi, S. Alavi and M. Saif, "An electrochemical model-based particle filter approach for Lithium-ion battery estimation," in *51st IEEE Conference on Decision and Control*, Hawaii-USA, 2012.
- [3] T. Ratniyomchai, S. Hillmansan and P. Tricoli, "Recent developments and applications of energy storage devices in electrified railways," *IET Electrical Systems in Transportation*, vol. 4, no. 1, p. 9-20, 2013.
- [4] J. Jaguemont, L. Boulon and Y. Dubé, "Characterization and Modeling of a Hybrid-Electric-Vehicle Lithium-Ion Battery Pack at Low Temperatures," *IEEE Transactions on Vehicular Technology*, vol. 65, no. 1, pp. 1-14, 2016.
- [5] J. J. Mwambeleko, T. Kulworawanichpong and K. A. Greyson, "Tram and Trolleybus Net Traction Energy Consumption Comparison," in *The 18th International Conference on Electrical Machines and Systems (ICEMS2015)*, Pattaya, 2015.
- [6] C. F. Bonnett, *Practical Railway Engineering 2nd Edition*, London: Imperial College Press, 2005.
- [7] S. Frey, *Railway Electrification Systems and Engineering*, Delhi: White Word Publications, 2012.
- [8] J. J. Mwambeleko, "Reducing Passenger Travel Fuel Cost And Emission: A Case Study of Tanzania Commuter Trains," Suranaree University of Technology, Nakhon Ratchasima, Thailand, 2016.
- [9] A. Steimel, *Electric Traction - Motive Power and Energy Supply*, Munich: Oldenbourg Industrieverlag GmbH, 2008.
- [10] A. Eddahech, O. Briat and J.-M. Vinassa, "Determination of lithium-ion battery state-of-health based on constant-voltage charge phase," *Journal of Power Sources*, vol. 258, pp. 218-227, 2014.
- [11] L. W. Yao, J. A. Aziz, P. Y. Kong and N. R. N. Idris, "Modeling of Lithium-Ion Battery Using MATLAB/Simulink," in *IECON 2013 - 39th Annual Conference of the IEEE Industrial Electronics Society*, Vienna, 2016.
- [12] I. Masatsuki, "Development of the battery charging system for the new hybrid train that combines feeder line and the storage battery," in *The 2010 International Power Electronics Conference (IPEC)*, 2010.
- [13] H. Hirose, K. Yoshida and K. Shibamura, "Development of Catenary and Storage Battery Hybrid Train System," in *Electrical Systems for Aircraft, Railway and Ship Propulsion (ESARS)*, 2012, 2012.
- [14] Y. Kono, N. Shiraki, H. Yokoyama and R. Furuta, "Catenary and Storage Battery Hybrid System for Electric Railcar Series EV-E301," in *The 2014 International Power Electronics Conference (IPEC)*, 2014.
- [15] N. Shiraki, K. Tokito and R. Yokozutsumi, "Propulsion system for catenary and storage battery hybrid electric railcar series EV-E301," in *IEEE-International Conference on Electrical Systems for Aircraft, Railway, Ship Propulsion and Road Vehicles (ESARS)*, Aachen, 2015.
- [16] T. Iwase, J. Kawamura, K. Tokai and M. Kageyama, "Development of battery system for railway vehicle," in *2015 International Conference on Electrical Systems for Aircraft, Railway, Ship Propulsion and Road Vehicles (ESARS)*, Aachen, 2015.
- [17] Wikipedia, "EV-E801 series," Wikimedia Foundation, Inc, 17 December 2016. [Online]. Available: [https://en.wikipedia.org/wiki/EV-E801\\_series](https://en.wikipedia.org/wiki/EV-E801_series). [Accessed 6 January 2017].
- [18] Wikipedia, "BEC819 series," Wikimedia Foundation, Inc, 10 December 2016. [Online]. Available: [https://en.wikipedia.org/wiki/BEC819\\_series](https://en.wikipedia.org/wiki/BEC819_series). [Accessed 7 January 2016].
- [19] T. Horiba, "Lithium-Ion Battery Systems," *Proceedings of the IEEE*, vol. 102, no. 6, pp. 939 - 950, 2014.
- [20] I. Dincer, C. O. Colpan and M. A. Ezan, *Progress in Clean Energy, Volume 2: Novel Systems and Applications*, Springer, 2015.
- [21] B. Tian, H. Xiang, L. Zhang, Z. Li and H. Wang, "Niobium doped lithium titanate as a high rate anode material for Li-ion batteries," *Electrochimica Acta*, vol. 55, p. 5453-5458, 2010.
- [22] S. Liu, J. Jiang, W. Shi, M. Zeyu, L. Y. Wang and H. Guo, "Butler-Volmer-Equation-Based Electrical Model for High-Power Lithium Titanate Batteries Used in Electric Vehicles," *IEEE Transactions on Industrial Electronics*, vol. 62, no. 12, pp. 7557-7568, 2015.
- [23] Proterra, "The proterra catalyst 40-foot transit vehicle," Proterra, 2016. [Online]. Available: <https://www.proterra.com/products/catalyst-40ft/#35-Foot-Catalyst>. [Accessed 6 January 2017].
- [24] Volvo Bus Corporation, "Think electric," Volvo Bus Corporation, 2015. [Online]. Available: <http://electric.volvobuses.com/>. [Accessed 7 January 2017].
- [25] Wikipedia, "Lithium-titanate battery," Wikipedia, 18 October 2016. [Online]. Available: [https://en.wikipedia.org/wiki/Lithium%E2%80%93titanate\\_battery](https://en.wikipedia.org/wiki/Lithium%E2%80%93titanate_battery). [Accessed 2 January 2017].
- [26] Škoda Transportation, "Electrobus with the fast-charging station ŠKODA Ultra Fast Charger," Škoda Transportation, [Online]. Available: <http://www.skoda.cz/en/products/electric-and-hybrid-buses/electrobus-skoda-hp-perun/>. [Accessed 18 July 2016].
- [27] TOSA, "Flash Mobility. Clean City. Smart Bus," TOSA, 2013. [Online]. Available: <http://www.tosa2013.com/en/#/>. [Accessed 17 September 2015].
- [28] ABB Communications, "Large-capacity, flash-charging, battery-powered pilot bus takes to the street," ABB, 30 May 2013. [Online]. Available: <http://www.abb.com/cawp/seitp202/9315e568e4e6a1f8c1257b7400302.fcd.aspx>. [Accessed 17 September 2015].
- [29] J. Swanson and J. Smatlak, "State of the Art in Light Rail Alternative Power Supplies," in *13th National Light Rail and Streetcar Conference*, Minnesota, 2015.
- [30] ABB, "Product data sheet, Propulsion and auxiliary converter for light rail vehicles (LRVs)," ABB, [Online]. Available: [https://library.e.abb.com/public/890771f0f07641609b94e5b21d4d9657/PDS%20BORDLINE%20CC400%20ESS\\_3BHS262329%20ZAB%20E07%20lowres.pdf](https://library.e.abb.com/public/890771f0f07641609b94e5b21d4d9657/PDS%20BORDLINE%20CC400%20ESS_3BHS262329%20ZAB%20E07%20lowres.pdf). [Accessed 7 January 2017].
- [31] Škoda Transportation, "Škoda transportation will deliver catenary-free trams to turkey," Škoda Transportation, 6 May 2013. [Online]. Available: <http://www.skoda.cz/en/press-room/news/skoda-transportation-will-deliver-catenary-free-trams-to-turkey/>. [Accessed 4 January 2017].
- [32] M. Chymera and C. J. Goodman, "The calculation of train performance," in *IET 13th Professional Development Course on Electric Traction Systems*, 2014.
- [33] Stadler Pankow GmbH; A Company of Stadler Rail Group, "Low-floor light rail vehicle, type Variobahn for Bochum-Gelsenkirchener Straßenbahnen AG (BOGESTRA)," 2014.
- [34] J. Laminie and J. Lowry, *Electric Vehicle Technology Explained*, 2nd ed., West Sussex, John Wiley & Sons Ltd, 2012.
- [35] Wikipedia, "Human body weight," Wikipedia, 23 September 2015. [Online]. Available: [http://en.wikipedia.org/wiki/Body\\_weight](http://en.wikipedia.org/wiki/Body_weight). [Accessed 24 September 2015].
- [36] R. Barrero, J. V. Mierlo and X. Tackoen, "Energy savings in Public Transport," *Vehicular Technology Magazine, IEEE*, vol. III, no. 3, pp. 26-36, September 2008.
- [37] Altair Nanotechnologies, "24 V 60 Ah Battery Module," 10 March 2011. [Online]. Available: <http://www.altairnano.com/wp-content/uploads/2015/11/24V-60Ah-BATTERY-MODULE-Data-Sheet.pdf>. [Accessed 28 September 2016].

File / Name		License
IEEJ-TER18010-PDF.pdf		
 IEEJ-TER18010-PDF.pdf (1.36MB) [0 downloads]		
Non-members: ¥ 660- , IEEJ: Academic members: ¥ 440-		
<b>Item type</b>	Study group materials	
<b>language</b>	English	
<b>keyword</b>	Simulator, Battery and catenary, light rail vehicle, Simulator, Battery and catenary, light rail vehicle	
<b>Author name</b>	Kulworawanichpong Thanatchai Mwambeleko Joachim	
<b>Author affiliation</b>	School of Electrical Engineering, Suranaree University of Technology, Nakhon Ratchasima, Thailand, School of Electrical Engineering, Suranaree University of Technology, Nakhon Ratchasima, Thailand	
<b>wrap up</b>	Urban traffic congestion and air pollution from petroleum powered vehicles call for efficient and ecological mobility system. Trams are currently one of the best options. For reasons such as electrification cost, safety and unsightliness of overhead lines, some routes are not fully electrified. Such routes Can be served by different combinations of pollution power delivery systems, battery and catenary hybrid is a common system. In this paper, a battery and catenary light rail vehicle simulator is developed. With the simulator, analyzing train and battery performances on a given route is done easily and quickly	
<b>Journal title</b>	[D] Industrial Application Division Transportation and Electric Railway Study Group	
<b>Year of issue</b>	2018-02-01	
<b>Paper No.</b>	TER18010	
<b>number of pages</b>	6	
<b>Edition type</b>	A4	

# Development of a battery and catenary hybrid light rail vehicle simulator for vehicle and battery performance analysis: version 01

Joachim J.Mwambeleko (Suranaree University of Technology, Thailand)  
Thanatchai Kulworawanichpong (Suranaree University of Technology, Thailand)

**Abstract** Urban traffic congestion and air pollution from petroleum powered vehicles call for efficient and ecological mobility system. Trams are currently one of the best options. For reasons such as electrification cost, safety and unsightliness of overhead lines, some routes are not fully electrified. Such routes can be served by different combinations of traction power delivery systems, battery and catenary hybrid is a common system. In this paper, a battery and catenary light rail vehicle simulator is developed. With the simulator, analyzing train and battery performances on a given route is done easily and quickly.

**Keywords** : simulator, battery and catenary, light rail vehicle

## 1. INTRODUCTION

With the growing population, mobility demand, urban traffic congestion and air pollution from petroleum powered vehicles, the need for efficient and environmental friendly transportation system in urban areas cannot be overstated. There has been a growing effort towards replacing petroleum traction systems with electric systems. As a reliable, environmental friendly and efficient traffic mode, an electric train is currently one of the best options that addresses urban mobility and air pollution challenges. Thanks to its low rolling friction and high passenger capacity. Having proved successful, electric light rail vehicles (ELRVs) are have been adapted in many cities. These vehicles draw power from overhead catenaries, third rail, underground (via inductive transfer) or onboard energy storage devices. Various technologies are used for onboard energy storage, these include batteries, super capacitors, hydrogen fuel cells and flywheels [1], [2], [3], [4].

For various reasons such as railway electrification cost and unsightliness of overhead lines in certain areas, some railway routes are not fully electrified. The former is true for lightly used lines while the latter is particularly true in historical centers. Safety is another concern especially when considering electrifying old routes which were designed with no electrification consideration. Routes that are not fully electrified can be served by hybrid trains, on non-electrified sections the trains draw power from onboard storage devices, and on electrified section the trains draw power from a power line, power drawn is also used to recharge the onboard energy storage devices. In recent years, battery technology has significantly improved with decline in cost. This has stimulated the production of electric buses and trains [5].

Having high power and energy densities, lithium ion battery is currently the best battery technology for electric vehicles. Common Li-ion batteries used in electric traction include lithium manganese oxide (LMO), lithium nickel manganese cobalt oxide (NMC), lithium nickel cobalt aluminum oxide (NCA), lithium iron phosphate (LFP) and lithium titanate (LTO) [6]

Battery and catenary hybrid trams are increasingly becoming popular in various countries like France, Turkey, Brazil, USA, China, and Japan [7]. In Japan alone there are more than 50 km (non-electrified) served by battery and catenary hybrid trams

operated by JR Kyushu and JR East with six battery and catenary hybrid trams in commercial service (see table). In the city of Naging, China, 15 battery and catenary trams were introduced in 2014. The trams serve two lines with a total distance of 17 km, 90% of the lines is without catenary [8]. With advancement in battery technology, the future of battery and catenary hybrid trams is promising.

Table 1. Battery catenary hybrid trams operating commercially in Japan [9], [10], [11], [12].

Manufacturer	J-TREC	Hitachi	Hitachi
Operator	JR East	JR Kyushu	JR East
Family name	Accum	Hitachi A-train	Accum
Series	EV-E301	BEC819	EV-E801
Number of cars per train	2	2	2
Weight (ton)	77.9	72.1	75.6
Length / width (m)	20 / 2.8	20 / 2.95	-
Passenger capacity	266	264	256
Entered service	March 2014	October 2016	March 2017
Operator	JR East	JR Kyushu	JR East
Number in operation	4 train sets	1 train set	1 train set
Number under construction	0	6 train sets	0
Distance	Non-electrified	20.4	10.8
Served (km)	Electrified	11.7	-
			13

- data not available

It is of great advantage to railway operators and government authorities if vehicle and battery performance can be preliminarily analyzed before a decision is made on which tram (transportation) system to be introduced on a particular route. Given route, vehicle and battery characteristics, a simulator can be used to determine (estimate) how will the vehicle and battery pack perform. But, these simulators are not readily available. In this paper a battery and catenary hybrid tram simulator is developed. The simulator is not only useful to railway operators and government authorities, but also to researchers and scholars who want to know how a particular vehicle with a particular battery pack would perform on a particular route.



## 2. VEHICLE AND BATTERY MODELING

**2.1 VEHICLE** A vehicle is modelled as a point mass, its mechanical driving power ( $P_m$ ) is given as a product of its tractive effort ( $T_E$ ) and velocity ( $v$ ), where  $T_E$  is calculated as in (1), neglecting curve (cornering) resistance which is usually very low at low speeds.

$$T_E = \bar{M} \frac{\Delta v}{\Delta t} + Mg \left( \mu + \frac{\Delta h}{\Delta l} \right) + 0.5 \rho_{air} C_d A_f v_{air}^2 \quad (1)$$

where

$\bar{M}$  and  $M$  are tram effective and normal masses given as  $\bar{M} = m_{tare}(1 + \lambda) + m_{load}$  and  $M = m_{tare} + m_{load}$  respectively, where  $m_{tare}$  is the vehicle tare mass,  $\lambda$  is rotary allowance accounting for angular acceleration of the rotating parts (motor rotors, gears and wheel sets) and,  $m_{load}$  is the mass of the vehicle load.  $\Delta v/\Delta t$  is the change in velocity per change in time,  $\mu$  is the rolling resistance coefficient and  $g$  is the gravitational acceleration constant ( $9.81 \text{ ms}^{-2}$ ),  $\rho_{air}$  is air density ( $1.23 \text{ kgm}^{-3}$ ),  $C_d$  is aerodynamic drag coefficient,  $v_{air}$  is air velocity relative to the tram body,  $A_f$  is the tram frontal area ( $\text{m}^2$ ) and  $\Delta h/\Delta l$  is change in vertical distance (altitude) per change in horizontal distance [13].

Vehicle tractive electric power ( $P_{te}$ ) and net energy consumption ( $E_E$ ) are given by (2) and (3) respectively.

$$P_{te} = \begin{cases} T_E v / \eta_{tr} & \text{if } T_E > 0 \\ \eta_{tr} T_E v & \text{if } T_E < 0 \text{ and } v > 10 \text{ km/h.} \\ 0 & \text{otherwise} \end{cases} \quad (2)$$

$$E_E = \int_{t_{start}}^{t_{stop}} (P_{te}(t) + P_{ax}/\eta_{ax}) dt \quad (3)$$

where  $T_E$  is the tractive effort (N) as given in (1),  $v$  is vehicle velocity (m/s),  $\eta_{tr}$  is the electrical-mechanical tractive power conversion efficiency, it is a product of VVVF converter efficiency, traction motor efficiency, gear box efficiency, DC-DC converter efficiency, and battery charge or discharge efficiency (from Fig. 1),  $t_{start}$  is the time at which the tram starts moving from its current station,  $t_{stop}$  is the time at which the tram stops at the next station,  $P_{ax}$  is the auxiliary power,  $\eta_{ax}$  is the efficiency of the auxiliary system, it is a product of DC-DC converter efficiency, battery charge or discharge efficiency and auxiliary power unit (APU) efficiency and,  $dt$  is the change in time (s).

**2.2 BATTERY** Different battery types have different

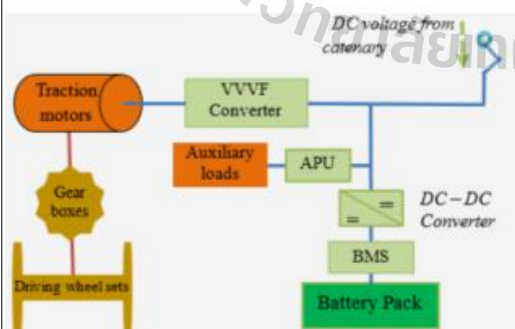


Fig. 1. Battery and catenary hybrid tram block diagram

models, but all models used in the simulator have the same input and output parameters. The input parameters are battery state of charge (SoC) and current (C-rate), and the output parameters are battery terminal voltage and internal resistance as shown in Fig. 2.

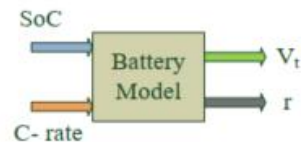


Fig. 2. Inputs and outputs of a battery model

State of charge of a battery charged or discharged from time  $t$  to  $t_f$  is given by (4), where  $SoC_t$  is the state of charge at time  $t$ ,  $SoC_{t_f}$  is the state of charge at time  $t_f$ ,  $\eta_b$  is the battery charge or discharge efficiency,  $C$  is C-rate which is the ratio of current to battery capacity (Amps-seconds) and  $dt$  is change in time (s)

$$SoC_{t_f} = \begin{cases} SoC_t + \int_t^{t_f} \eta_b C(t) dt & \text{if charging} \\ SoC_t - \int_t^{t_f} \frac{C(t)}{\eta_b} dt & \text{if discharging} \end{cases} \quad (4)$$

**2.3 SPEED PROFILE** Generally, a vehicle's speed profile, consist of four operating modes namely: i) accelerating, ii) cruising mode, iii) coasting mode and, iv) braking mode. In accelerating mode the vehicle accelerates to the desired maximum speed, in cruising mode the vehicle maintains its speed (acceleration is zero), tractive effort equals summation of forces opposing the motion. In coasting mode, tractive power supply is cut off, and the vehicle is left to move with its own kinetic energy. This is one of techniques used to minimize energy consumption. In braking mode, brakes are applied to stop the vehicle or reduce its speed. Braking system can be regenerative (vehicle kinetic energy is converted back to electrical energy and stored or used by other loads) or non-regenerative (vehicle kinetic energy is lost mainly as heat). Maximum traction force and braking force at a given speed are dictated by vehicle tractive and braking effort curves. A vehicle speed profile must include accelerating and braking modes but not necessarily cruising and coasting modes. [14], [15], [16].

## 3. THE SIMULATOR

Simulator's Graphical User Interface (GUI) consists of main GUI shown in Fig. 2. and sub GUIs. The main GUI is divided into five parts which are i) Vehicle, ii) Battery, iii) Route and, iv) Speed profile and, v) Simulation controls. Sub GUIs appear only when called/triggered. Examples of the sub GUIs are those shown in Fig. 4 through Fig. 6.

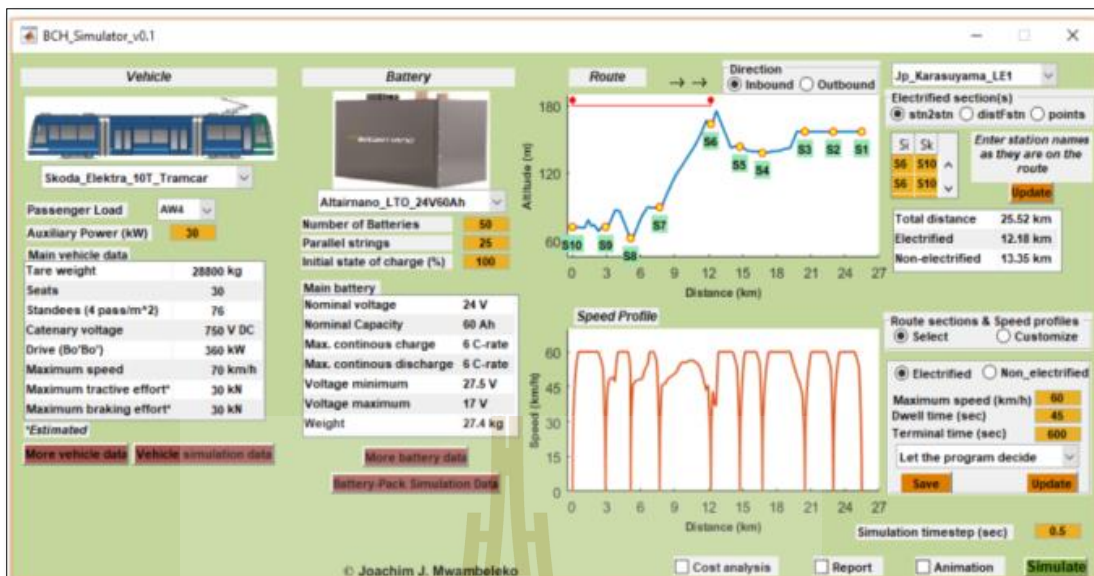


Fig. 3. Simulator main GUI

With vehicle 'skoda elektrika 10T tram', and passenger loading 'AW4' selected, and auxiliary power typed in, vehicle details (displayed after pressing 'vehicle more data' push button) are as shown in Fig 4 and vehicle simulation data (displayed after pressing 'vehicle simulation data' push button) are as shown in Fig 5.

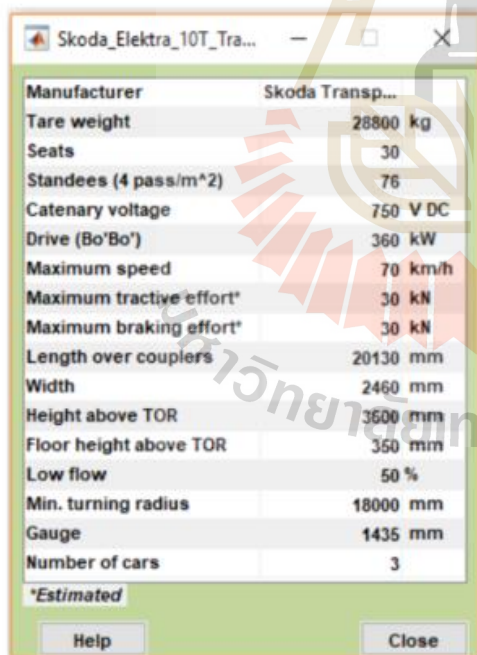


Fig. 4. More vehicle data, for a selected vehicle

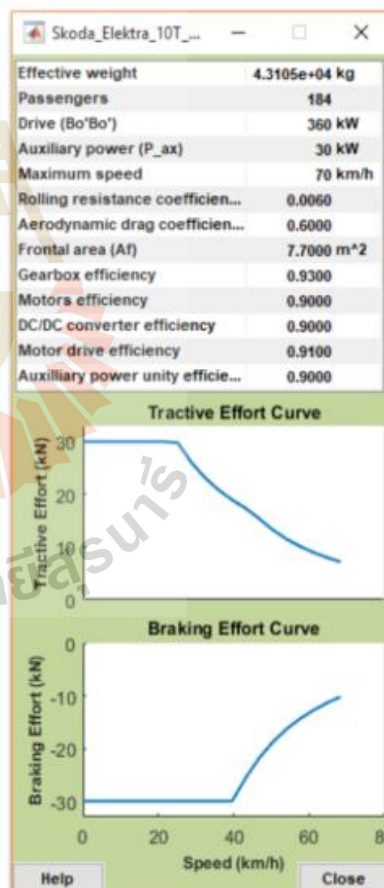


Fig. 5. Vehicle simulation data

Simulation data for the selected battery, and specified number of



batteries in a battery pack, are as shown in Fig. 6 (after pressing the 'Battery-pack simulation data' push button). The figure also shows a battery model that will be used in the simulation.

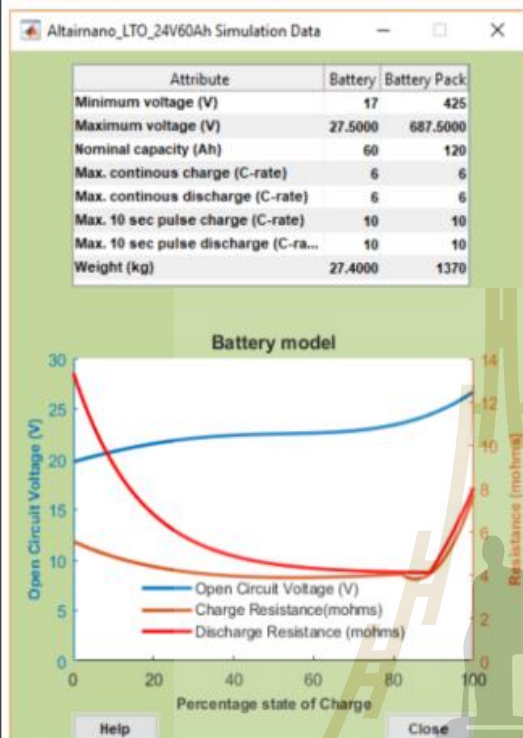


Fig. 6. Battery pack simulation data

Some of user inputs are explained in Table 2.

Table 2. Some of the user inputs

Item	remarks
<b>Vehicle</b>	
Vehicle name	A vehicle name selected from the menu list. When a vehicle is selected, its image and parameters are loaded
Passenger load	Passenger load (added weight) AW0: fire weight of a vehicle. AW1: AW0 + crew + seated passengers AW2: AW1 + standees at 0.251m <sup>2</sup> per standee AW3: AW1 + standees at 0.167m <sup>2</sup> per standee Passenger weight is taken as 70.3 kg AW4: AW1 + standees at 0.125m <sup>2</sup> per standee
Auxiliary power	Vehicle power demand apart from traction power. E.g. power for lighting, air conditioning, and passenger information system
<b>Battery</b>	
Battery name	Battery name, when a battery name is selected, its parameters are loaded.
Number of batteries	Total batteries forming a battery pack
Parallel strings	Number of battery strings connected in parallel
Initial state of charge	Battery initial state of charge (state of charge before a tram starts moving) in percentage

Route	
direction	Tram moving direction (a selection), if outbound direction was selected, the route figure would be as shown in Fig. 7, signifying the tram will be moving from S1 to S10.
Electrified sections	Route electrified section, the input can be in terms of station to station (sta2sta), distance from a station (distFsta), or from any one point (specified by distance) to another(points)
Speed profile	
Vehicle speed profile for electrified and non-electrified sections	Speed profile can be either selected by a user or decide by a program. Six selections are available as shown in Fig. 8. Acc_brake: cruising and coasting are given least priority Acc_coast_brake: cruising is given least priority Acc_cruise_brake: accelerating, coasting is given least priority Let the program decide: the program chooses a speed profile based on distance between stations. Find optimal: the program seeks for the optimal speed profile.  Speed profile can also be customized for different interstation sections



Fig. 7. Route direction, outbound

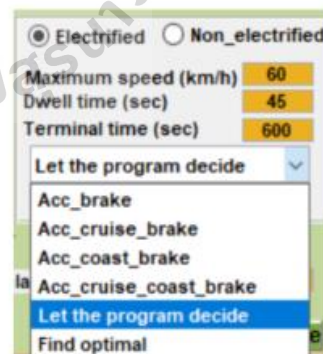


Fig. 8. Speed profile options

With the given inputs, simulation results were as shown in Fig.9.

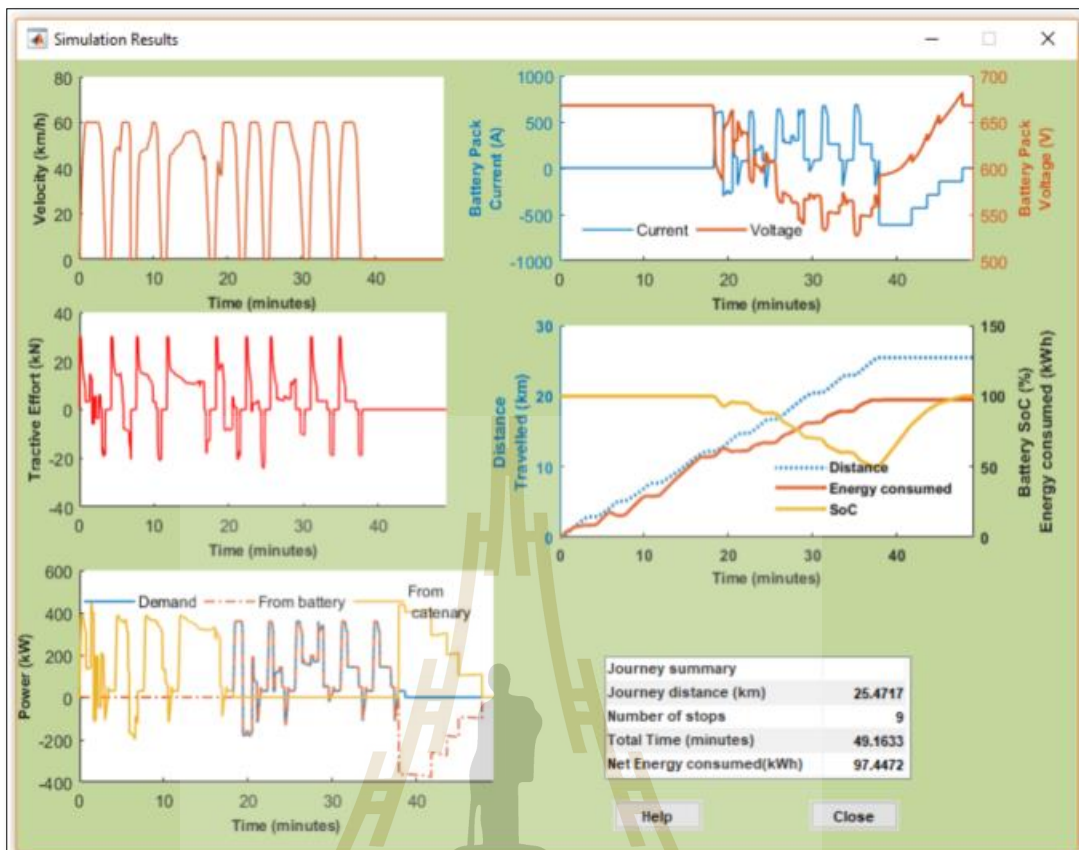


Fig. 9. Simulation results

#### 4. CONCLUSION

For either electrification cost, safety or aesthetical reasons some routes are not fully electrified. With advancements in battery technology, battery and catenary hybrid trams are becoming increasingly popular. Given route, vehicle and battery characteristics, a simulator can be used to determine (estimate) how will the vehicle and battery pack perform. But, these simulators are not readily available. In this paper a battery and catenary hybrid tram simulator is developed. The simulator is useful to railway operators and city planners, researchers and scholars. Performance of different vehicles equipped with different battery pack (or battery pack size) on different routes, can be quickly and easily analyzed.

#### References

- (1) L. Yang, KepingLi, ZiyouGao and XiangLi, "Optimizing trains movement on a railway network," *Omega*, vol. 40, p. 619-633, 2012.
- (2) M. Samadi, S. Alavi and M. Saif, "An electrochemical model-based particle filter approach for Lithium-ion battery estimation," in *51st IEEE Conference on Decision and Control*, Hawaii-USA, 2012.
- (3) T. Rattiyomchai, S. Hillmansen and P. Tricoli, "Recent developments and applications of energy storage devices in electrified railways," *IET Electrical Systems in Transportation*, vol. 4, no. 1, p. 9-20, 2013.
- (4) J. Jaguemont, L. Boulon and Y. Dubé, "Characterization and Modeling of a Hybrid-Electric-Vehicle Lithium-Ion Battery Pack at Low Temperatures," *IEEE Transactions on Vehicular Technology*, vol. 65, no. 1, pp. 1-14, 2016.
- (5) J. J. Mwanjeleko and T. Kulworawanichpong, "Battery electric multiple units to replace diesel commuter trains," *Journal of Energy Storage*, vol. XI, p. 7-15, 2017.
- (6) J. J. Mwanjeleko, "Reducing Passenger Travel Fuel Cost And Emission: A Case Study of Tanzania Commuter Trains," Suranaree University of Technology, Nakhon Ratchasima, Thailand, 2016.
- (7) J. Swanson and J. Smatlak, "State of the Art in Light Rail Alternative Power Supplies," in *13th National Light Rail and Streetcar Conference*, Minnesota, 2015.
- (8) Bombardier Transportation, "PRIMOVE TRAM: First catenary-free trams with Bombardier's lightweight battery technology," 2015. [Online]. Available: [http://primove.bombardier.com/fileadmin/primove/content/GENERAL/PUBLICATIONS/English/PT\\_PRIMOVE\\_Datasheet\\_2015\\_Nanjing\\_EN\\_print\\_110dpi.pdf](http://primove.bombardier.com/fileadmin/primove/content/GENERAL/PUBLICATIONS/English/PT_PRIMOVE_Datasheet_2015_Nanjing_EN_print_110dpi.pdf) [Accessed 10 11 2017].
- (9) Y.Kono, N.Shiraki, H.Yokoyama and R.Furuta, "Catenary and Storage Battery Hybrid System for Electric Railcar Series EV-E301," in *The 2014 International Power Electronics Conference (IPEC)*, 2014.
- (10) Wikipedia, "EV-E301 series," Wikimedia Foundation, Inc, 14 April 2017. [Online]. Available: [https://en.wikipedia.org/wiki/EV-E301\\_series](https://en.wikipedia.org/wiki/EV-E301_series). [Accessed 21 April 2017].
- (11) Wikipedia, "EV-E801 series," Wikimedia Foundation, Inc, 1 April 2017. [Online]. Available: [https://en.wikipedia.org/wiki/EV-E801\\_series](https://en.wikipedia.org/wiki/EV-E801_series).

[Accessed 21 April 2017].

- (12) Wikipedia, "BEC819 series," Wikimedia Foundation, Inc, 13 March 2017. [Online]. Available: [https://en.wikipedia.org/wiki/BEC819\\_series](https://en.wikipedia.org/wiki/BEC819_series). [Accessed 21 April 2017].
- (13) J. J. Mwambeleko, T. Kulworawanichpong and K. A. Greyson, "Tram and Trolleybus Net Traction Energy Consumption Comparison," in *2015 18th International Conference on Electrical Machines and Systems (ICEMS2015)*, Pattaya, January 2016, pp. 2164 - 2169.
- (14) J. J. Mwambeleko, T. Kulworawanichpong and K. A. Greyson, "Tram and Trolleybus Net Traction Energy Consumption Comparison," in *The 18th International Conference on Electrical Machines and Systems (ICEMS2015)*, Pattaya, 2015.
- (15) J. J. Mwambeleko, K. Somsai and T. Kulworawanichpong, "The potential of Battery Electric Multiple Units to Replace Diesel Commuter Trains and Reduce Fuel Cost," in *Proceedings of the 2016 IEEE/SICE International Symposium on System Integration*, Sapporo, 2016.
- (16) M. Chymera and C. J. Goodman, "The calculation of train performance," in *IET 13th Professional Development Course on Electric Traction Systems*, 2014.





## Effect of Partial Charging at Intermediate Stations in Reducing the Required Battery Pack Capacity for a Battery Powered Tram

Joachim J. Mwambeleko, Uthen Leeton and Thanatchai Kulworawanichpong

**Abstract**— Despite the fact that electric trains are ideal for commuter rail service, most often the cost to electrify idle railway routes is unjustifiable. In an effort to replace diesel commuter trains serving short and idle routes, with battery powered trams; this paper evaluates three battery charging options. If batteries are only to be charged at terminal stations, the battery powered tram simulated in MATLAB would need a 57.6 kWh battery pack to travel a distance of 12 km with six intermediate stations, limiting the minimum state of charge to 40%. A one minute, 5C partial charging at one and two of the intermediate station(s), reduced the needed battery pack capacity by 10% and 20% respectively. Having a battery chemistry with high charging rate capability, multiple small trams rather than one big tram, and a good timetable will result into more reduction of the overall required number of batteries. Thus, increase the attractiveness of an intermediate charging station.

**Keywords:** diesel commuter train; battery powered tram; battery charging options

### I. INTRODUCTION

The growing mobility demand, environmental concerns, energy prices, and traffic congestion in cities; keep accelerating the need for efficient and sustainable intracity transportation systems [1, 2]. Having high passenger capacity and efficiency, low energy cost and emission levels; an electric train is currently one of the best solutions to urban mobility challenges [3-5]. Electric trains come with other advantages such as, low maintenance cost, quiet operation, and increased passenger comfort. However, railway electrification is often applied to heavily-used routes where the density of traffic movement is sufficient to justify the high fixed costs [6, 7]. It is for this reason that there are still existing non-electrified railway networks served by diesel commuter trains (DCTs).

In comparison to a traction motor, a diesel engine has very low efficiency and high maintenance cost, the efficiency of a DCT is even much lower in a short journey with frequent stops. The low efficiency of a diesel traction system makes the cost of its fuel per kWh output, much higher than that of grid electricity [4, 7, 8].

Keen to address the growing concern over fossil fuel shortage and environmental issues while benefiting from low operating cost; there have been several attempts to replace DCTs with battery electric multiple units (BEMUs). Most currently, Japanese railway companies: JR East and JR West, have been developing catenary and battery hybrid train

systems since 2011, utilizing lithium-ion (Li-ion) batteries [9-12]. In November 2015, Bombardier's battery powered tram was reported to set a range record when it successfully completed a 41.6 km catenary-free test-run using Li-ion batteries [13]

Recently, lithium titanate (LTO) battery which uses a lithium titanate oxide ( $\text{Li}_4\text{Ti}_5\text{O}_{12}$ ) as a negative electrode instead of graphite, has emerged as a leading candidate for fast charging and power assist vehicular applications, thanks to its power capability, long circle life, low energy cost per cycle life, and chemical stability [14-16]. The battery chemistry has proven successful powering several electric buses and trains [16-19]. Taking the advantage of the low rolling resistance (between a steel wheel and steel rail, with a very small contact area), rail transport consumes less energy per passenger kilometer than road transport for the same traffic [2], [8]. Thus, LTO batteries are expected provide longer drive range in trains than in buses.

Using a 12 km commuter train route in Dar es Salaam, Tanzania; This paper evaluates three battery charging options. Option I, batteries are fully charged only at the terminal stations, option II, batteries are fully charged at terminal stations and partially charged at one of the intermediate stations, and option III, batteries are fully charged at the terminal stations and partially charged at two of the intermediate stations. The aim of the intermediate charging being to reduce the battery pack size. In all cases the battery pack minimum state of charge ( $\text{SoC}_{\min}$ ) is limited to 40%.

The rest of the paper content have been structured as follows: The subject of research is described in section II. A condensed review on train movement is given in section III. Simulation details and results are presented and discussed in section IV, and finally, section V concludes the paper.

### II. THE SUBJECT OF RESEARCH

To ease travelling within the congested Tanzanian commercial city of Dar es Salam; the government of Tanzania introduced commuter train services in October 2012. Tanzania Railways Limited (TRL) operates a diesel commuter train which serves a 12 km route from Central-station (city center) to Ubungu-Maziwa as shown in Fig. 1. The train makes three trips in the morning and evening throughout the week excluding Sundays and public holidays [20-21]. For convenient purposes, in this paper the stations are named as S1, S2, ..., S8 starting from the city center (Central station)

Joachim J. Mwambeleko, Uthen Leeton and Thanatchai Kulworawanichpong are with the School of Electrical Engineering, Institute of Engineering, Suranaree University of Technology, Nakhon Ratchasima, Thailand.

(emails: jo.mb@outlook.com,  
thanatchai@gmail.com)

uthen.leeton@gmail.com,



Fig. 1. TRL commuter train route

Unfortunately, attributed by low efficiency of the train especially in a short journey with frequent stops, high fuel consumption leading to high operating cost and carbon-dioxide (CO<sub>2</sub>) emission has been a challenge. In November 2013, the TRL commuter train was reported to have caused a loss of approx. US\$ 334000, operating at a daily loss of approx. US\$ 1000 [22]. This paper then, studies different battery charging options for BEMUs to replacing DCTs serving short and idle routes. And hence, reduce fuel cost and CO<sub>2</sub> emissions

### III. TRAIN MOVEMENT AND ENERGY CONSUMPTION

#### A. Train kinematics

Generally, a train's speed profile consists of four operating modes which are acceleration, constant speed, coasting and, braking. Normally a train starts accelerating with a constant tractive force to a base speed. From the base speed to a desired speed, tractive power is kept constant, and tractive force reduces inversely to speed till it balances the forces opposing the motion [4], [23]. The adhesion between the driving wheels and the rail determines the minimum and maximum tractive force above which the wheels will start rolling and slipping respectively.

With tractive force equals to the forces opposing the motion, the train maintains the attained speed. As a technique to minimize tractive energy consumption, before brakes are applied, tractive power is cut off and the train is left to coast with its own momentum. The train speed starts decreasing on account of resistance to the motion. Finally, brakes are applied and the train is brought to a stop [23-24]. Like the tractive force, the maximum braking force is determined by the adhesion between the braking wheels and the rail. Modern trains use regenerative braking to recapture train's kinetic energy.

#### B. Train dynamics

Train's movement calculations are governed by the Newton's laws of motion. A free body diagram showing the forces acting upon an uphill moving train is shown in Fig. 2. The relationship between the forces is as expressed in (1)

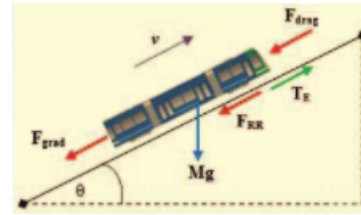


Fig. 2. Free body diagram of a train going uphill

$$F_E = M \frac{dv}{dt} + F_{RR} + F_{grad} + F_{drag} \quad (1)$$

where  $F_E$  is the tractive effort (N),  $F_{RR}$  is the rolling resistance force (N),  $F_{drag}$  is the aerodynamic drag force (N),  $F_{grad}$  is the gradient force (N),  $\frac{dv}{dt}$  is the acceleration (ms<sup>-2</sup>), and  $M$  is the effective vehicle mass (kg) [2]. The effective vehicle mass  $M$  is given as  $m_{tare}(1 + \lambda) + m_{load}$ , where  $m_{tare}$  is the vehicle tare mass,  $\lambda$  is rotary allowance (representing the rotary inertial effect) and,  $m_{load}$  is the vehicle load (passenger or freight mass) [24].

**Aerodynamic Drag,  $F_{drag}$ :** A vehicle moving in air faces air resistance (it has to displace air), aerodynamic drag is due to the friction of the vehicle body moving through air [4]. It is common to express the aerodynamic resistance force in the basic form as in (2) [2].

$$F_{drag} = 0.5 \rho_{air} C_d A_f V_{air}^2 \quad (2)$$

where  $\rho_{air}$  is the air density (kgm<sup>-3</sup>),  $C_d$  is an aerodynamic drag coefficient,  $A_f$  is the projected vehicle frontal area (m<sup>2</sup>) and,  $V_{air}$  is the speed of air relative to the vehicle body (ms<sup>-1</sup>) [26]

**Gradient Force,  $F_{grad}$ :** Gradient force is the component of the vehicle weight acting along a slope. Gradients on railways are usually small such that, taking  $\sin \theta \approx \tan \theta$  ( $\theta$  being the slope angle) is sufficiently accurate. With  $g$  representing acceleration due to gravity, the gradient force of a train with effective mass  $M$  can be expressed as a function of  $h/l$  where  $h$  is the vertical distance and  $l$  is the horizontal distance moved to rise  $h$  units. From (1), the force is negative when the vehicle is moving downhill and vice versa, mathematically expressed, as in (3) [2], [24].

$$F_{grad} = \pm Mg \sin \theta \approx \pm Mg \frac{h}{l} \quad (3)$$

**Rolling Resistance Force,  $F_{RR}$ :** Rolling resistance force is the force resisting the motion of the rotating parts. At the most elementary level the rolling resistance of a vehicle is mathematically expressed, as in (4) [27].

$$F_{RR} = \mu Mg \quad (4)$$

where  $M$  is vehicle effective mass,  $g$  acceleration due to gravity and,  $\mu$  is the rolling resistance coefficient. Some literatures combine (2) and (4) into one equation called Davis' equation as in [28].

### C. Train tractive energy consumption computation

In a computer simulation, the approach to calculate tractive energy consumed by a train travelling from one station to the next is as summarized in Fig. 3.

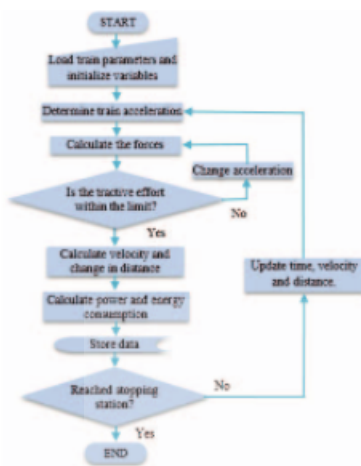


Fig. 3. Train tractive energy consumption, calculation flow chart

## IV. SIMULATION, RESULTS AND DISCUSSION

### A. Simulation details

For the purpose of this paper, a Stadler-bidirectional tram and Altairnano lithium-titanate batteries were chosen. The tram in operation drawing power from a catenary system is shown in Fig. 4 and its technical data are given in TABLE I, its construction overview can be found in [29].



Fig. 4. Stadler-bidirectional tram, type Variobahn [29].

TABLE I. STADLER VARIOBAHN TRAM DETAILS [29].

Attribute	Value	
Maximum speed	70 km/h	
Passenger capacity	56 Sitting 256 Standing (8 persons/m <sup>2</sup> )	
Tram weight	38800 kg	
Catenary's voltage	600 / 750 V	
Drive	8 x 45 kW	
Dimensions	length	29.62 m
	width	2.3m
	height	3.35 m
Gauge	1000 mm	

As the  $SoC_{min}$  was limited to 40%, for most of the time the batteries will operate in a linear (almost flat) zone where the difference between the battery actual voltage (as the function

of state of charge) and nominal voltage is very small. Therefore, in this study a battery is simply modelled as an ideal voltage source (with open circuit voltage equals to the nominal voltage) in series with the equivalent internal impedance. Converters, motors and motor drives are presented by their respective efficiency parameters. The battery and tram details used in the simulation are given in TABLE II and TABLE III respectively. Modelled as a BEMU as shown in Fig. 5, the tram is simulated in MATLAB, using the 12 km TRL commuter train route which has a total of eight (8) stations as shown in Fig. 1. As the route is fairly flat, the gradient force is assumed to be negligible.

TABLE II. BATTERY PACK DETAILS [30].

Attribute	Value
Voltage limit	19-27 V
Nominal voltage	24 V
Nominal capacity	60 Ah
Typical discharge energy (1C rate, 25°C)	1.44 kWh
Maximum continuous charge	360 A
Maximum continuous discharge	360 A
Internal impedance	4 mΩ
Weight	27.4 kg

TABLE III. TRAM DETAILS USED IN THE SIMULATION [1], [25], [31]

Attribute	Value
Maximum allowable speed (km/h)	50
Passenger capacity	312
Vehicle effective weight (kg) <sup>a</sup>	63102
Rolling resistance coefficient	0.006
Aerodynamic drag coefficient	0.6
Frontal area (m <sup>2</sup> )	7.7
Gearbox efficiency	0.93
Motors efficiency	0.9
DC/DC converter (bidirectional) efficiency	0.91
Motor drive efficiency	0.91
Auxiliary load (kW)	20

<sup>a</sup>The weight corresponding to option I, it changes slightly with the number of batteries

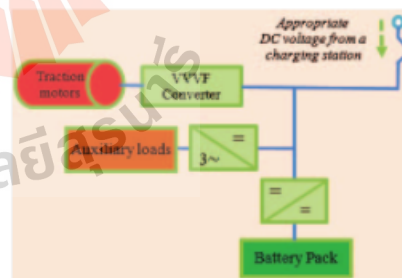


Fig. 5. BEMU block diagram



**B. Simulation results**

Since velocity profile (drive cycle) is the same in all the three cases considered in this paper, and the change in effective weight of the tram due to change in the size of the battery pack is too small to cause notable changes in the tractive effort. The tram velocity and tractive effort profiles are shown just once in Fig. 6. Dwelling for one minute at intermediate stations, the tram takes approx. 30 minutes travelling from S1 (Central station) to S8 (Ubungo-maziwa). When it reaches at the terminal station, batteries are recharged to full charge within 10 minutes. At any charging station, battery charging is done at 5C rate if the states of charge (SoC) is below 80% and at 3C rate otherwise, provided the battery is not fully charged. Perhaps it is worth mentioning at this point that: i) the drive cycles used in this study were optimized to minimize energy consumption, adapted from [5], and ii) these simulation results assume that the tram uses regenerative braking. However, as it can be seen in Fig. 8, the regenerative energy is very little due to low maximum speed, long coasting and relative flat route thus, little kinetic energy is available at a point of braking.

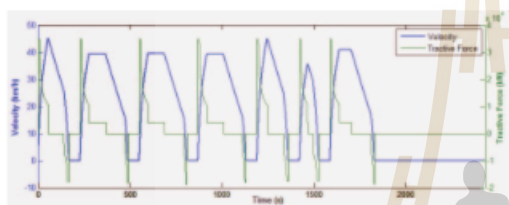


Fig. 6. Tram velocity and tractive force profiles

**Option I:** With option I, batteries are only charged at the terminal stations (charging starts immediately after the tram has come to a stop) as shown in Fig. 7. The needed battery pack consists of 40 batteries (20 in series) with equivalent capacity of 57.6 kWh. The tram power demand, battery current and voltage profiles are shown in Fig. 8. Battery pack SoC, tram net energy consumption and, distance travelled profiles are shown in Fig. 9.

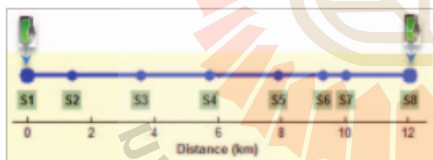


Fig. 7. Option I: Charging points installed only at the terminal stations

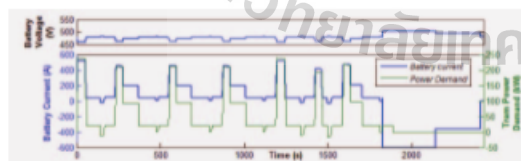


Fig. 8. Option I: Tram power demand, battery pack current and voltage profiles

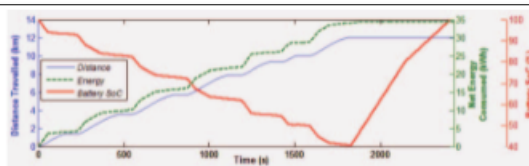


Fig. 9. Option I: Distance travelled, net energy consumed and battery SoC profiles

**Option II:** With option II, batteries are fully charged at the terminal stations and partially charged at one of the intermediate stations (in both cases, charging starts immediately after the tram has come to a stop) as shown in Fig. 10. The needed battery pack consists of 36 batteries (18 in series) with equivalent capacity of 51.84 kWh. Tram power demand, battery current and voltage profiles are shown in Fig. 11. Battery pack SoC, tram net energy consumption and, distance travelled profiles are shown in Fig. 11.



Fig. 10. Option II: Charging points installed at terminal stations and one of the intermediate stations

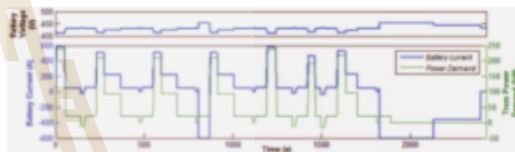


Fig. 11. Option II: Tram power demand, battery pack current and voltage profiles

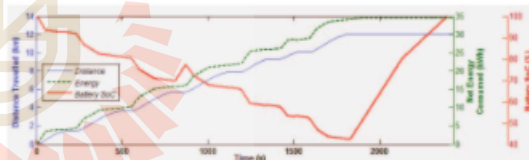


Fig. 12. Option II: Distance travelled, net energy consumed and battery SoC profiles

**Option III:** With option III, batteries are fully charged at the terminal stations and partially charged at two of the intermediate stations as shown in Fig. 13. The needed battery pack consists of 32 batteries (16 in series) with equivalent capacity of 46.08 kWh. Tram power demand, battery current and voltage profiles are shown in Fig. 14. Battery pack SoC, tram net energy consumption and, distance travelled profiles are shown in Fig. 15. A summary of the three options is given in TABLE IV.



Fig. 13. Option III: Charging points installed at terminal stations and one of the intermediate stations

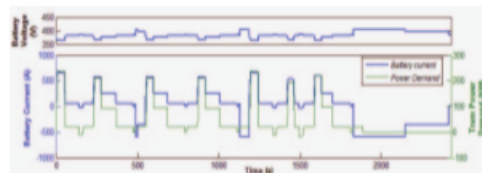


Fig. 14. Option III: Tram power demand, battery pack current and voltage profiles

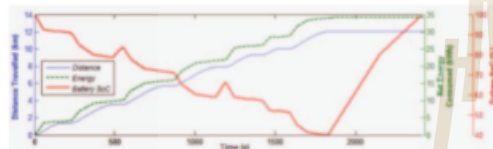


Fig. 15. Option III: Distance travelled, net energy consumed and battery SoC profiles

TABLE IV. SUMMARY OF THE THREE OPTIONS

Summary	Batteries needed	Battery pack Capacity (kWh)	Intermediate-station charging	Total energy Consumed (kWh)
Option I	40	57.6	N/A	34,365
Option II	36	51.84	1, (S4)	34,328
Option III	32	46.08	2, (S3 and S5)	34,283

### C. Discussion

With one intermediate charging station, four batteries (which have an equivalent of 5.76 kWh) could be reduced. That made a 10% reduction of required battery pack capacity. With two intermediate charging stations, the required battery pack capacity was reduced by 20%. Intermediate charging stations come with extra cost. Depending on the number of the trains and a battery pack size for each, different systems will have different battery-pack-reduction to intermediate-charging-station cost ratios.

With regard to the TRL commuter train service, the current DCT has a passenger capacity of 1200. Thus, four BEMUs (as the one used in this study) will be needed to replace the train. One intermediate charging station will reduce 16 batteries in total, equivalent to 23.04 kWh battery pack reduction. And, two intermediate charging stations will reduce 32 batteries in total, equivalent to 46.08 kWh battery pack reduction. Such a reduction is significant; currently, a lithium titanate battery costs around US\$ 1000 to US\$ 1500 per kWh [32], [33].

Having a battery chemistry with high charging rate capability, and multiple small trams rather than one big tram will increase the utilization factor of the intermediate charging station(s). Thus, the overall intermediate charging time will be increased, resulting into more reduction of the overall required number of batteries. That will further enhance the attractiveness of an intermediate charging station. In case of a double track, a good time table that minimizes the number of trains charging simultaneously at a station will help to reduce the size of the charging infrastructure needed.

### V. CONCLUSION AND FUTURE WORK

In an effort to replace DCTs serving short and idle routes with BEMUs, this paper evaluated three battery charging options. A commuter train route, currently served by a DCT in Dar es Salaam Tanzania was used. With option one, where batteries are only charged at the terminal stations, a 57.6 kWh battery pack was needed. With option two, where batteries are fully charged at the terminal stations and partially charged at one of the intermediate stations, the needed battery pack capacity was reduced by 10%. And with option three, where batteries are fully charged at the terminal stations and partially charged at two of the intermediate stations, the needed battery pack capacity was reduced by 20%. In all the three options the battery pack minimum state of charge was limited to 40%.

To replace the current DCT, four BEMUs (as the one used in this study) will be needed. Thus, one and two intermediate charging station(s) will reduce a total of 23.04 kWh and 46.08 kWh battery size respectively. Such a reduction is significant; currently, a lithium titanate battery costs around US\$ 1000 to US\$ 1500 per kWh.

Having a battery chemistry with high charging rate capability and, multiple small trams rather than one big tram will result into more reduction of the overall required number of batteries. Thus, increase the attractiveness of an intermediate charging station. In case of a double track, a good time table that minimizes the number of trains charging simultaneously at a station will help to reduce the size of the charging infrastructure needed.

In the future the authors are expecting to expand this study by considering the actual cost of installing (design and costing of) an intermediate charging stations, and analyze their cost effectiveness for different systems including battery powered buses.

### REFERENCES

- [1] R. Barrero, J. V. Mierlo and X. Tackoen, "Energy savings in Public Transport," *IEEE Vehicular Technology Magazine*, vol. 3, no. 3, pp. 26-36, September 2008.
- [2] J. J. Mwambeleko, T. Kulworawanichpong and K. A. Greyson, "Tram and Trolleybus Net Traction Energy Consumption Comparison," in *The 18th International Conference on Electrical Machines and Systems (ICEMS2015)*, Pattaya, 2015.
- [3] X. Li and H. K. Lo, "An energy-efficient scheduling and speed control approach for metro rail operations," *Transportation Research Part B*, vol. 64, p. 73-89, 2014.

- [4] A. Steimel, *Electric Traction - Motive Power and Energy Supply*, Munich: Oldenbourg Industrieverlag GmbH, 2008.
- [5] J. J. Mwambeleko, "Reducing Passenger Travel Fuel Cost And Emission: A Case Study Of Tanzania Commuter Trains," 2016.
- [6] C. F. Bonnett, *Practical Railway Engineering 2nd Edition*, London: Imperial College Press, 2005.
- [7] S. Frey, *Railway Electrification Systems and Engineering*, Delhi: White Word Publications, 2012.
- [8] V. Profillidis, *Railway Management and Engineering - Fourth Edition*, Wey Court East: Ashgate Publishing Limited, 2014.
- [9] I. Masatsuki, "Development of the battery charging system for the new hybrid train that combines feeder line and the storage battery," in *The 2010 International Power Electronics Conference (IPEC)*, 2010.
- [10] H. Hirose, K. Yoshida and K. Shibanuma, "Development of Catenary and Storage Battery Hybrid Train System," in *Electrical Systems for Aircraft, Railway and Ship Propulsion (ESARS)*, 2012, 2012.
- [11] Y. Kono, N. Shiraki, H. Yokoyama and R. Furuta, "Catenary and Storage Battery Hybrid System for Electric Railcar Series EV-E301," in *The 2014 International Power Electronics Conference (IPEC)*, 2014.
- [12] T. Iwase, J. Kawamura, K. Tokai and M. Kageyama, "Development of battery system for railway vehicle," in *2015 International Conference on Electrical Systems for Aircraft, Railway, Ship Propulsion and Road Vehicles (ESARS)*, Aachen, 2015.
- [13] Bombardier, "Bombardier's Battery Powered Tram Sets Range Record," Bombardier, 3 November 2015. [Online]. Available: <http://www.bombardier.com/en/media/newsList/details.BT-20151103-Bombardiers-Battery-Powered-Tram-Sets-Range-Record-01.bombardiercom.html>. [Accessed 6 June 2016].
- [14] I. Dincer, C. O. Colpan and M. A. Ezan, *Progress in Clean Energy, Volume 2: Novel Systems and Applications*, Springer, 2015.
- [15] B. Tian, H. Xiang, L. Zhang, Z. Li and H. Wang, "Niobium doped lithium titanate as a high rate anode material for Li-ion batteries," *Electrochimica Acta*, vol. 55, p. 5453-5458, 2010.
- [16] S. Liu, J. Jiang, W. Shi, M. Zeyu, L. Y. Wang and H. Guo, "Butler-Volmer-Equation-Based Electrical Model for High-Power Lithium Titanate Batteries Used in Electric Vehicles," *IEEE Transactions on Industrial Electronics*, vol. 62, no. 12, pp. 7557-7568, 2015.
- [17] Škoda Transportation, "Electrobus with the fast-charging station ŠKODA Ultra Fast Charger," Škoda Transportation, [Online]. Available: <http://www.skoda.cz/en/products/electric-and-hybrid-buses/electrobus-skoda-hp-perun/>. [Accessed 18 July 2016].
- [18] TOSA, "Flash Mobility. Clean City. Smart Bus," TOSA, 2013. [Online]. Available: <http://www.tosa2013.com/en/#/>. [Accessed 17 September 2015].
- [19] ABB Communications, "Large-capacity, flash-charging, battery-powered pilot bus takes to the street," ABB, 30 May 2013. [Online]. Available: <http://www.abb.com/cawp/seitp202/9315e568e4c6a1f8c1257b7400302fd.aspx>. [Accessed 17 September 2015].
- [20] Tanzania Railways Limited, "Transport Services," Tanzania Railways Limited, 2016. [Online]. Available: [http://www.trl.co.tz/?page\\_id=43](http://www.trl.co.tz/?page_id=43). [Accessed 29 July 2016].
- [21] Wikipedia, "Dar es Salaam commuter rail," Wikipedia, 29 September 2015. [Online]. Available: [https://en.wikipedia.org/wiki/Dar\\_es\\_Salaam\\_commuter\\_rail](https://en.wikipedia.org/wiki/Dar_es_Salaam_commuter_rail). [Accessed 19 May 2016].
- [22] H. Nachilongo, "A train ride worth Sh2m loss," Mwananchi Communications Ltd, 11 November 2013. [Online]. Available: <http://www.thecitizen.co.tz/News/A-train-ride-worth-Sh2m-loss/-/1840392/2068448/-/acnhks/-/index.html>. [Accessed 5 June 2016].
- [23] R. Rajput, *Utilisation of Electrical Power: Including Electrical Drives and Electric Traction*, New Delhi: Laxmi Publications (P) Ltd, 2006.
- [24] M. Chymera and C. J. Goodman, "The calculation of train performance," in *IET 13th Professional Development Course on Electric Traction Systems*, 2014.
- [25] J. Larminie and J. Lowry, *Electric Vehicle Technology Explained*, 2nd ed., West Sussex: John Wiley & Sons Ltd, 2012.
- [26] T. Kulworawanichpong and S. Punnaisam, "Dynamic Simulation of Electric Bus Vehicle," *The Standard International Journals (The SIJ)*, vol. II, no. 3, pp. 99-104, May 2014.
- [27] T. D. Gillespie, *Fundamentals of vehicle dynamics*, Warrendale, PA: Society of Automotive Engineers, 1992.
- [28] S. Lu, S. Hillmansen, T. k. Ho and C. Robert, "Single Train Trajectory Optimization," *IEEE Transactions On Intelligent Transportation Systems*, vol. XII, no. 2, pp. 743-750, June 2013.
- [29] Stadler Pankow GmbH; A Company of Stadler Rail Group, "Low-floor light rail vehicle, type Variobahn for Bochum-Gelsenkirchener Straßenbahnen AG (BOGESTRA)," 2014.
- [30] Altairmano, "24 V 60 Ah Battery Module," Altairmano, [Online]. Available: <http://www.altairmano.com/products/battery-module/>. [Accessed 30 May 2016].
- [31] D. P.-M. Sarah Catherine Walpole Email author, P. Edwards, J. Cleland, G. Stevens and I. Roberts, "The weight of nations: an estimation of adult human biomass," *BMC Public Health*, 2012.
- [32] ebay, "Toshiba 27v 40Ah lithium titanate Li-ion Battery Pack Module Lto Low Temperature," ebay, [Online]. Available: [http://www.ebay.com/itm/Toshiba-27v-40ah-Litio-titanate-Li-ion-Lto-bateria-Pack-Modulo-De-Baja-Temperatura-/181942232478?\\_ul=BO](http://www.ebay.com/itm/Toshiba-27v-40ah-Litio-titanate-Li-ion-Lto-bateria-Pack-Modulo-De-Baja-Temperatura-/181942232478?_ul=BO). [Accessed 4 August 2016].
- [33] Alibaba, "Deep cycle Lithium Titanate Battery 48v 52Ah LTO Battery for power bank system," Alibaba, [Online]. Available: [https://wholesaler.alibaba.com/product-detail/Deep-cycle-Lithium-Titanate-Battery-48v\\_60258805243.html](https://wholesaler.alibaba.com/product-detail/Deep-cycle-Lithium-Titanate-Battery-48v_60258805243.html). [Accessed 4 August 2016].

## BIOGRAPHY

Mr. Joachim Julius Mwambeleko was born in Morogoro, Tanzania. He received his Bachelor of Science in Electrical Engineering (BSCEE) from Saint Augustine University of Tanzania (SAUT), Mwanza, Tanzania in 2013. He received a Master Degree of Engineering in Electrical Engineering from Suranaree University of Technology (SUT), Nakhon Ratchasima, Thailand in 2016. He is doing PhD studies at the same university, Suranaree University of Technology (SUT). While continuing with his PhD studies, he was a temporary lecturer at Walailak University (WU), Nakhon Si Thammarat, Thailand. His areas of interest are DC electric traction, Solar PV energy and energy efficiency, Artificial intelligence (AI), and Internet of things (IoT).

